DEPOSITIONAL FACIES AND RESERVOIR ANALYSIS OF THE TYLER

FORMATION IN THE CENTRAL WILLISTON BASIN,

NORTH DAKOTA

By

PAUL DAVID MONAHAN

Presented to the Faculty of the Graduate School of

The University of Texas at Arlington in Partial Fulfillment

of the Requirements

for the Degree of

MASTER OF SCIENCE IN GEOLOGY

THE UNIVERSITY OF TEXAS AT ARLINGTON

MAY 2014

Acknowledgements

Abstract

DEPOSITIONAL FACIES AND RESERVOIR ANALYSIS OF THE TYLER

FORMATION IN THE CENTRAL WILLISTON BASIN,

NORTH DAKOTA

Paul David Monahan, M.S.

The University of Texas at Arlington, 2014

Supervising Professor: John Wickham

Traditionally, the Pennsylvanian Tyler Formation has been targeted as a conventional reservoir consisting of barrier island and channel sand deposits in the southwestern Williston basin, North Dakota. The purpose of this study is to investigate the cyclothemic stacking patterns in the Tyler Formation near the depocenter of the basin to improve the petroleum system model. Utilizing one core located in central McKenzie County, the litho-stratigraphy of the cyclothems is characterized. Six facies were identified and described in each cyclothem. A network of six structural and stratigraphic cross sections was constructed. Structural cross sections and structural maps illustrate that the Tyler Formation dips to the northeast. The stratigraphic cross sections illustrate that the Tyler cyclothems were deposited during a period of sea level transgression and high stand. These cross sections and isopach maps also depict a discontinuous sand facies which does not occur in the core studied.

New permeability and porosity data of two carbonate intervals as well as publically available data from several other intervals in the core were used to characterize the reservoir model of these cyclothems. The majority of the identified facies had less than one nanodarcy of permeability, strongly indicating this was a very tight formation.

It is concluded that the overall tight-rock characteristics of the carbonate and siliciclastic rocks within the lower Tyler Formation may indicate an unconventional petroleum play. The sand facies within the upper Tyler Formation might lead to a conventional approach if hydrocarbons are present.

Table of Contents

List of Figures

List of Tables

Chapter 1

Introduction

       The Tyler Formation is of Morrowan age during the Early Pennsylvanian. The formation is underlain by the Mississippian Big Snowy Group and is overlain by the Middle Pennsylvanian Amsden Formation. The Tyler Formation in North Dakota was one of the first formations to be produced for oil and gas in the Williston basin. To date, the Tyler Formation has produced 84 million barrels of oil from approximately 285 wells (Anon., 2011). Historically, the majority of these wells were drilled in the Dickinson, Fryburg, Medora, Rocky Ridge, and Tracy Mountain fields (Figure 1.1). Traditionally a conventional vertical well play, more recently companies have drilled horizontally to tap undiscovered reservoirs. Several of these horizontal wells have been quite productive, such as the Federal #2-13 and Federal #3-13, drilled by Upton Resources (Nordeng & Nesheim, 2012). Both of these were drilled in the sandstone intervals of the Tyler Formation that dominates the Tracy Mountain field in South Billings County. Together these two wells have a cumulative production of more than 500,000 barrels of oil. High oil prices along with developed unconventional technology and knowledge may be key to the development of the Tyler Formation in a viable unconventional petroleum play.

       The Tyler Formation commonly consists of an upper and a lower unit. In the Dickinson, Fryburg, Medora, Rocky Ridge, and Tracy Mountain fields (Figure 1.1), the formation produces from channel and bar sandstones found in the lower unit. The Lower unit, as described by Sturm (1982), is sourced from organic rich shales intercalated with the channel/bar sandstones. The heterogeneous distribution of these reservoir quality sandstone bodies in the lower unit makes exploration and production difficult. The Upper unit of the Tyler Formation, which consists of organic-rich limestone and reservoir quality sandstone layers, has been studied extensively (Sturm, 1982). The strata in the upper unit are more aerially extensive than the lower unit. The high porosity and permeability (8-15% average porosity) in these sandstone layers have made the Tyler play in these fields ideal for conventional drilling. The geographic focal point for this study (Figure 1.1 and Figure 1.3) is adjacent to the Tyler Formations' depocenter, and the

1

stratigraphic and sedimentological history has not been well studied. In this region, the upper and

lower units do not show the characteristics described by Sturm (1982), as shown in Figure 1.2.

The goal of the study is to see if a conventional or unconventional play be developed in the area.
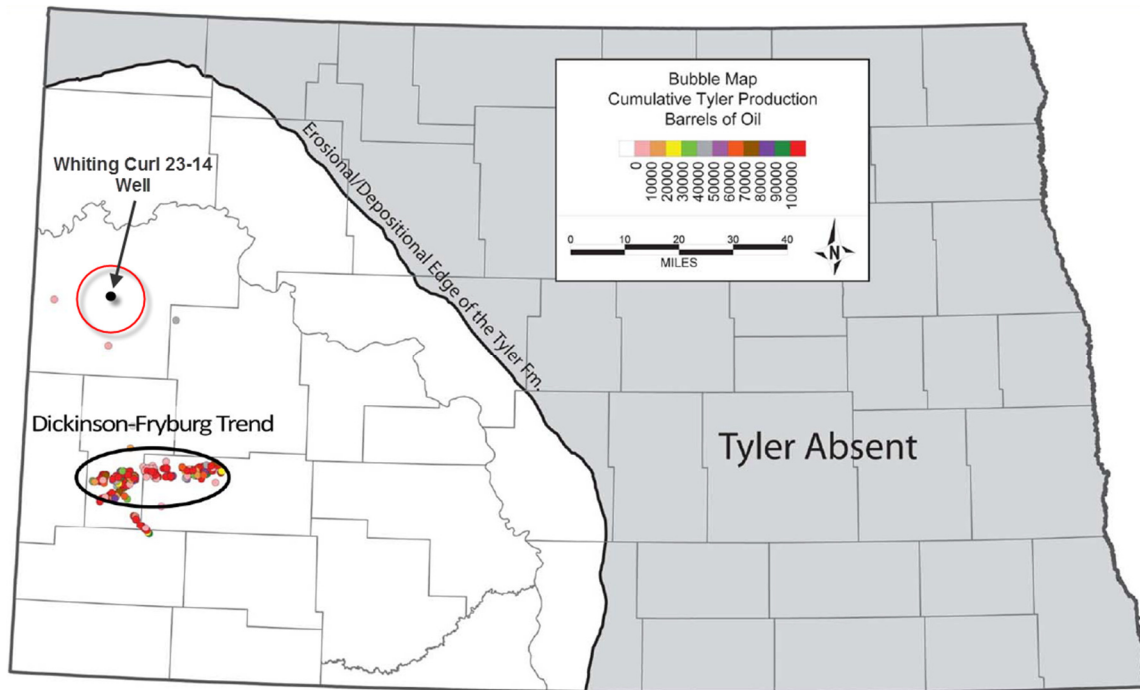
Figure 1.1 Historical production of the Tyler Formation in the Williston basin, North Dakota.

Wells that produced from the Tyler Formation are marked by circles along with the main
production trend. Area of study is circled in red and Whiting's Curl 23-14 well location identified.
Modified from Nesheim & Nordeng (2013).
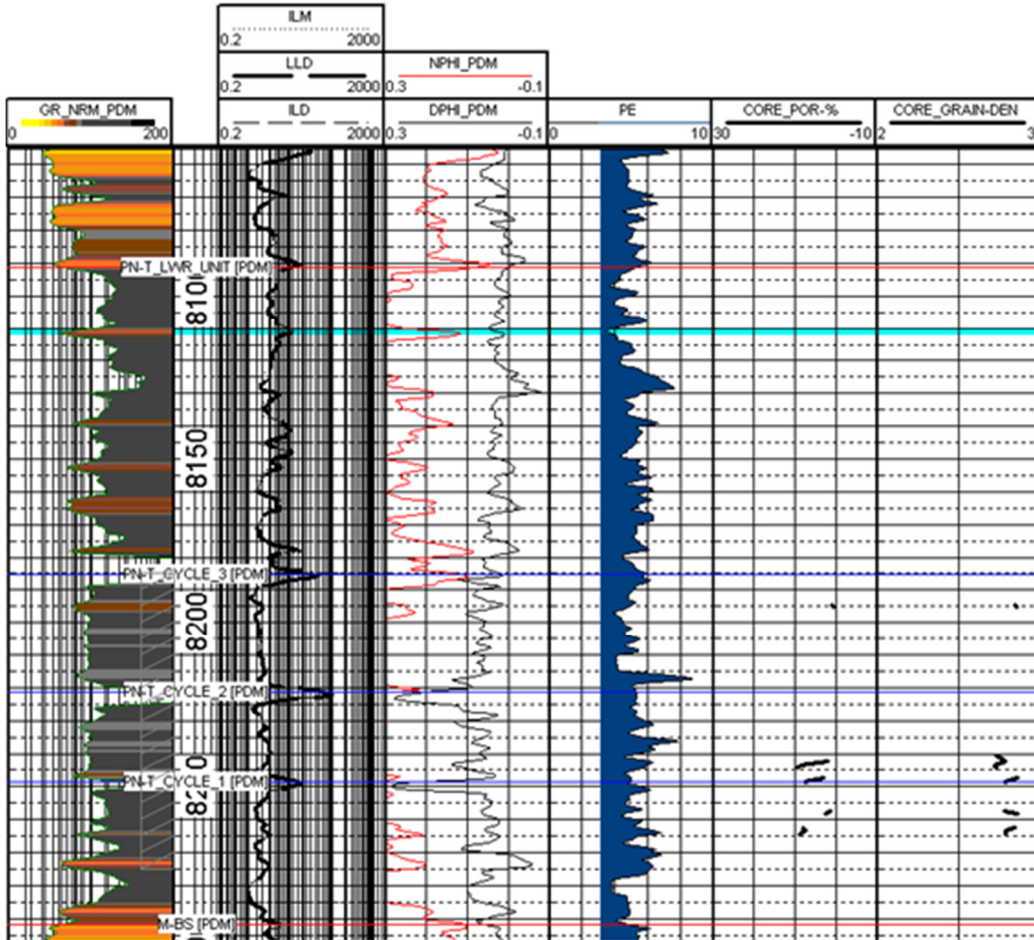
Figure 1.2 Central basin Tyler Formation type log.

Type log for Whiting Oil and Gas Corporations' Curl 23-14 well. Three cyclothems can be seen in the lower half of the formation. Cored interval is located in the interval of 8,185 – 8275 feet. Available core analysis data is shown in far right two tracks.

1.1 Location of Study Area

The study area is geographically located in western North Dakota. It encompasses Townships 148-150 N and Ranges 102-99 W in central McKenzie County, and covers an area of approximately 12,960 square miles (33,556 square Kilometers), as seen in Figure 1.3. The geographic focus of this study overlies one of the locations for potential Tyler Formation productivity described the in North Dakota Geological Survey Report of Investigations No. 111. That focused on the characteristics of the Tyler Formations' source rocks and found the central basin to be a possible locality for future Tyler Formation production (Nordeng & Nesheim, 2012).
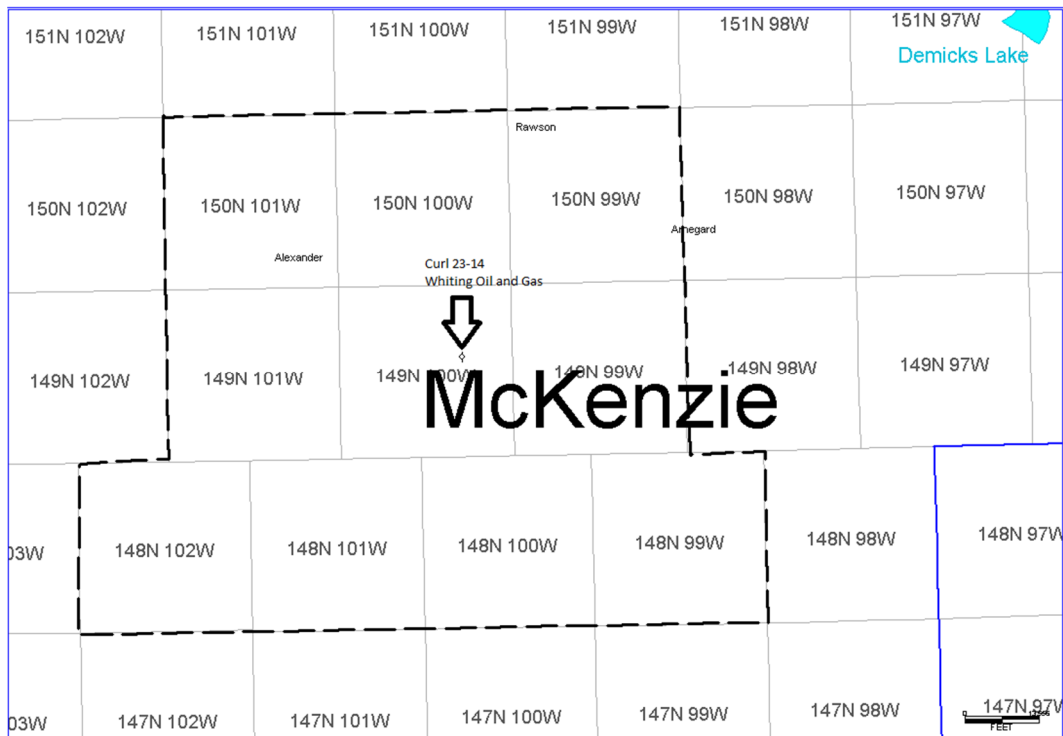
Figure 1.3 Study area with the Curl 23-14 well indicated.

1.2 Research Objectives and Methods

The major contributions of this study are to:

- Establish a more detailed understanding of the facies and depositional environments of the Tyler Formation in the central Williston Basin.

- Conceptualize the relationship between facies and reservoir rock properties.

  - Provide an analysis of porosity and qualitative permeability through well-log interpretation

The main objectives of this research to:

- Understand the depositional environment of the Tyler Formation in the central basin region by determining the facies associations, geometry, and continuity of the formation. The following are detailed steps which were performed to understand the depositional environment:

  1) Describe the Curl 23-14 Tyler core in the central basin in order to identify vertical facies variations.

  2) Correlate 429 digital and raster logs in the central McKenzie County in order to construct structural, isopach maps, and stratigraphic and structural cross sections, from which a depositional model is inferred for the region.

- Determine reservoir quality by applying an integrated petrophysical analysis. The petrophysical analysis and facies interpretation were combined to determine whether the facies correlated with the reservoir properties identified in well logs. The integration of these two methods involved the following:

  1) Determine reservoir quality from a core analysis report and the rock properties from core measurements.

  2) Determine porous intervals of all wells in study area within the Tyler Formation by conventional well log analysis, then correlated these intervals and map the lateral thickness variation in the field.

3) Analyze the relationship between facies and rock property to determine factors controlling reservoir quality.

1.3 Previous work

Historically, the Tyler Formation has been studied near the producing fields incorporated in the Dickinson-Fryburg trend, seen in Figure 1.1. The first investigations of the formation began with Ziebarth and Land (1972 &1976) who studied the economic and stratigraphic characteristics of the Tyler sandstones in the Dickinson area. The Tyler Formation sandstones were found to have finely laminated to ripple cross-stratification and burrow structures (Land, 1976). Ziebarth (1972) noted the thickening of the Tyler Formation towards the northwest, indicating that this apparent thickness could be caused by the facies change of the overlying bedding from carbonate to shale, matching facies of the Tyler Formation. Ziebarth (1972) also noted that prominence of limestone in the southwestern portion of the state.

Following these two studies, Grenda (1978) did a paleozoology study utilizing thirty-four cores. The majority of the cores are located in the Fryburg-Dickinson trend, while two are located near his study. Grenda (1978) concluded that the fauna suggested a depositional environment that constantly fluctuated with depth and salinity. He also mentioned that within the same core, repetition of these depositional environments were evident, implying the presence of cyclothems.

Sturm (1982) divided the Tyler Formation in southwestern North Dakota into two units, a lower, and an upper. Sturm also indicated that in the southwestern portion of North Dakota, the Tyler Formation consists of three cyclothems. The first cyclothem starts from an erosional surface that incised the Big Snowy Group surface during a major regression, and includes channel sandstone filled the incised valleys during a subsequent marine transgression, and mudstone and limestone, formed during the subsequence high stand of seal level. The second cyclothem is similar to the first and these two cyclothems form the lower unit of the Tyler Formation (Sturm, 1982).The lower Tyler Formation is of deltaic depositional environment and the distributary channel sands were sourced from the Transcontinental Arch and Cedar Creek Anticline to the

south of the basin (Sturm, 1982). Progradation of the delta front to the north encased

sandstones and coals in marine to non-marine shales and mudstones (Sturm, 1982). The third

cyclothem is the upper unit of the Tyler Formation. The upper unit consists of a basal sandstone

which is succeeded by limestone locally. The basal sandstone and limestone lenses are overlain

by intercalated black shale with limestone, and sandstone. These sandstone and limestone are

interpreted as deposits of barrier island environment occurred during marine regression, and are

typically laterally inconsistent. The laterally inconsistent sequence in the upper unit indicates that

the barrier island complex prograded and the associated estuarine and lagoonal environments

migrated north towards the productive fields (Sturm, 1982). Paleosols and coals found in the

upper unit show that marsh and swamp environments succeeded the barrier island environment.

The North Dakota Geological Survey Report of Investigations No. 11 focuses on the

southwestern North Dakota region and the shale intervals. These shale intervals occur

repetitively and were found to be highly organic-rich. Total organic content (TOC) was measured

along with thermal maturation, and a pressure analysis. TOC percentage has an average of

1.81% with a variance of 16.4 (Nordeng & Nesheim, 2012). Pressure data from thirty drill stem

tests conducted in producing Tyler Formation fields and wildcats were examined. Ten of the tests

concluded high fluid pressures while the other twenty were at hydrostatic pressure (Nordeng &

Nesheim, 2012). The ten over pressured wells were located in existing Tyler Formation fields and

four were in west-central North Dakota, near this thesis' area of focus.

The study concluded that the Tyler Formation has two possible plays, one of which has

been exploited to date as seen in Figure 1.4. The second play was located in the mid-basin in

McKenzie and Dunn Counties, because of the presence of over-pressured zones, high TOC, and

thermal maturity of the specific shale intervals. Although the study focused on these shales,

which are the source of this potential play, no study has yet focused on the other lithologies in the

cyclothems that could potentially be the reservoir and seal rocks in the central basin.
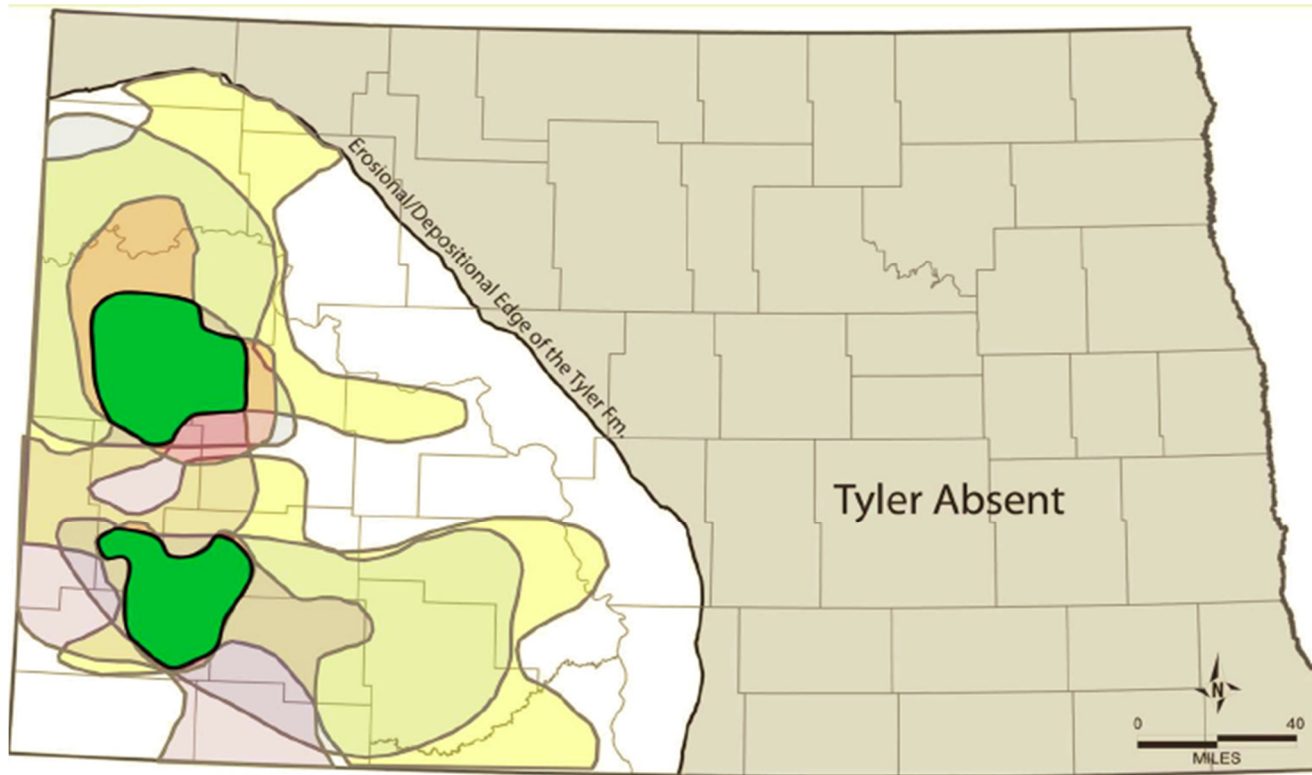
Figure 1.4 Lateral extent of the Tyler Formation with producible zones shaded.

The solid green shading indicates the overlapped area of highest TOC, overpressured zones, and thermal maturity. From Nesheim & Nordeng (2012).

Chapter 2

Geologic Setting

2.1 Williston Basin Structural History

The Williston Basin is a 133,000 mi^2 (344,468 km^2) elliptical intracratonic basin located on the western edge of the North American Platform (Gerhard, et al., 1990). The basin is bounded by the Canadian Shield to the north and east; the Alberta shelf, Little Rocky Mountains, and the Black Hills to the west; and the Trans-Continental Arch to the south (McCabe, 1957). The Big snowy trough to the west connected the Williston basin to the Antler Foredeep (Peterson, 1981; Dorobek, et al., 1991).

As an intracratonic basin the Williston basin had a thermal origin. A thermal anomaly located directly below the lithosphere would have caused expansion of the crust, which subsequently appears on the surface as epeirogenic uplift (Crowley, et al., 1985). Crowley et al., (1985) suggest that the thermal anomaly was the result of either dynamic upwelling or diapirism of asthenosphere into lithosphere. As uplift occurred, erosion of the basement, which was aerially exposed, occurred. As the heating mechanism beneath the lithosphere subsided, so did the uplift, forming the basin.

The eastern portion of the basin is underlain by the Archean Superior Province (King, 1976). In the Precambrian, the Archean Superior craton was sutured to the Archean Wyoming craton by the Trans-Hudson Belt (Anna, et al., 2011). This resulted in a north-south trending strike-slip fault and shear belt that created zones of weakness that controlled the location of several anticlines in the basin today. A weak zone was developed by the Trans-Hudson orogenic belt to the west of the basin and led to sagging during the Cambrian, creating the Williston basin. Controversial rifting which aided in the sagging of the basin was caused by regional uplift (Green, et al., 1985a) although Nelson et al (1993) state that there is no evidence of rifting. With thermal subsidence of the region creating accommodation space, the Williston basin became a center for deposition from the Cambrian to the Jurassic.

10

The Red Wing Creek structure is located in the western flank of the Williston basin. Geophysical studies indicate that this subsurface structure has a central uplift which is surrounded by an annular crater moat and a raised rim (Koeberl, et al., 1996). The diameter of the structure is approximately 5.5 miles (9 kilometers and buried underneath about 6,500 feet (2,000 meters) of sediment (Koeberl, et al., 1996). This structure might be a part of a series of meteor impacts that occurred simultaneously during the late Triassic in Rochechouart (France), Manicouagan and Saint Martin (Canada), and Obolon' (Ukraine) (Spray, et al., 1998). These craters, when plotted on a tectonic reconstruction of the Laurentian and Eurasian plates for 214 Ma, are found to be co-latitudinal at 22.8º and share a similar declination. This indicates that the five impact craters were formed at the same time within hours of each other by a fragmented comet or asteroid (Spray, et al., 1998). Production from this structure is mostly from the Madison Group due to large fracture and fault networks formed from the deformation.

2.2 Regional Stratigraphy and Sedimentology

In the Williston basin there are six major depositional sequences including, from oldest to youngest, the Sauk, Tippecanoe, Kaskaskia, Absaroka, Zuni, and Tejas (Anna, et al., 2011). In total, these account for nearly 16,000 feet (4,877 meters) of sedimentary rock present from the Cambrian to the Tertiary. The deposition of these major sequences has been controlled by eustatic change in sea level. Water depths in the basin during the Phanerozoic were shallow; thus a small change in sea level resulted in substantial depositional environment and sedimentation changes (Anna, et al., 2011).

A stratigraphic column of the basin is shown in Figure 2.1. Figure 2.2 features a diagram showing the geologic time scale, major stratigraphic sequences of Sloss (1984), first- and second-order sea level curves from Vail et al (1977), and ages of petroleum source and reservoir rocks in the Williston Basin.

The Sauk sequence consists of the Upper Cambrian Deadwood Formation that was deposited on a low-relief Precambrian erosional surface during a first-order transgression as

11

shown in Figure 2.2. The Depositional environments in the Deadwood include shallow marine, coastal plain, and alluvial plain (Anna, et al., 2011). Several minor transgression-regression cycles separate the Deadwood Formation into multiple members (LeFever, 1996). A major unconformity occurs at the end of Deadwood deposition that truncates most of the upper members near the basin margins.

The Kaskaskia sequence is part of a first-order regressive cycle that commenced at the beginning of the Devonian and ended at the end of the Mississippian (Figure 2.2). During this time the basin was subjected to restricted marine conditions that was followed by episodes of regular circulation due to sea level change. This produced a variety of lithologically different formations in the sequence. The first few were deposited during the initial transgression. These were the Ashern and Winnipegosis Formations overlain by the Prairie Formation. The Prairie Formation is dominated by evaporites and minor clastics, representing a period of regression and restricted water flow. A secondary transgression occurred and deposited the Dawson Bay Formation. As the sea level regressed once more, the Souris River, Duperow, Birdbear, and Three Forks Formations were deposited.

The third and final major transgression occurred during the late Devonian and deposited the highly organic-rich Bakken Formation (Anna, et al., 2011). Sea level receded once more and the Mississippian Lodgepole Formation was deposited under subtidal conditions, forming low porosity limestone. The Madison Group was deposited above the Lodgepole Formation and represents a time with minor transgression-regression cycles. Open marine and intertidal limestone with peritidal and sabkha anhydrite and salt were deposited during the Mississippian (Anna, et al., 2011). At the end of the Mississippian the Big Snowy Group was deposited, overlaying the Madison Group. The Big Snowy Group consists of interbedded sandstones, shales, and limestone. This regression ended major Paleozoic marine sedimentation in the Williston Basin, with exception of the Pennsylvanian and Permian (Anna, et al., 2011; Gerhard, et al., 1982).

The Absaroka sequence lasted from Pennsylvanian to Triassic. The Tyler Formation was deposited during the initial first-order regression of this sequence in the Morrowan stage of the Early Pennsylvanian. The Early Pennsylvanian Williston Basin was recreated by Blakey (2013) and shown in Figure 2.3. Uplift to the east, west, and south became major sources of clastic sediment during this time. The Tyler Formation includes interbedded sandstone, siltstone, shale, and limestone and will be discussed in the following sections. The Tyler Formation overlies the erosional boundary (sequence boundary) above the Big Snowy Group. The Amsden Formation overlies the Tyler Formation and had input from the Ancestral Rocky Mountain orogenic belt and Transcontinental Arch (Anna, et al., 2011). Continued regression caused restrictive conditions that produced thick accumulations of salt as well as subaerial exposure during the Permian (Gerhard, et al., 1982; Anna, et al., 2011).

The Zuni sequence occurred during the Jurassic and Cretaceous Periods and contains strata deposited during a first-order cycle (Figure 2.2) and bounded by regional unconformities (Anna, et al., 2011). During the Jurassic there were marine subtidal and intertidal environments that deposited anhydrite and salt at the basin center. Shale and calcareous shale were deposited near basin margins while carbonates and sandstone are on the basin margins. At the end of the Jurassic the lithology switched to continental sandstone and mudstone. In the Lower Cretaceous the lithologies are mostly sandstone, siltstone, mudstone, and shale (Anna, et al., 2011). The Upper Cretaceous consists of four major transgression-regression cycles with the same lithology as the Lower
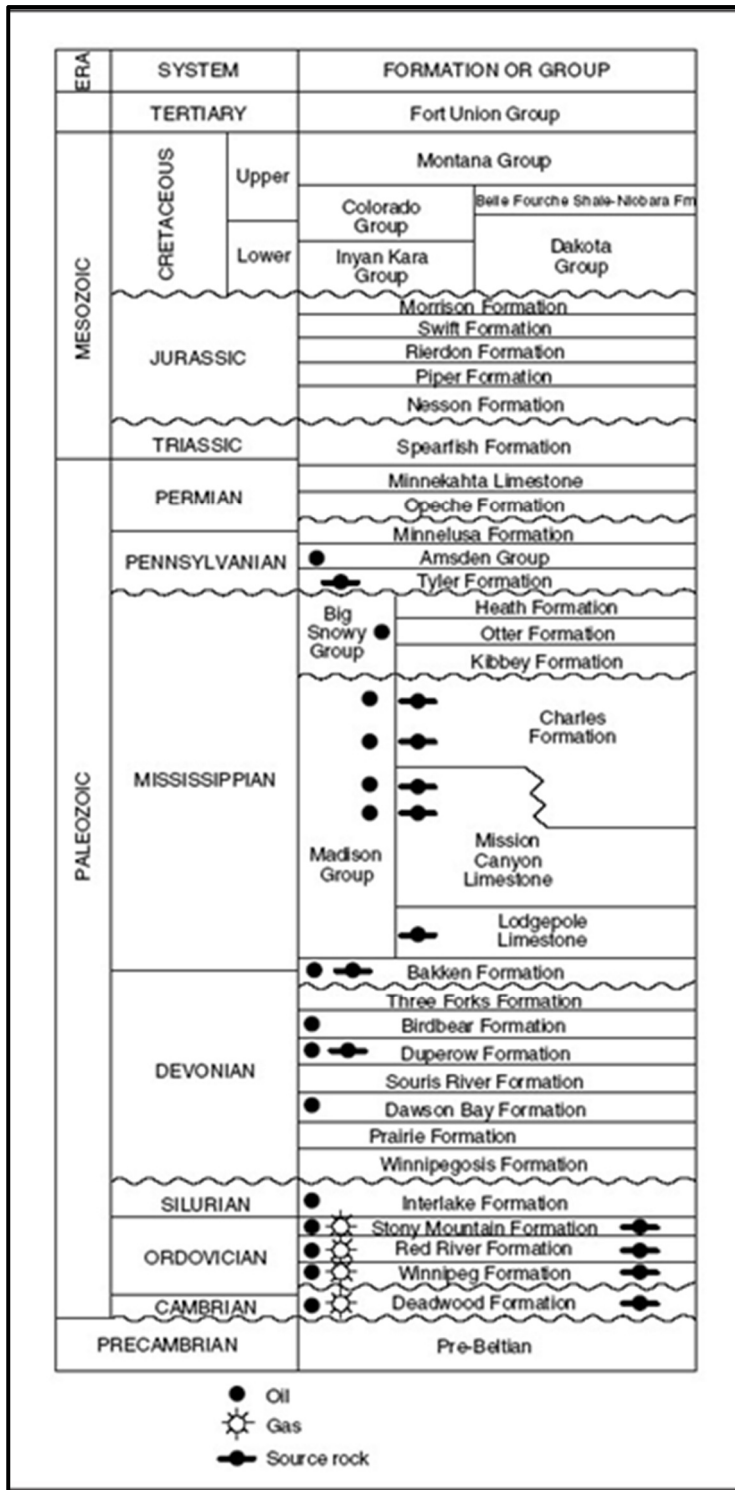
Figure 2.1 Williston Basin stratigraphic column.

This column highlights known source rocks and production.
From (Peterson, 1995).
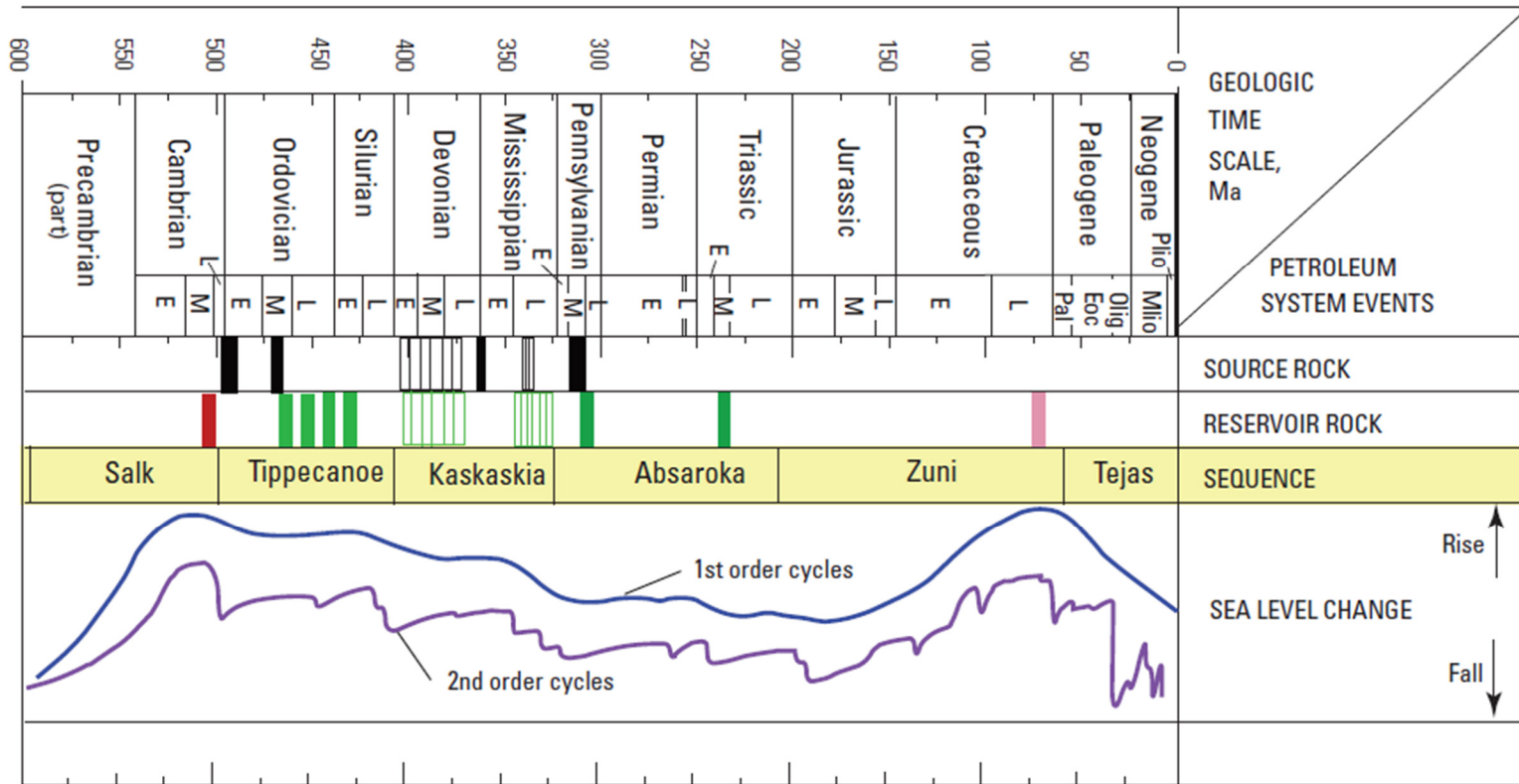
Figure 2.2 Milankovitch Cycles and Petroleum Plays in the Williston Basin.

Solid black intervals in the source rock column are for thick accumulations; thin lines indicate an association with carbonate depositional cycles. In the reservoir rock column, green is for oil and red for gas; thin lines indicate generalized reservoir rock and do not necessarily represent the full spectrum of possible reservoirs. E, Early; M, Middle; L, Late; Pal, Paleocene; Eoc, Eocene; Olig, Oligocene; Mio, Miocene; Plio, Pliocene (Anna, et al., 2011). Diagram from Anna et al (2011).

Cretaceous.

The Tejas sequence identifies the final first-order regression in the basin, seen in Figure 2.2. It is comprised of three regional cycles with strata ranging in age from mid-Paleocene through Quaternary and consists of continental gravel, sandstone, siltstone, mudstone, and low-grade coal (Anna, et al., 2011). Coal bed methane has been produced in this sequence but no other forms of hydrocarbons have been found.
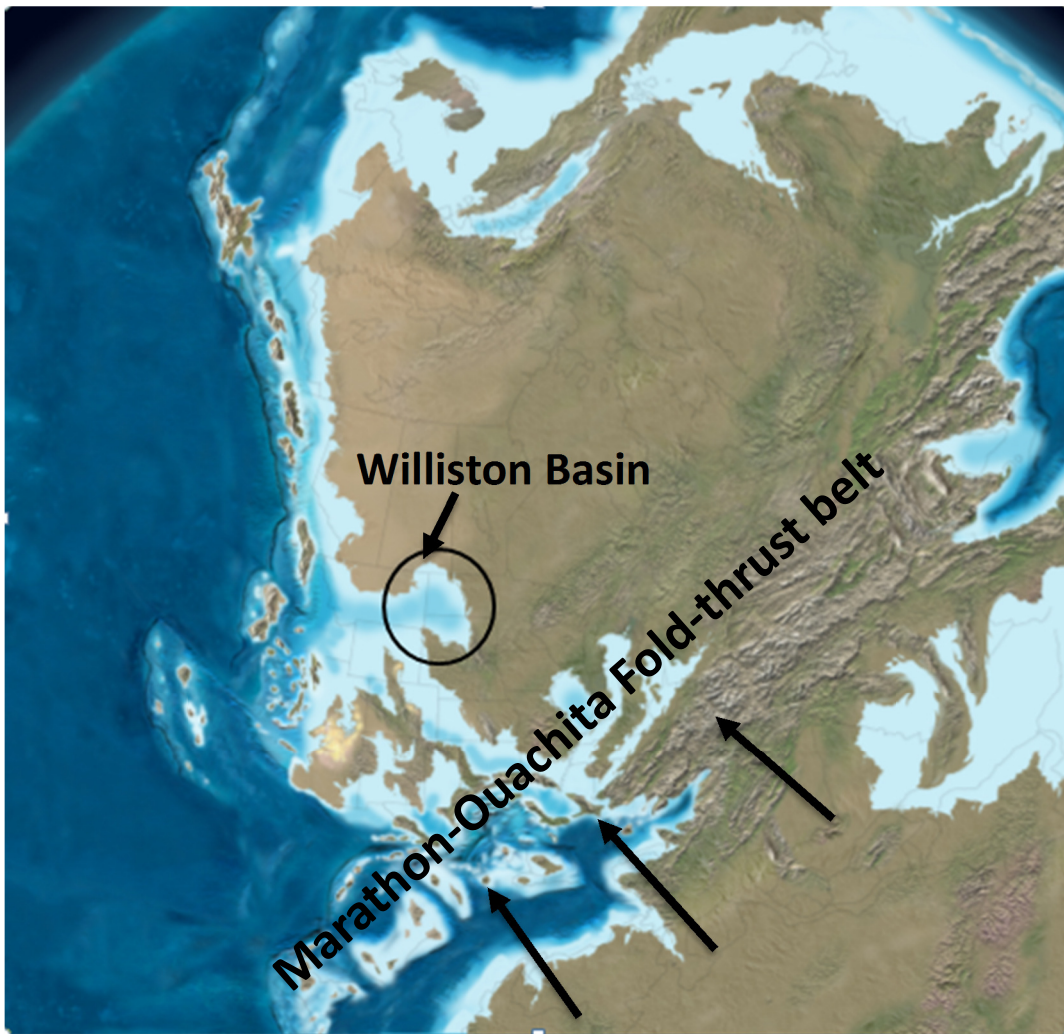
Figure 2.3 Early Pennsylvanian paleogeography in North America.

Modified from Blakey (2013).

Chapter 3

Methodology

There are three cores available for the Tyler interval in McKenzie County, but only one was described in this study. Analysis of this core helped identify facies variation and create a depositional model for the Tyler Formation in the central Williston basin and nearby regions.

3.1 Facies Interpretation and Core Description

The core that was used for this study is from Whiting Oil and Gas Corporations' Curl 23-14 well, API number 3305302794 and its location is shown in Figure 1.3. The core was analyzed in Grand Forks, North Dakota at the Wilson M. Laird Core and Sample Library. The core is 90 feet long from a measured depth of 8,195 to 8,275 feet from a Kelly bushing elevation of 2,225 feet; subsea depth is -5,970 to -6,050 feet. The conventional core was photographed previously by the Wilson M. Laird Core and Sample Library, and photographs can be found on the North Dakota Industrial Commission's (NDIC) website. Special emphasis was placed on identifying sequence boundary surfaces and depositional environments. The core description follows a modified guideline of Bebout and Loucks (1984) for facies identification which included: lithological variations, grain-size distribution, mineralogical composition, fossil and trace fossil associations, rock textures, and sedimentary structure. Grain size was determined using a hand lens and a well card provided by the Wilson M. Laird Core and Sample Library.

The presence of calcite and dolomite minerals in core samples was identified using 10% HCl. The distinction between calcite and dolomite minerals is based on the reactivity of calcite to HCl compared to dolomite.

Determination of facies was a primary focus of this study. Facies are defined as "a body of rock characterized by a particular combination of lithology, physical and biological structures that exhibit an aspect different from the bodies of rock above, below and laterally adjacent" (Walker, 2006). Six facies were identified from core data in the central Williston basin. Facies D is

17

subdivided into facies D1 and D2 based on sedimentary features and carbonate concentration. For the purpose of this study, shale was categorized as mudstone.

3.2 Subsurface Well Log Interpretation and Depositional Model

All available digital and raster copies of the petrophysical logs from 496 wells were loaded into the geological mapping and correlation software, IHS Petra©, and geologic information for the wells were entered into the appropriate zones in the database. Log data was obtained through the North Dakota Geological Survey's website: https://www.dmr.nd.gov-oilgas/. Although more wells exist in the study area, most operators begin logging at the top of the Charles salt which underlies the Tyler Formation, creating a relative lack of data compared to other petroleum plays underlying the Tyler Formation in the basin such as the Madison, Bakken, and Three Forks Formations.

Well logs were utilized to show cyclic deposition in wells away from the Curl 23-14 well. The Curl 23-14 well was chosen as the type well because of the modern log suite and core available for the well. Gamma ray (GR) logs were used primarily to depict cyclical deposition unless a combination of GR, Resistivity, Neutron, and Density logs were available at the Tyler Formation's interval.

The GR log measures the degree of natural radioactivity in the targeted interval of rock measured in API units. The API measurement comes from the addition of the three most common components in parts per million of naturally occurring radiation: potassium, thorium, and uranium (Asquith, et al., 2004). This is the most widely used log and is commonly run with an electrical tool which measures the natural resistivity of the formation, depending on the penetration of the tool. The GR log in this study is shown on a scale of 0 to 200 API.

The density log determines the formation density and estimates the formation porosity. The density tool emits gamma rays from a source at the base of the tool which penetrates into the surrounding rocks. The rays which are not absorbed into the formation are detected at the top of the tool. The quantity of gamma rays which arrive at the detector at the top of the tool is inversely

proportional to the electron density of the rock (Asquith, et al., 2004). This is then proportional to the rock density. The density and neutron log are both on the same scale of -0.10 to 0.30, indicating percentage of porosity.

The neutron log evaluates formation porosity. An apparent porosity value is given by measuring the density of neutrons from the formation to the tool (Asquith, et al., 2004). A pitfall of the neutron log is that the hydrogen content of the formation can force the neutron log to have incorrect values.

Tops were picked to correlate and show continuity of the cycles in the mid basin region. These tops were based on the high organic rich mudstones that normally read more than 200 API on the GR log and are characterized by much higher resistivity than the surrounding lithologies. These tops include the top of the Tyler Formation (PN-T) , cyclothem 1-3 (PS-(1-3)), channel sand top(PN-T_CHANNEL_SAND_TOP) and base (PN-T_CHANNEL_SAND_BASE) , Mississippian Big Snowy Group (M_BS), Mississippian Kibbey Lime (M-KL) and Mississippian Charles salt (M-Charles). The type log of the Tyler Formation used for this study is shown in Figure 1.2.

These tops were picked in all 496 wells, if present, and were used to create subsurface structure and isopach maps. Several north-south and east-west cross sections were constructed in order to visualize the subsurface structure and stratigraphic thickening or thinning for each interval in interest. The wells used in this project and cross section lines created for the study can be seen in Figure 3.1. For correlation purposes, facies were lumped together in the stratigraphic cross sections due to difficulty in depicting individual facies through the well log responses.
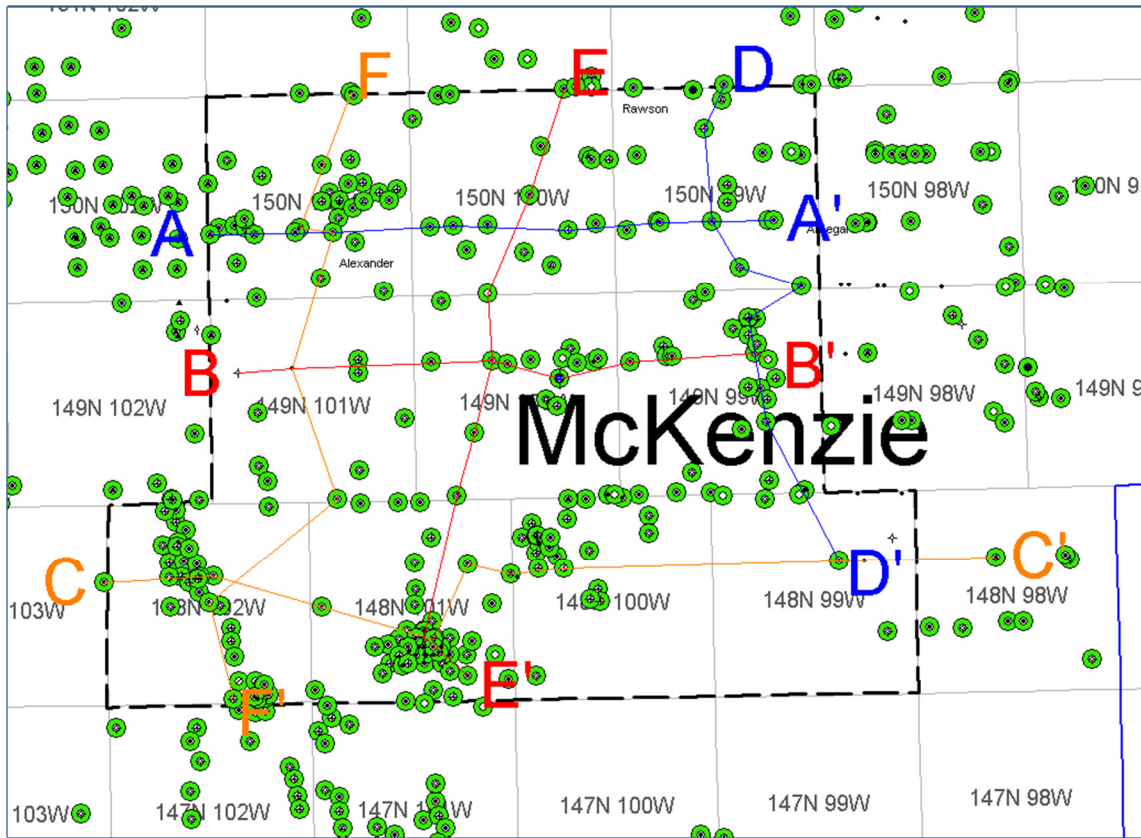
Figure 3.1 All wells and cross sections in the study area.

Digital and raster logs are highlighted in green. The study area is indicated by the dashed black line. Cross-section lines for A-F are indicated as well.

3.2.1 Construction of Cross Sections

Six structural cross sections across the study area, oriented north-south and east-west, were constructed to gain an understanding of the structural behavior of the Tyler Formation in the central Williston basin (Figure 3.1). Cross sections A-A', B-B', and C-C' have an east-west orientation in the study area (Figures 4.9- 4.11). Cross sections D-D', E-E', and F-F' have a north-south orientation in the study area (Figures 4.12- 4.14).

The same six structural cross sections were converted to stratigraphic cross sections for the study using the stratigraphic cross section tool in IHS PETRA©. The stratigraphic cross sections were created by taking the same structure cross sections and flattening on the top of the Tyler Formation (PN-T) picked throughout the study area. These stratigraphic cross sections were correlated with the facies to gain a basic understanding of the facies development within the Tyler Formation in the study area. These cross sections depict a change in deposition, thickness variations, and sediment variation in their lateral and vertical extents in the study area. Cross sections A-A', B-B', and C-C' have an east-west orientation in the study area (Figures 4.15- 4.17). Cross sections D-D', E-E', and F-F' have a north-south orientation in the study area (Figures 4.18- 4.20). Differentiation of the facies within the cyclothems was not possible because several of the facies are too thin for the resolution of the logging tool. Thus, they were lumped together and compared to the highly organic mudstone that was identified by (Nordeng & Nesheim, 2012).

3.2.2 Construction of Subsurface Maps

Subsurface structure maps were created utilizing the tops picked for the Tyler Formation and underlying strata. Structure maps were constructed from the top of the Tyler, Big Snowy Group, Kibbey Lime, and Charles Formations (Figures 4.21- 4.28). Each structure map has its own scale except for the structure maps of the three cyclothems and the top of the Tyler Formation. These were kept at the same scale to show a crude visualization of the progressive basin fill of the formation during deposition.

Isopach maps were constructed utilizing the tops picked within the Tyler Formation. The

isopach tool within IHS PETRA© calculated thicknesses within chosen tops and then that value was used for each well to map thickness of each interested zone. These isopach maps are found in Figures 4.29 to 4.33. The isopach maps of the three cyclothems were kept on a similar scale for comparison.

3.2.3 Depositional Model

The depositional model was constructed using the facies interpreted from the Curl 23-14 core. A paleogeographic reconstruction was created in the form of a block diagram depicting the Tyler Formation depositional environments. Major flooding surfaces were identified utilizing the organic-rich mudstone marker found in the GR logs and a basic sequence stratigraphic evaluation was implemented in order to better understand the control of eustasy on depositional environments.

3.3 Mercury Injection Porosimetry (MIP)

Seventeen intervals of porosity and five intervals of permeability measurements were provided by Whiting Oil and Gas Corporation. Porosity and permeability measurements were also made on two additional plugs that was taken from the core using the Mercury Injection Porosimetry (MIP) procedure created by Giesche (2006) and modified by Gao & Hu (2013). The core plugs were cut to a cube with dimensions no greater than 1.5 cm. These cubes were subjected to low-pressure and a high-pressure analysis. The low pressure analysis measures pore-throat diameters down to 300 μm. The high pressure analysis measures pore-throat diameters down to three nm and reach the highest pressure in step. Time to allow for equilibrium was fifty seconds before continuing to the next pressure level. Before measurements are made the samples were be evacuated to 50 μmHg (equivalent to 0.05 Torr or 6.7 Pa).

The porosity of these samples can be directly obtained through the MIP procedure's raw data. Permeability was calculated utilizing the KT method. Using the raw data from the MIP test, the inflection point from the cumulative intrusion curve will represent the threshold pressure P_t, and V_t, the volume at threshold pressure, is obtained directly from the cumulative intrusion curve

(Gao & Hu, 2013). In order to obtain L_{max}, the pore throat diameter at which hydraulic conductance is maximum, and V_{Lmax} the volume corresponding to L_{max}, V_t has to be subtracted from each cumulative intrusion volume V_c at each pressure step after P_t until the maximum pressure is reached (Gao & Hu, 2013). The net volume (V_c-V_t) multiplied by the diameter-cubed (up to 1.5 cm for diameter) for the corresponding pressure is plotted as function of pore-throat diameter. S(Lmax), the fraction of connected pore space composed of pore width size L_{max} and large, is calculated dividing the V_{Lmaxt} by $V_{tot,}$ which is found using the Cumulative intrusion vs. intrusion pressure plot (Gao & Hu, 2013). Knowing these variables, a calculation of permeability can be done by using the equation found in Figure 3.2.

A cross plot of porosity and permeability was created in order to determine the relationships within the potential reservoirs (Figure 4.35). The x-axis represents porosity values while the y-axis represents permeability values. Higher porosity and permeability values mean better reservoir quality. Each data point is categorized according to its facies in order to view reservoir quality trends within the facies.

$$k = \frac{1}{89}(L_{max})^2(L_{max}/L_c)\phi S(L_{max})$$

Figure 3.2 Permeability equation for use with MIP data.

Introduced by Kats and Thompson (1986, 1987).

Chapter 4

Results and Discussion

4.1 Facies Interpretation and Core Description

I described the core of the Curl 23-14 well, which is stored at the North Dakota

Geological Survey Core Library in Grand Forks, North Dakota. Figures 4.1-4.7 show photographs

of the facies identified in the Tyler Formation. Figures 4.8-4.9 are the core description and legend,

which illustrate the facies, lithology, bioturbation intensity, porosity, and permeability at depth.

4.1.1 Facies A- Organic-Rich, Whole Fossil Pyritic Black Mudstone

4.1.1.1 Description

Facies A is characterized by dark gray to black, carbonaceous, and occasionally

calcareous mudstone (is fissile). In this interval the pyrite nodules are of silt to medium sand size.

The pyrite is usually disseminated throughout the mudstone, but does occasionally occur as thin

laminations (Figure 4.1). Fractures in the mudstone are generally cemented by calcite or pyrite of

fine sand size. Lenses and nodules of carbonate mudstones are scattered throughout this

interval. Benthic fossil fragments are common but are difficult to identify in certain intervals

(Figure 4.1). These benthic fossil fragments include crinoids, ostracods, and skeletal shell

fragments which are commonly replaced by pyrite (Figure 4.1). Algal laminations occur above the

transgressive limestone and grade upward from coarse to fine. Pelagic fossils such as conodonts,

fish debris, radiolarians, and ammonoids might be present in Facies A, but were not identified in

the core. Locally developed black mudstone occurs directly above Facies E before the limestone

deposition. Sparse organics and minor bioturbation are found in this mudstone.

4.1.1.2 Interpretation

Facies A is representative of marine shelf to restricted basin black mudstone.

Preservation of organic material and laminations indicate an environment with a stratified water

column, which is possibly slightly anoxic. The algal laminations could be produced from algal

blooms occurring during deposition. The abundant benthic skeletal fragments in certain intervals

indicates organic overload in the environment originating from algal blooms (Pederson, 1990). This oxygen-deprived environment in the Williston basin would have been caused by a restricted basin coupled with high organic production. Poor water circulation cannot supply the oxygen demanded by decomposing organisms. This process creates an anoxic environment found in the Tyler Sea (Tourtelot, 1979). Pyrite is an indicator of bacterial decomposition of organic material during deposition in a reducing environment, which produces pyrite during diagenesis if the zone has detrital iron minerals (Berner, 1984). The thin carbonate intervals indicate minor fluctuations in sea level; enough to allow carbonate precipitation.

The near shore black mudstone found above Facies E is not laterally extensive and contains a sparse benthic fauna characteristic of restricted near shore to shoreline environments (Bisnett & Heckel, 1996). Formation of the black mudstone was caused by preexisting organic material from the underlying peat or by local high organic productivity during an early transgression (Pederson, 1990). The depositional environment for the mudstone was described as dysoxic shallow-marine bay or lagoonal (Pederson, 1990). Fractures in this facies could indicate possible overpressure in the formation and migration of hydrocarbons laterally or up section depending on connectivity, unless the fractures were sealed by pyrite or calcite before pyrolysis.
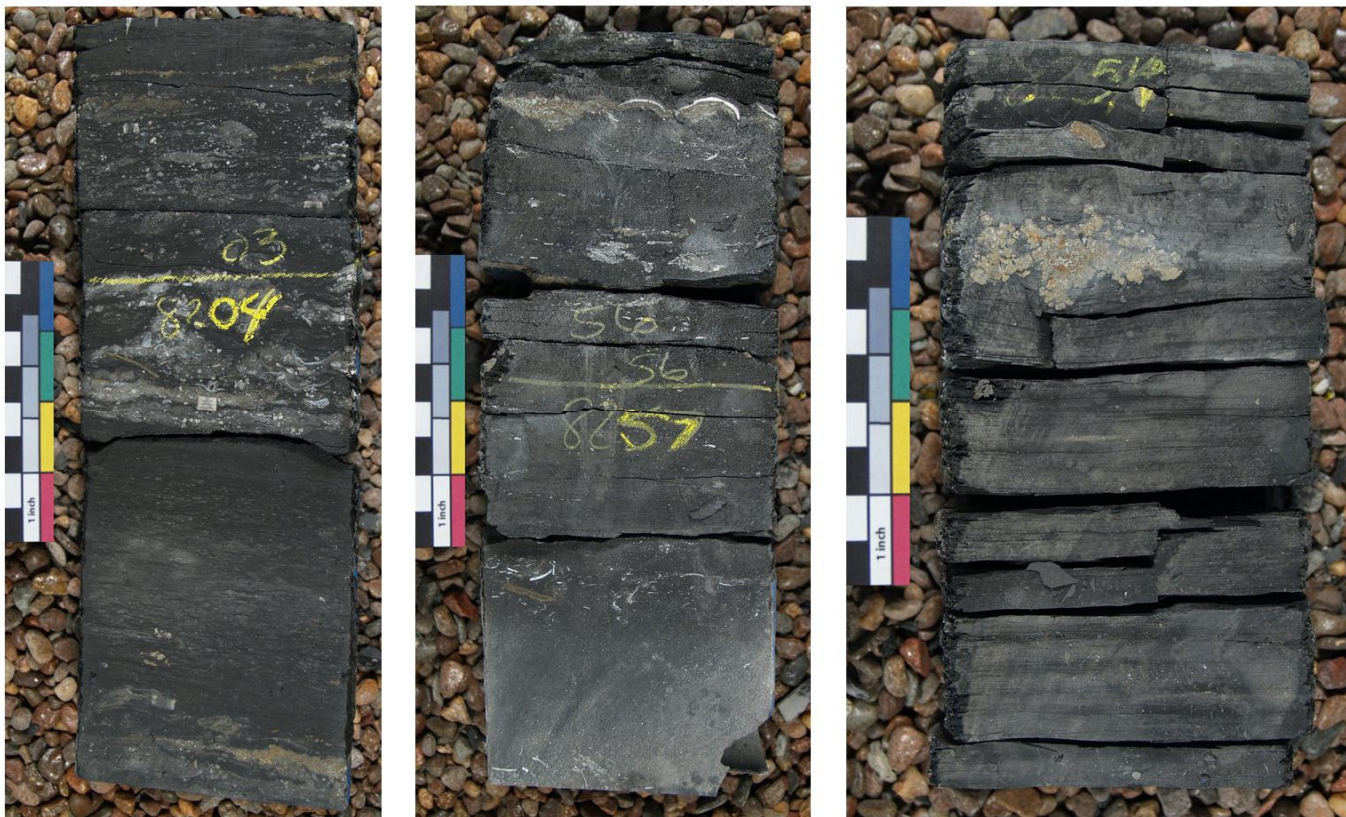
Figure 4.1 Facies A of the Tyler Formation with 1 inch scale.

Photographs were taken by the Wilson M. Laird Core and Sample Library.

4.1.2 Facies B- Gray to Dark Gray Muddy Limestone

4.1.2.1 Description

Facies B consists of a muddy wackestone that contains occasional shell fragments and/or Ostracods as seen in Figure 4.2 (photographs 1, 3, and 4). The majority of these have been pyritized. This facies has extremely strong effervesce due to the dominating presence of calcite. These thin beds are found underlying, overlying, and interbedded with the dark gray mudstone of facies A. Porosity is intergranular with calcite and, occasionally, pyrite as the cements. An abrupt but conformable basal contact is commonly present between facies A and facies B as seen in Figure 4.2 (photographs 1 and 4), but a graded boundary may also occur. The top boundary tends to grade from a limestone to calcareous mudstone then finally into the dark gray mudstone found in facies A, depicted in photograph 2 (Figure 4.2). Photograph 3 shows a basal contact which grades from calcareous mudstone into Facies B limestone. Effervescence differences between the two facies was enough to show a grading in the amount of calcareous material present. Laminations can be found in the uppermost example of facies B in the red beds of the core. This facies ranges in thickness from four inches to three feet making it difficult to be picked up with wireline logging tools. When thick enough to be detected by the logging tools, a slight decrease in the GR API is seen. The top foot of the core contains a red bed interval consisting of Facies B and a small interval of Facies A. Within the red bed interval lies calcitic cone-in-cone structures.

4.1.2.2 Interpretation

Limestone beds overlying the coal beds are typically deposited during transgression and are thin, possibly due to the poor preservation of lime mud due to low pH conditions, or because calcareous algae were unable to survive on the surface of decaying peat (Bisnett & Heckel, 1996). This phenomenon was seen in the Illinois basin and may occur in the Tyler Formation as well. Regressive limestone in the Tyler Formation shows subaerial exposure and could be associated with caliche, which is also typical of midcontinent cyclothems during the

Pennsylvanian (Watney, 1980). This was seen in two zones where the regressive limestone may grade into the caliche facies, known as facies D1. These regressive limestone are capped by blocky mudstones, identified as paleosol from Facies D2 (Bisnett & Heckel, 1996).

The red beds dominated by Facies B could have possibly been caused by pyrite oxidation. This type of oxidation is an excellent example of telodiagenesis, or late diagenesis (Mücke, 1994). These red beds are typically linked to sub-aerial exposure and surface weathering. The cone-in-cone structure found at the top of the core could possibly have been caused by burial-induced pressure solution and clay layers which remain as insoluble residues (Fairbridge & Rampino, 2003).

4.1.3 Facies C- Terrestrial to Near Shore Brown/Tan Mudstone

4.1.3.1 Description

These mudstone are commonly dark gray to brown in color, are extremely fissile, and more brittle than its counterpart in Facies A. Very fine-grained pyrite nodules are found near base of the facies. Nodular and disseminated pyrite increased in size towards the top and can be easily seen in photograph 1 from Figure 4.3. The lowest extent of calcrete formation can be seen in this facies and is shown in Figure 4.3 photograph 1. Mild effervescence was seen in this mudstone. The contact between the lighter mudstone and underlying black mudstone is gradational (Figure 4.3 photograph 2).

4.1.3.2 Interpretation

Facies C represents mudstone that are sparsely fossiliferous prodeltaic mudstone deposited during low sea level stands. The increase in brittleness in this facies may indicate a higher percentage of silica and/or calcite within the mudstone compared to Facies A. This facies typically grades into channel sands or paleosols following the regressive limestone from Facies B (Heckel, 2008). The light tan coloring seen at depths from 8242.5-8244 feet is most likely caused by leaching of carbonate material from the caliche overlying the mudstone, and the commencement of calcrete formation (Figure 4.3).

4.1.4 Facies D1.Bioturbated Tan /Brown Caliche

4.1.4.1 Description

Facies D1 represents bioturbated tan to brown caliche. Paleosol was deposited between the limestone nodules. A strong effervesce is present on the nodules and none for the clay in between. Rootlets are found bored along the limestone karst and paleosol (Figure 4.4). Slickenslides are present in the paleosol matrix. The contact with the underlying mudstone and overlying paleosol is gradational. Slight gradation in the calcrete sizes can be seen in Figure 4.4, photograph 3. Calcretes tend to be largest near the base and become smaller going toward the top.

4.1.4.2 Interpretation

Facies D1 represents caliche deposited below the paleosol horizon or a previous carbonate bed which was sub-aerially exposed and weathered. This caliche was deposited when the paleosol horizon was located in the vadose zone and water flowed through the horizon freely. Carbonate minerals in solution precipitated and formed carbonate nodules, creating a horizon of caliche. Micro-organisms such as algae, fungi, bacteria, or actinomycete in the vadose zone most likely aided in the diagenesis of this facies (Jones, 1986). Recognition of these organisms would be difficult due to the high amount of calcification. Another possibility for the origin of the caliche is a carbonate bed that was sub-aerially exposed and weathered by meteoric water. The high amount of clay and calcitic cement would make this zone's permeability extremely low for a reservoir. With the minimal amount of organics it is also a poor source rock.

Figure 4.2 Facies B in the Tyler Formation with 1 inch scale.

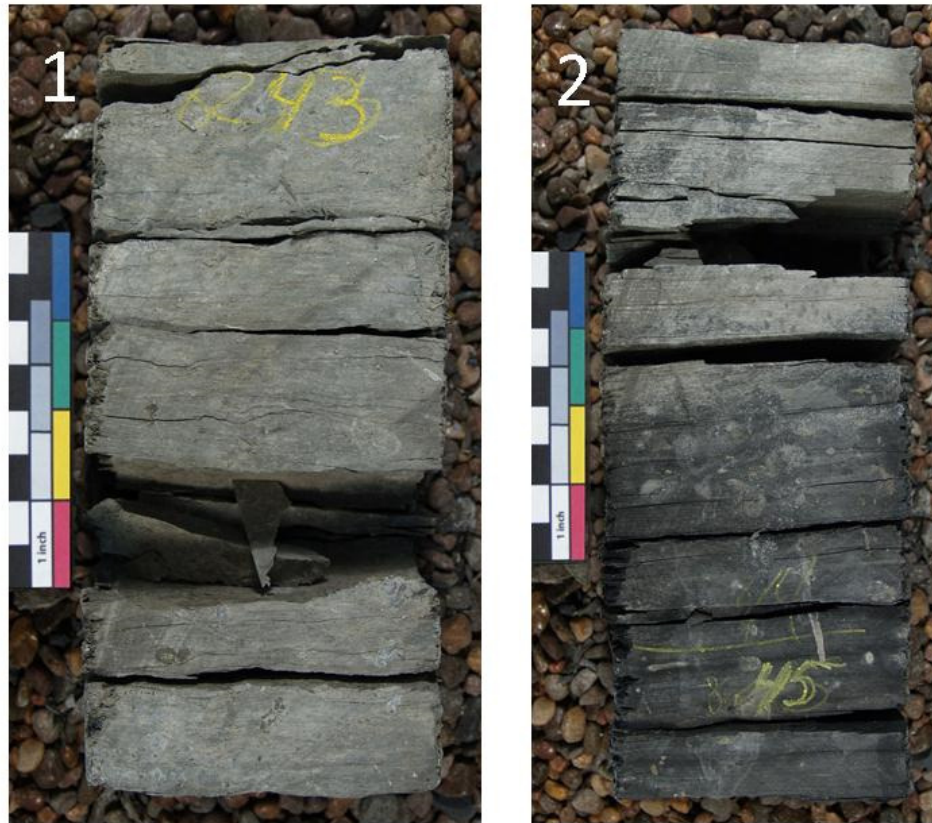Photographs were taken by the Wilson M. Laird Core and Sample Library.

Figure 4.3 Facies C of the Tyler Formation with 1 inch scale.

Photographs were taken by the Wilson M. Laird Core and Sample Library.
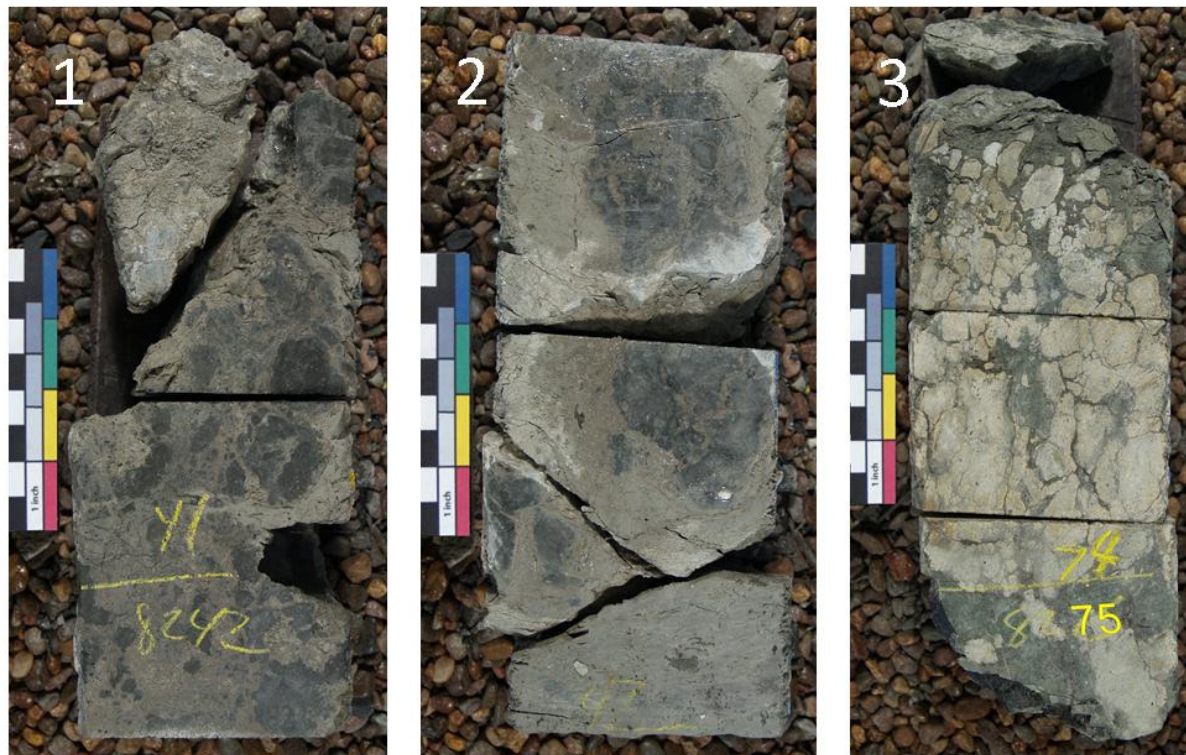
Figure 4.4 Facies D1 of the Tyler Formation with 1 inch scale.

Photographs were taken by the Wilson M. Laird Core and Sample Library.

4.1.5 Facies D2 Gleyed, Carbonaceous, Calcic, Vertisol

4.1.5.1 Description

This facies has the characteristic of poor to moderate layering due to pedoturbation. Slickenslides are prominent in this facies along with bioturbation from roots. Dark brown laminations were observed due to organic material accumulation (Figure 4.5, photographs 1-3). The facies also has calcretes; shown in Figure 4.5 photographs 1-3, earning the calcic modifier from Mack et al. (1993). Scattered carbonate nodules and tubules indicate a stage II morphology according to a Gile et al. (1966) (Figure 4.5). This facies is typically overlain by coal in response to the early stage of sea level rise. The contact between the overlying coal is abrupt while the contact with the underlying caliche is gradual, as shown in Figure 4.5 (photographs 2-3).

4.1.5.2 Interpretation

Facies D2 represents a paleosol deposited in a near-marine deltaic flood plain environment. Slickenslides were caused by shrinkage and swelling of expandable clays found within the paleosols (Mack, et al., 1993). The calcretes formed when the paleosol was beneath the water table; carbonate minerals were in solution and precipitated in the soil. Periodic waterlogging is evident due to the drab colors of the paleosol and presence of very-fine grained pyrite crystals. Organic material accumulations in the facies are remnants of the deltaic environment during the early Pennsylvanian. With the high clay content this facies has low potential as a reservoir or seal, and a poor source rock due to the insufficient amount of organic material.
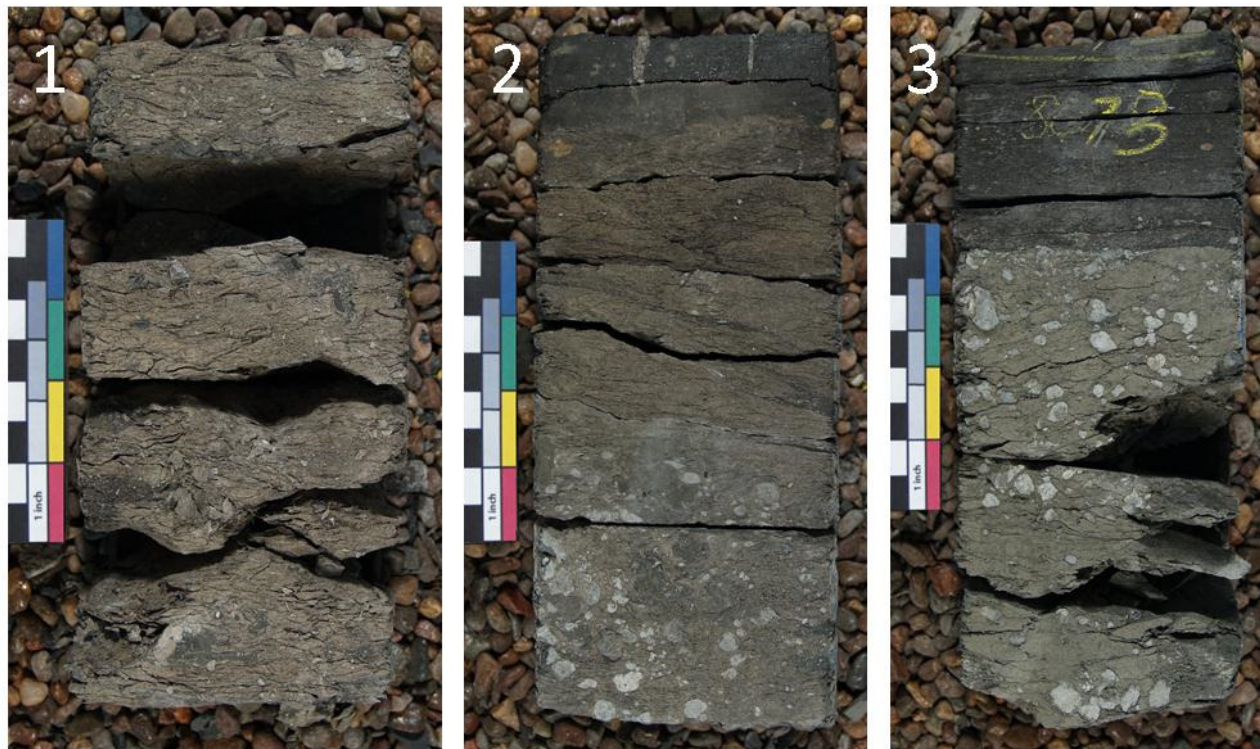
Figure 4.5 Facies D2 of the Tyler Formation with a 1 inch scale.

Photographs were taken by the Wilson M. Laird Core and Sample Library.

4.1.6 Facies E. Bioturbated Black Bituminous Coal

4.1.6.1 Description

This facies is highly bioturbated and contains evidence of roots and rootlets (Figure 4.6, photographs 2-3). It is generally very thin in the study area, reaching a maximum thickness of 8.5 inches (~22 cm). According to the Glossary of the American Geological Institute (bates and Johnson, 1984), a coal is "a readily combustible rock containing more than 50% by weight, and more than 70% by volume of carbonaceous material formed from compaction and induration of variously altered plant remains…' Vertical features in the coal are present, produced by large root systems. Large concentrations of pyrite are present in the coal, seen in Figure 4.6 photograph 1. Portions of this interval alternate from high to dull luster and leave black dust on fingers upon touch. The contact between the overlying black mudstone and underlying paleosol is sharp (Figure 4.6 photographs 1-3).

4.1.6.2 Interpretation

Facies E consists of black bioturbated coal derived from peat forming in low areas during early stages of sea-level rise. Fresh water run off was ponded to form swamps on low relief surfaces. This facies subsequently migrated up-shelf during the marine transgression (Heckel, 1996). Coal can be referred to as a Histosol in a paleosol regime due to coal forming in a waterlogged surface horizon e.g., Mack et al. (1993). The alternation between high to dull luster is indicative of Bituminous to Anthrathitic coal. The thick and elongate vertical roots in the coal are remnants of the Carboniferous swamplands. The presence of pyrite in the coal indicates that the depositional environment was sub-aqueous occasionally, if not dominantly. Deposition of coal is generally found to indicate the beginning of a transgressive systems tract (Boggs, 2005). Type III hydrocarbon (gas prone hydrocarbon) is produced from this interval due to the high amount of lignin in the coal, also visible in the core.
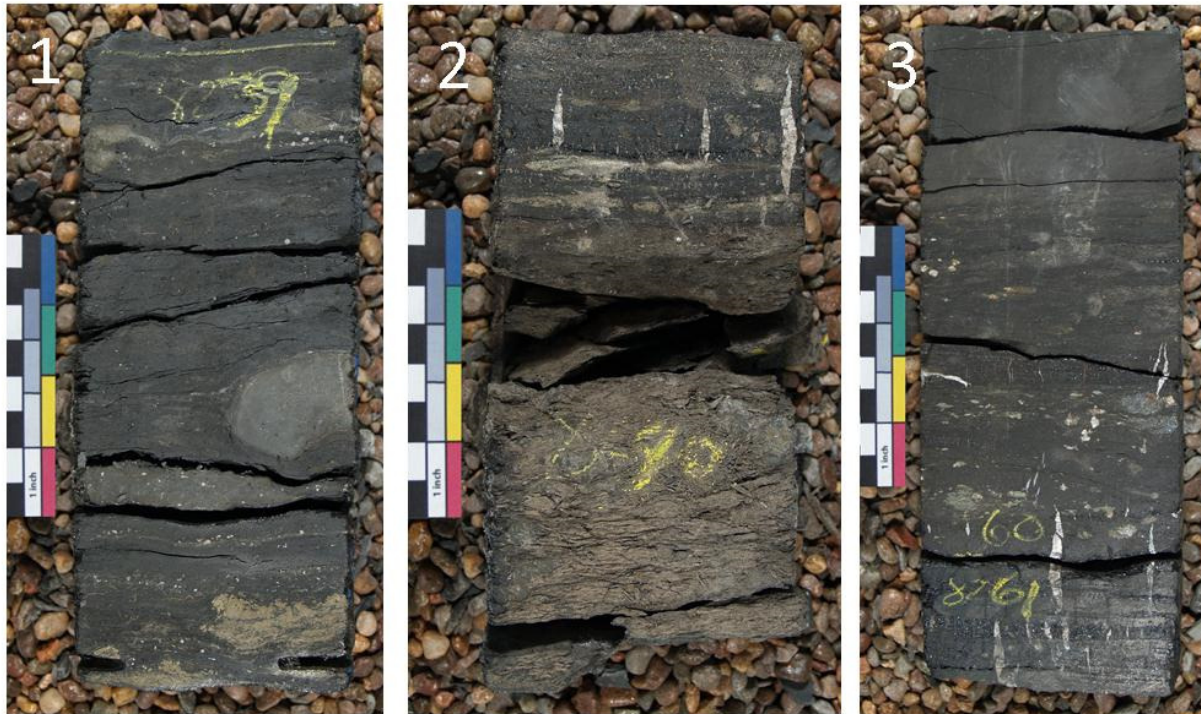
Figure 4.6 Facies E of the Tyler Formation with a 1 inch scale.

Photographs were taken by the Wilson M. Laird Core and Sample Library.
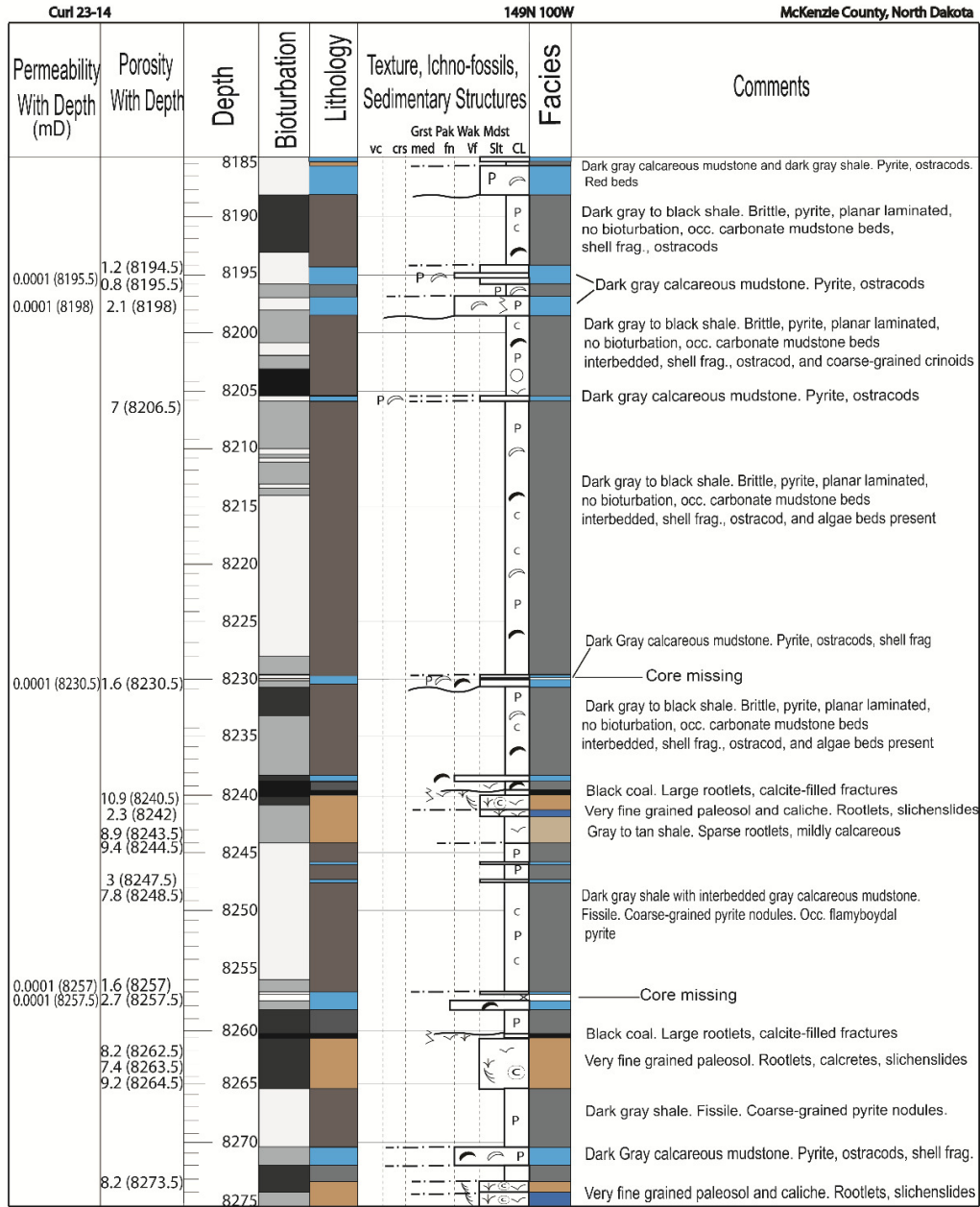
4.1.7 Graphical summary of core facies

Figure 4.7 Curl 23-14 core descriptions.

Associated rock characteristic values at depth.

Core Description Legend
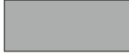
Lithology

Siltstone	Coal	Limestone	Mudstone

Sedimentary Structures

Plant remains — Calcretes — Shell fragments — Crinoid fragments — Ostracod remains

Bioturbation — Vertical fracture — Horizontal fracture — Carbonate lense

Pyrite — Slichenslides — Sharp, Irregular contact — Gradational contact

Bioturbation

Abundant	Common	Present	Rare

Colored Facies Legend

Facies E. Bioturbated black bituminous coal

Facies D2. Gleyed, carbonaceous calic, vertisol

Facies D1. Bioturbated brown/tan caliche

Facies C. Gray-tan shale

Facies B. Gray muddy limestone

Facies A. Organic rich pyritic black shale

Figure 4.8 Curl 23-14 core description legend.

4.2 Structural Cross Sections

The structural cross sections document the northeast dip of the Tyler Formation in the basin with the depocenter being near the far east-northeast corner of the study area. No major structural features such as faults, are indicated through the structural cross sections with exception of the Red Wing Creek structure (Figure 4.13). The Tyler Formation dips approximately 13 feet per mile (0.14° dip) and steadily decreases heading to the east to about 12.7 feet per mile (0.1381° dip) in the study area.

Cross sections A-C (Figures 4.9-4.11) show a dip towards the basin from west to east. Cross sections D-F (Figures 4.12-4.14) do not show a decline in dip because of their orientation along strike. In cross section E-E' (Figure 4.13) the Red Wing Creek structure is shown. About 1,650 feet of uplift is shown in the center the astrobleme in the True Oil LLC BN 21-27 well. The Tyler Formation was decimated in the impact, thus no tops were picked for the wells in the central peak (Koeberl, et al., 1996). The True Oil LLC BN 32-35 well is located in the concentric bowl surrounding the central uplift due to its lower elevation compared to the uplift and also to the Tyler Formation situated away from the astrobleme.

These cross sections also depict a different sequence of deposition from the cyclothems in the Tyler Formation. The terrestrial-marine cyclical deposition ceases and a period of marine mudstone, limestone, and submarine sand deposition begins, following a large transgressive event. This interval is called the upper Tyler Formation in this study. The cyclothems' well log response studied in the core does not match the lithology/facies of the upper Tyler Formation in the cross sections.

Figure 4.9 Structural cross-section of section line A-A'.

Location of cross section is shown in Figure 3.1. The GR log is shaded in from yellow (0 to 20 API) to black (greater than 150 API), having intermediate colors in between. The top of the Tyler Formation, cyclothems at base of the Tyler Formation are colored red and blue. The Kibbey Lime and Charles Salt tops are colored light blue.
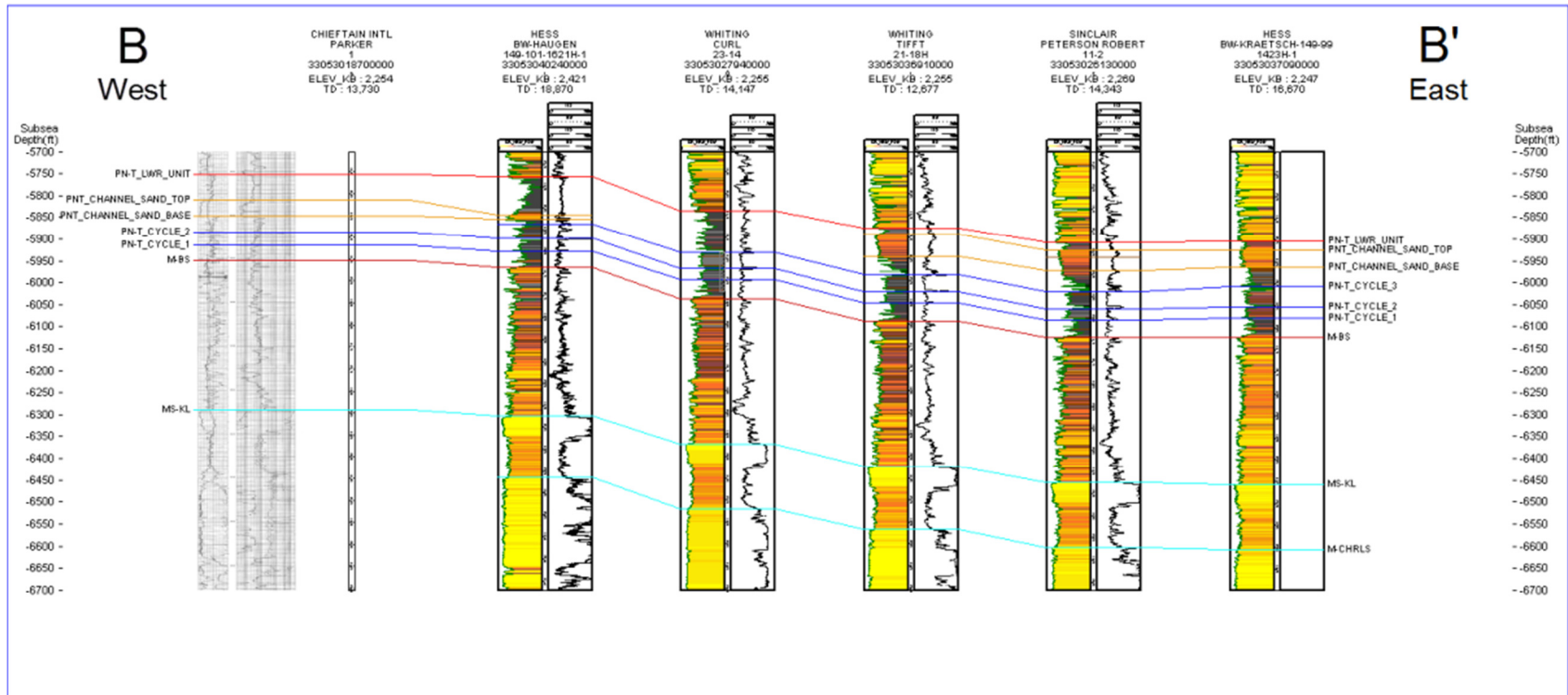
Figure 4.10 Structural cross-section of section line B-B'.

Location of cross section is shown in Figure 3.1. The GR log is shaded in from yellow (0 to 20 API) to black (greater than 150 API), having intermediate colors in between. The top of the Tyler Formation, cyclothems at base of the Tyler Formation are colored red and blue. The Kibbey Lime and Charles Salt tops are colored light blue.
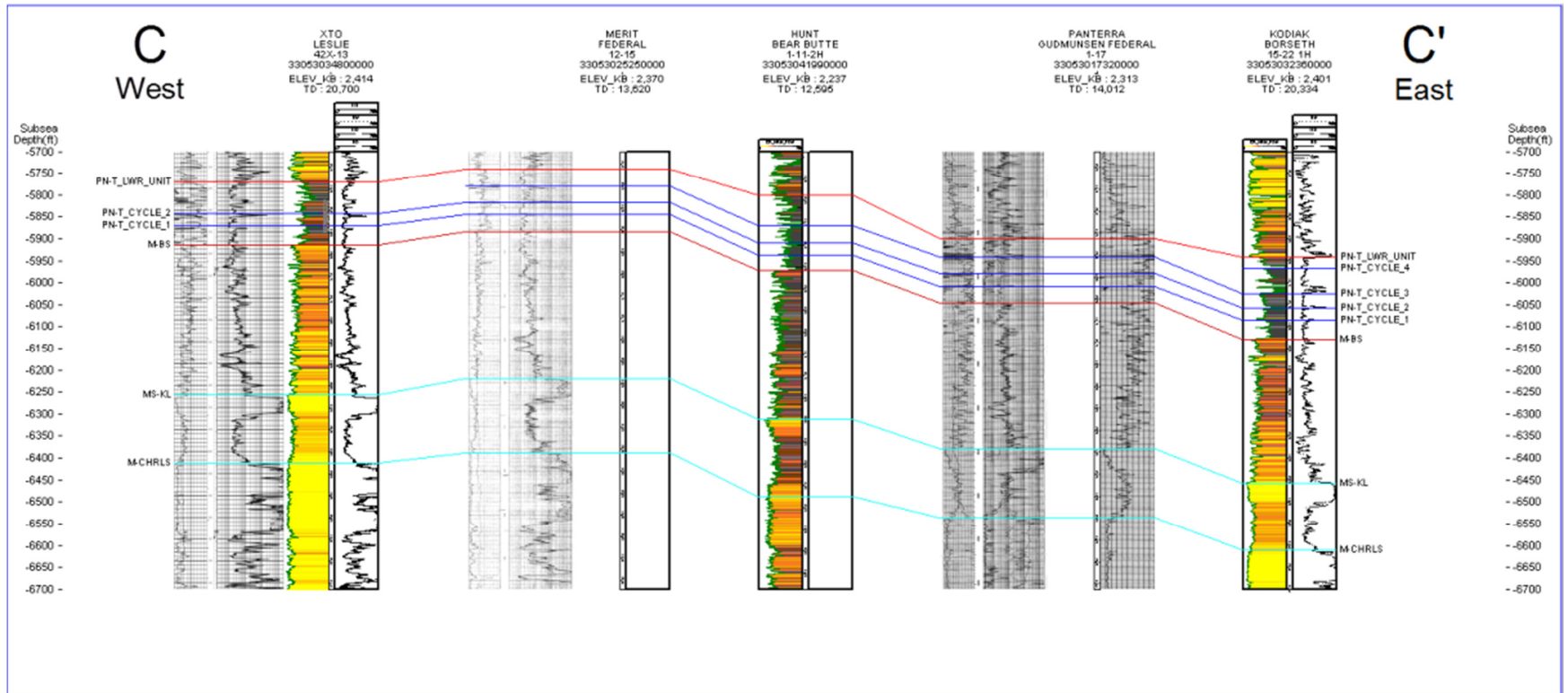
Figure 4.11 Structural cross-section of section line C-C'.

Location of cross section is shown in Figure 3.1. The GR log is shaded in from yellow (0 to 20 API) to black (greater than 150 API), having intermediate colors in between. The top of the Tyler Formation, cyclothems at base of the Tyler Formation are colored red and blue. The Kibbey Lime and Charles Salt tops are colored light blue.
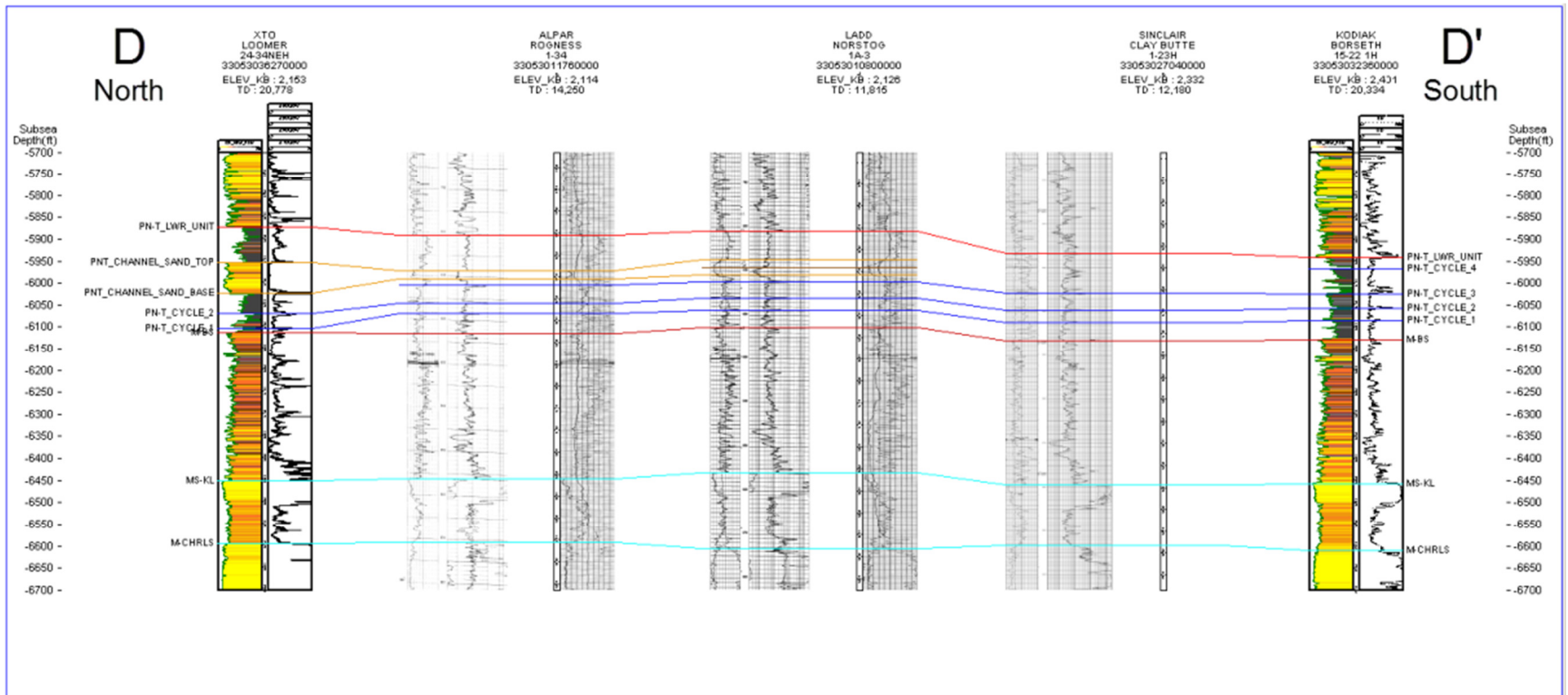
Figure 4.12 Structural cross-section of section line D-D'.

Location of cross section is shown in Figure 3.1. The GR log is shaded in from yellow (0 to 20 API) to black (greater than 150 API), having intermediate colors in between. The top of the Tyler Formation, cyclothems at base of the Tyler Formation are colored red and blue. The Kibbey Lime and Charles Salt tops are colored light blue.
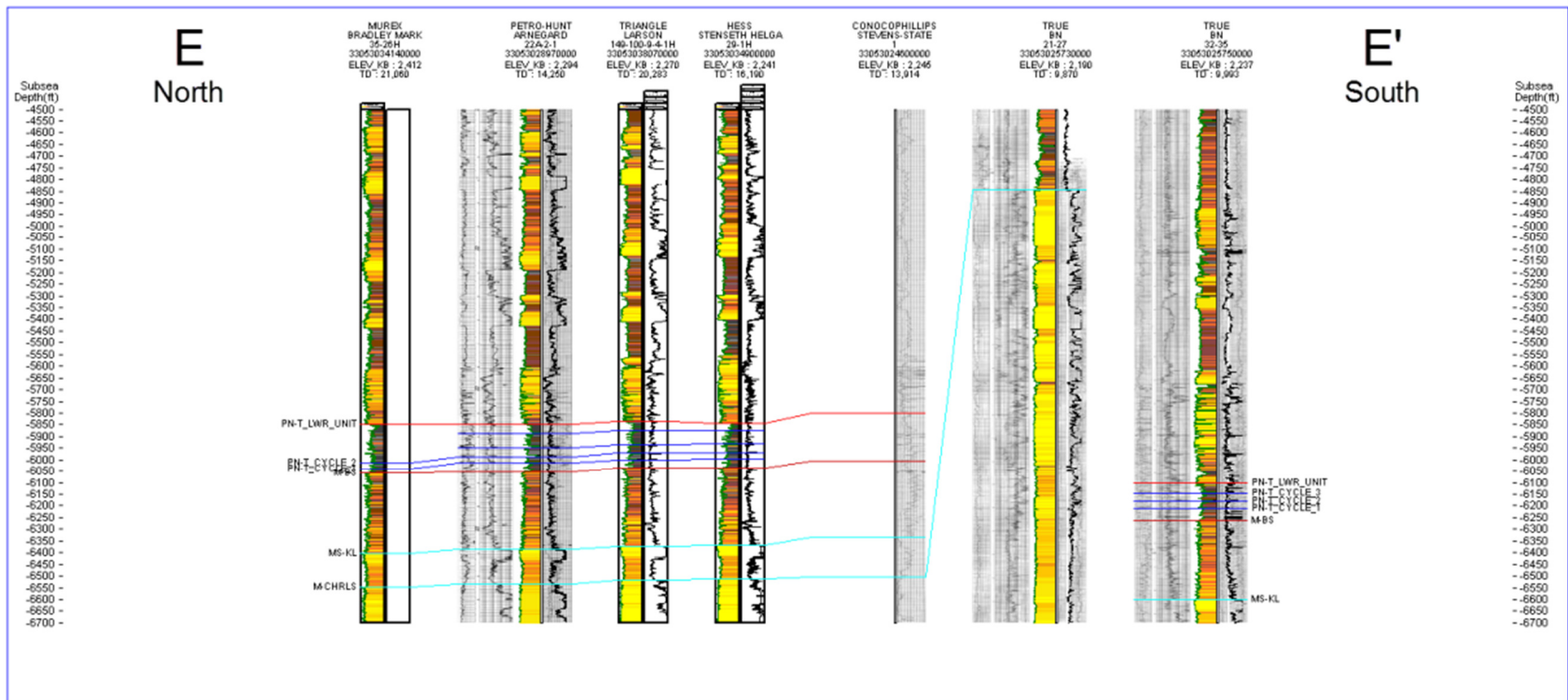
Figure 4.13 Structural cross-section of section line E-E'.

Location of cross section is shown in Figure 3.1. The GR log is shaded in from yellow (0 to 20 API) to black (greater than 150 API), having intermediate colors in between. The top of the Tyler Formation, cyclothems at base of the Tyler Formation are colored red and blue. The Kibbey Lime and Charles Salt tops are colored light blue.

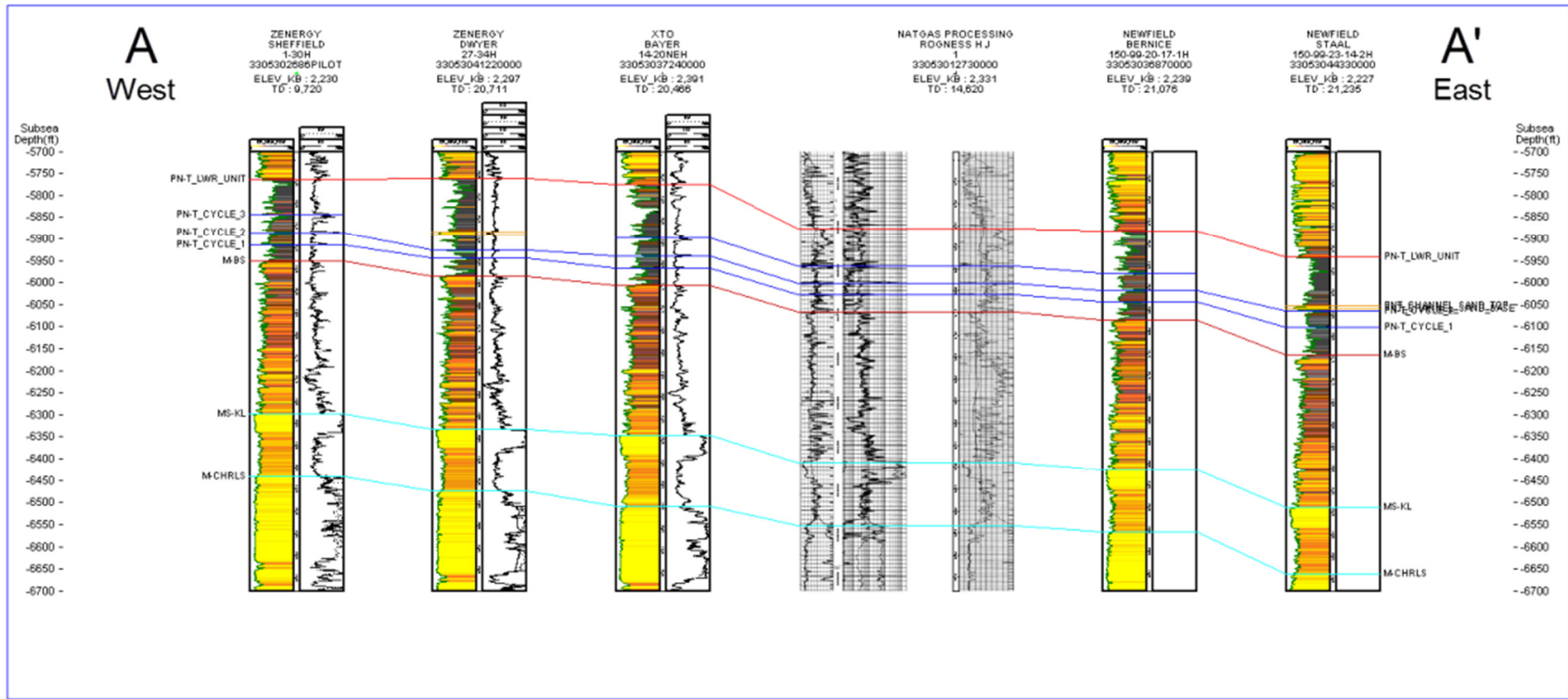44

Figure 4.14 Structural cross-section of section line F-F'.

Location of cross section is shown in Figure 3.1. The GR log is shaded in from yellow (0 to 20 API) to black (greater than 150 API), having intermediate colors in between. The top of the Tyler Formation, cyclothems at base of the Tyler Formation are colored red and blue. The Kibbey Lime and Charles Salt tops are colored light blue.

4.3 Stratigraphic Cross Sections

Each mudstone interval in the Tyler Formation has a unique thickness. The mudstone located in the first cyclothem has an average thickness of 5 feet (1.5 meters) and shows slight thinning from north to south and west to east. The mudstone in the second cyclothem has slight thinning from north to south and slightly thickens in the north of the study area as shown in cross section A-A' (Figure 4.15). It has an average thickness of 10 feet (3 meters). This interval along with the third mudstone interval was eroded by the upper Tyler Formation sands overlying the cyclothems in the Tyler Formation in portions of the study area. This can be seen in cross section A-A' (Figure 4.15). The mudstone interval deposited in the third cyclothem has an average thickness of 14 feet (4.3 meters). It shows a variation in thicknesses throughout the study area. In the west and central portion of the study area there is a general thinning of the interval while towards the east there is a thickening. This interval is commonly eroded due to the overlying upper Tyler Formation and its associated sands. This is seen in cross sections A-A', B-B', D-D', and F-F'; figures 4.15, 4.16, 4.18, and 4.20, accordingly.

The lower-most cyclothem in the Tyler Formation has an average thickness of 35 feet (10.7 meters). There is a variation in thickness throughout the study area for this interval. Furthermore, deposition appears to have taken place above an erosional surface (sequence boundary) as indicated by the Big Snowy Group structure map (Figure 4.24) and wireline logs. A general trend of thinning occurs in the central and south portion of the study area in the west to east direction. A more uniform thickness is seen from north to south with slight thickening in certain areas.

The second cyclothem is thinner than the others and has an average thickness of 18 feet (5.5 meters). This cyclothem has a uniform thickness from west to east while thickening slightly between the north and central portion of the study area as seen in cross sections D-D' and E-E' (Figures 4.18-4.19). In these cross sections the second cyclothem is shown to reach further into

46

the basin. Because the greatest thickness is in the northernmost wells, this cyclothem probably extended furthest out towards the depocenter.

The uppermost cyclothem in the Tyler Formation has an average thickness of 30 feet (9.1 meters) and shows a uniform thickness with occasional local thickening. This cyclothem is also commonly incised by the upper Tyler Formation sands which overlie it. This is seen in all the cross sections with exception to C-C' (Figures 4.15-4.20).

The upper Tyler Formation overlying the cyclothems has an extremely variable thickness in the study area. From west to east this depositional package does not show any trend of variable thickness. This behavior is shown in cross sections A-A', B-B', and C-C' (Figures 4.15-4.17). Thickness variation is seen clearly from north to south as this depositional package thins up the basin shelf. There is a clear trend of thinning towards the south for this system, shown in cross sections D-D', E-E', and F-F' (Figures 4.18-4.20). The sub-marine sands in this system occasionally eroded through the third and second cyclothem. Their thicknesses change significantly going from a few feet to up to sixty feet thick in the north-eastern townships.
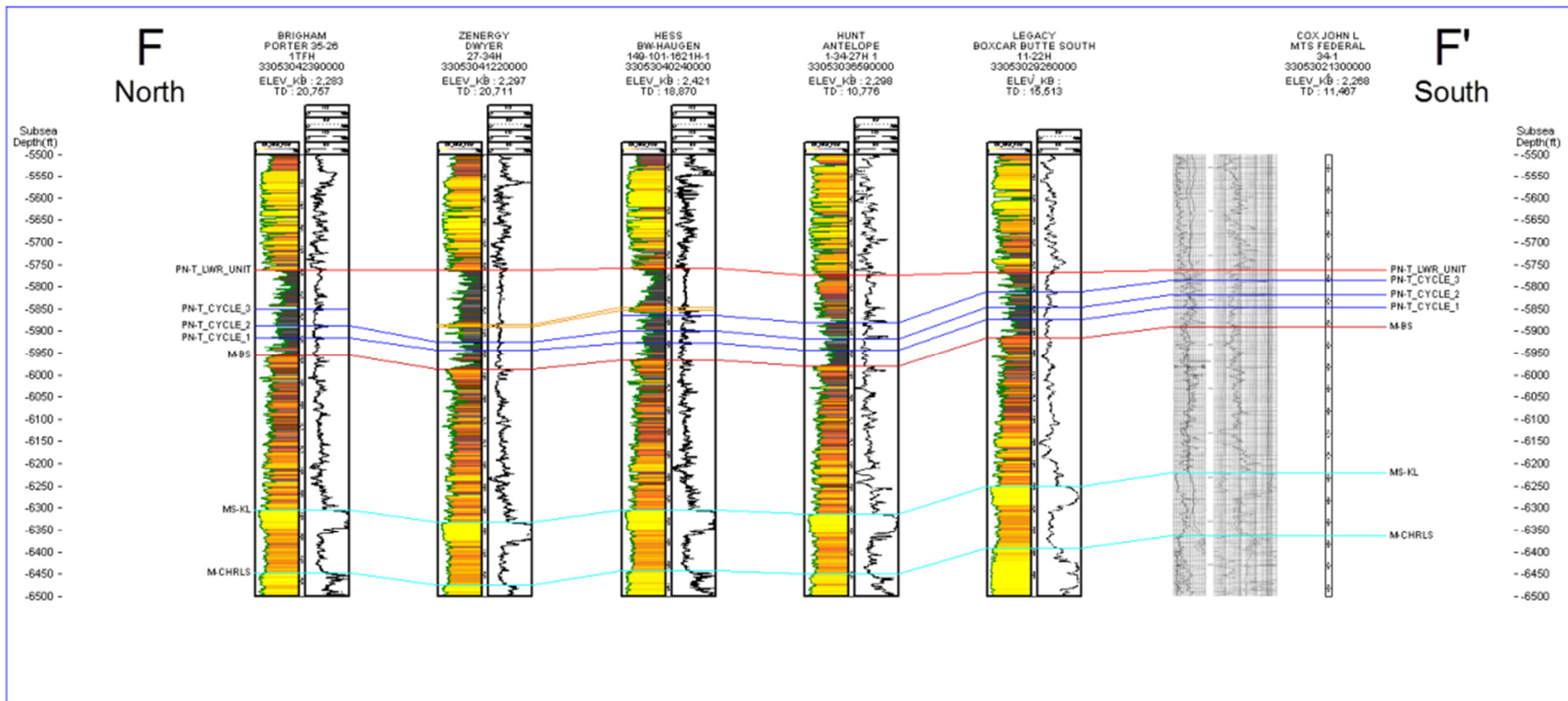
Figure 4.15 Stratigraphic cross-section of section line A-A'.

Location of cross section is shown in Figure 3.1. The GR log is shaded in from yellow (0 to 20 API) to black (greater than 150 API), having intermediate colors in between. The top of the Tyler Formation, cyclothems at base of the Tyler Formation are colored red and blue. The upper Tyler Formation interval is shaded in cyan and the non-organic rich black mudstone intervals of the cyclothems are shaded in neon green. The organic rich black mudstone intervals are shaded in black, and the sandstones in yellow.
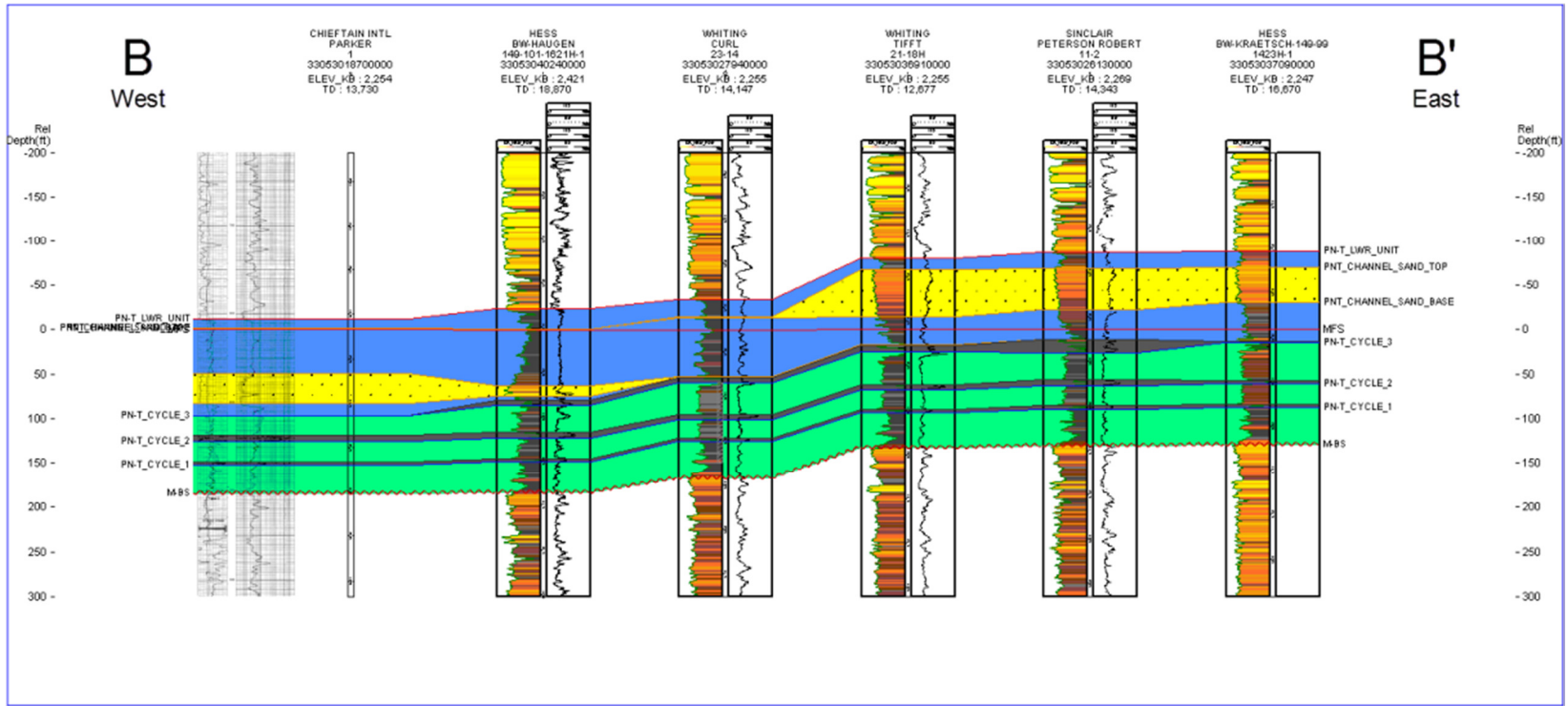
Figure 4.16 Stratigraphic cross-section of section line B-B'.

Location of cross section is shown in Figure 3.1. The GR log is shaded in from yellow (0 to 20 API) to black (greater than 150 API), having intermediate colors in between. The top of the Tyler Formation, cyclothems at base of the Tyler Formation are colored red and blue. The upper Tyler Formation is shaded in cyan and the non-organic rich black mudstone intervals of the cyclothems are shaded in neon green. The organic rich black mudstone intervals are shaded in black, and the sandstones in yellow.
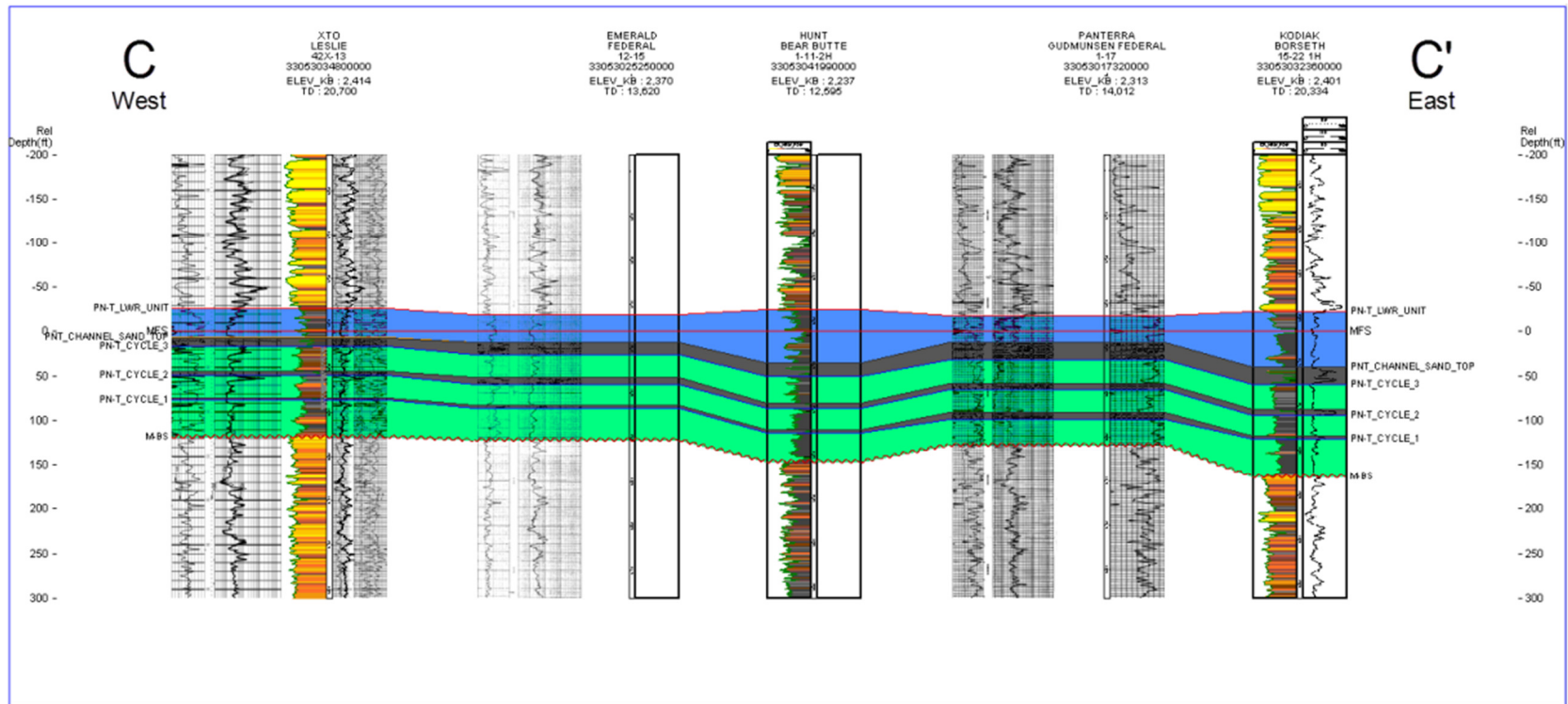
Figure 4.17 Stratigraphic cross-section of section line C-C'.

Location of cross section is shown in Figure 3.1. The GR log is shaded in from yellow (0 to 20 API) to black (greater than 150 API), having intermediate colors in between. The top of the Tyler Formation, cyclothems at base of the Tyler Formation are colored red and blue. The upper Tyler Formation is shaded in cyan and the non-organic rich black mudstone intervals of the cyclothems are shaded in neon green. The organic rich black mudstone intervals are shaded in black.
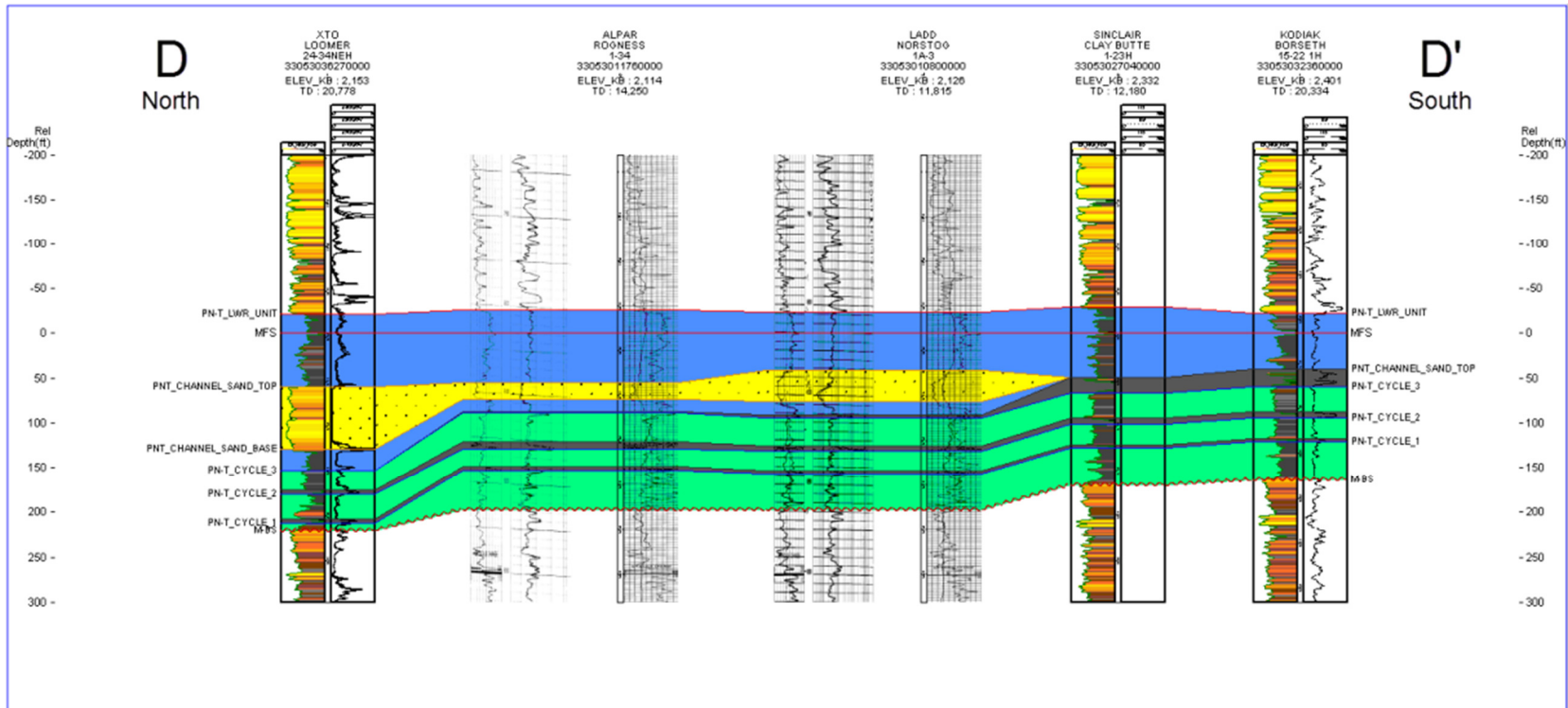
Figure 4.18 Stratigraphic cross-section of section line D-D'.

Location of cross section is shown in Figure 3.1. The GR log is shaded in from yellow (0 to 20 API) to black (greater than 150 API), having intermediate colors in between. The top of the Tyler Formation, cyclothems at base of the Tyler Formation are colored red and blue. The upper Tyler Formation is shaded in cyan and the non-organic rich black mudstone intervals of the cyclothems are shaded in neon green. The organic rich black mudstone intervals are shaded in black, and the sandstones in yellow.
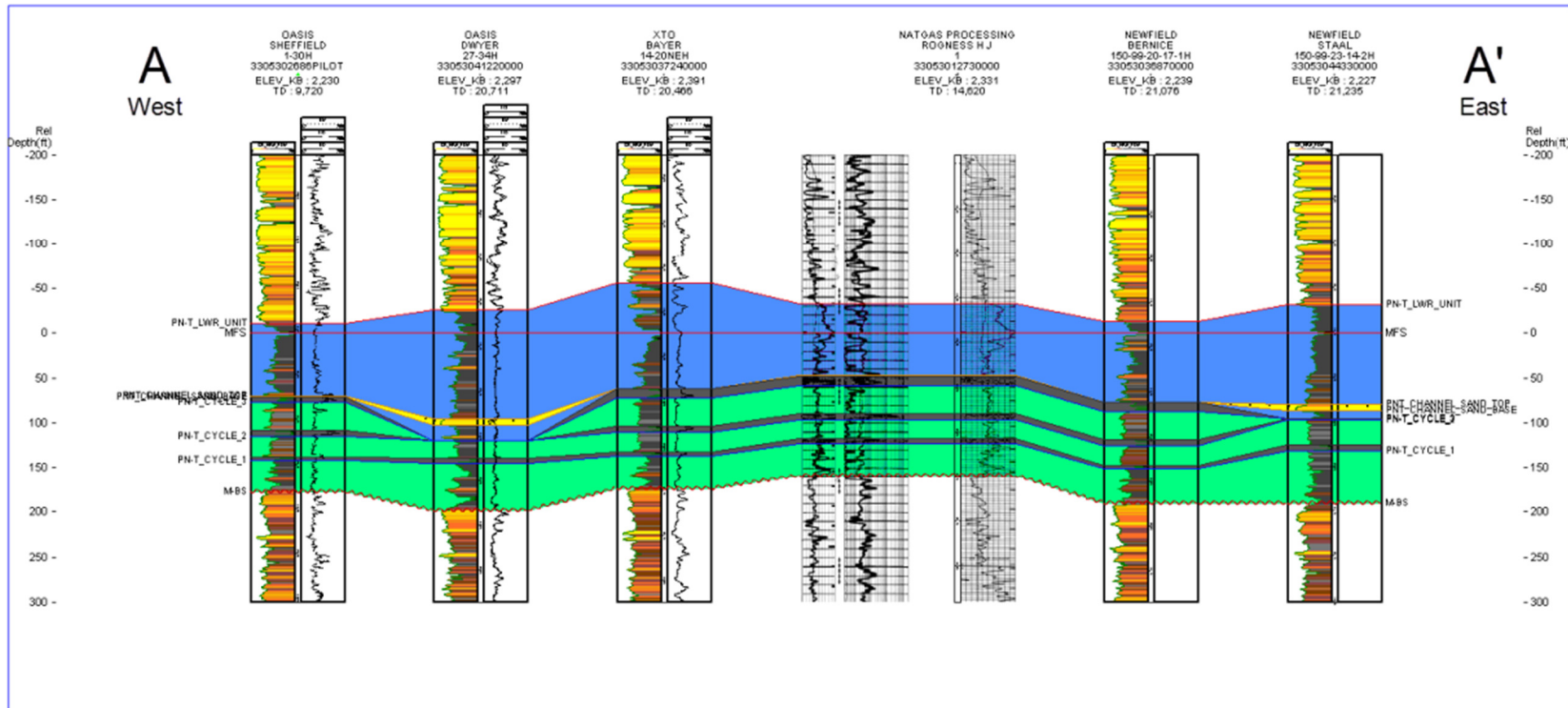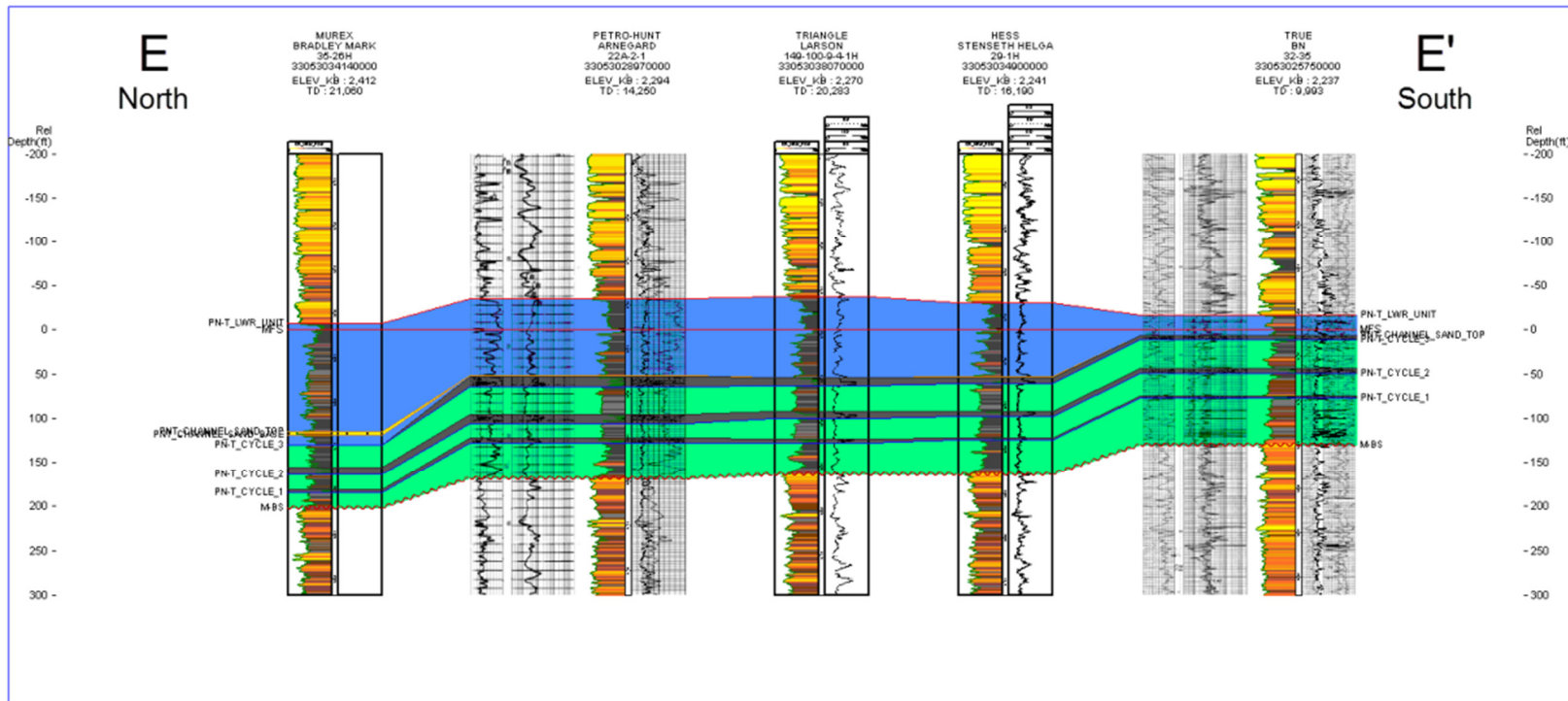
Figure 4.19 Stratigraphic cross-section of section line E-E'.

Location of cross section is shown in Figure 3.1. The GR log is shaded in from yellow (0 to 20 API) to black (greater than 150 API), having intermediate colors in between. The top of the Tyler Formation, cyclothems at base of the Tyler Formation are colored red and blue. The the upper Tyler Formation is shaded in cyan and the non-organic rich black mudstone intervals of the cyclothems are shaded in neon green. The organic rich black mudstone intervals are shaded in black, and the sandstones in yellow.
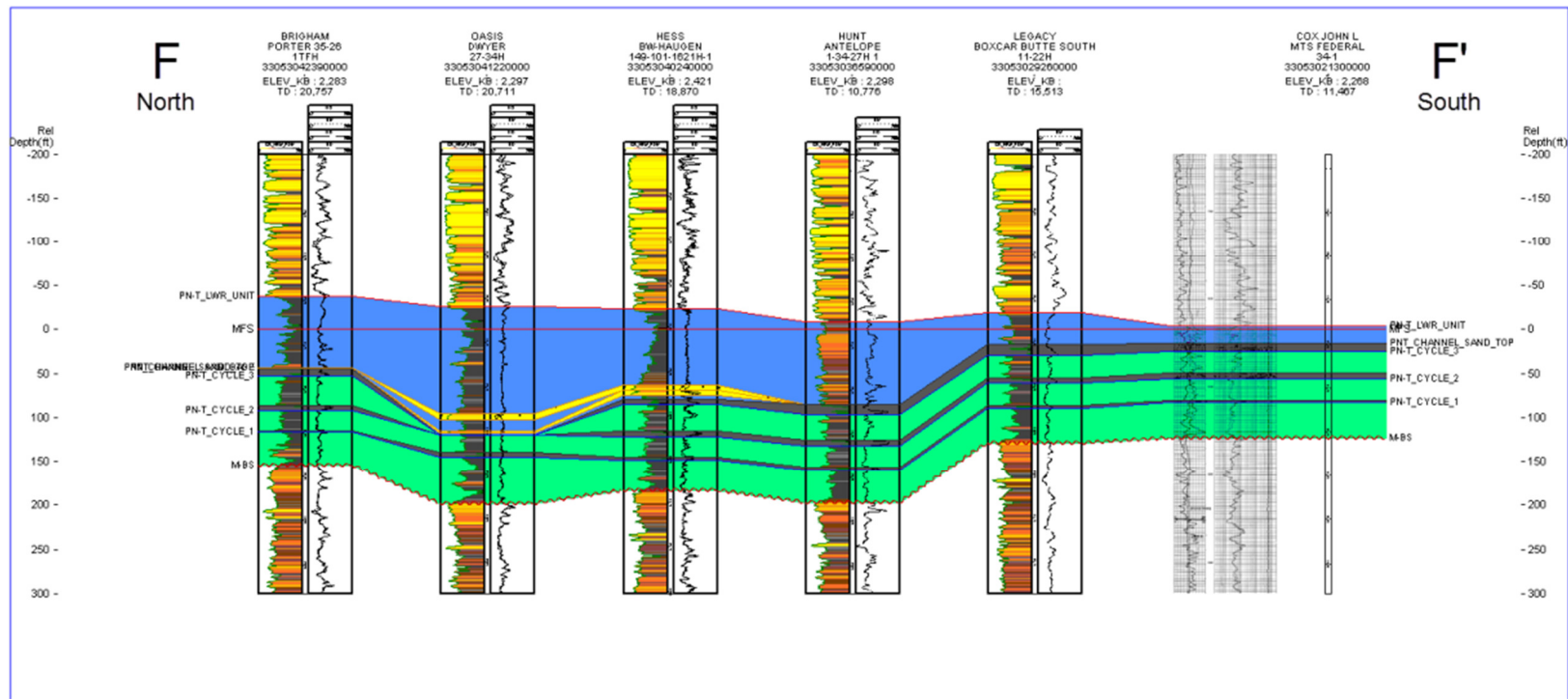
Figure 4.20 Stratigraphic cross-section of section line F-F'.

Location of cross section is shown in Figure 3.1. The GR log is shaded in from yellow (0 to 20 API) to black (greater than 150 API), having intermediate colors in between. The top of the Tyler Formation, cyclothems at base of the Tyler Formation are colored red and blue. The upper Tyler Formation is shaded in cyan and the non-organic rich black mudstone intervals of the cyclothems are shaded in neon green. The organic rich black mudstone intervals are shaded in black, and the sandstones in yellow.

4.4 Structure Maps

Structure maps were constructed for the Tyler, Big Snowy Group, Kibbey Lime, and Charles Formation from the top of these intervals (Figures 4.21-4.28). The Tyler, Big Snowy Group, Kibbey Lime, and Charles Formation all dip toward the east – northeast approximately 13 feet per mile. No obvious faults are present based on the log interpretations. The Red Wing Crater is located in township N148 W101 and can be seen clearly in the Tyler, Big Snowy Group, Kibbey Lime, and Charles structure maps. The Tyler Formation does not exist in the Red Wing central uplift due to the impact of the meteor and the proximity of the formation to the surface at the time of impact (Koeberl, et al., 1996). The value seen in the structure maps in place of the Tyler Formation are actually the Charles salt top. In the basin-wide structure map, the Nesson (north-east) and Billings (south-west) Anticlines are visible. This map also shows a rough estimate of the amount of accommodation space that is available for Tyler deposition at the commencement of the Early Pennyslvanian. It does not take into account subsidence and/or compression of sediments.

The Charles Formation structure map was made to show changes in the structure caused by salt dissolution. Minor features such sudden depressions are found throughout the Kibbey Lime and Tyler structure maps in Figures 4.23 and 4.28, indicating a possible zone of salt dissolution in the Charles Formation or underlying salts such as the Prairie Formation. An excellent depiction of the Red Wing Creek structure is shown in both the Charles and the Kibbey lime structure map (Figures 4.22-4.23). The Big Snowy Group structure map (Figure 4.24) depicts the amount of accommodation space available to the Tyler Formation at the onset of deposition. The depocenter in the Williston basin at this time is at the eastern margin of the study area.

The structure maps of the cyclothems and of the top of the Tyler Formation are shown in Figures 4.25-4.28. A rough estimate of basin fill is provided through these structure maps. Minor depressions found in these structure maps within the **Tyler** Formation are located at the same

areas shown on the Charles Formation structure map. This indicates there may be a relationship
between them, such as salt dissolution from the Charles Formation post-deposition.
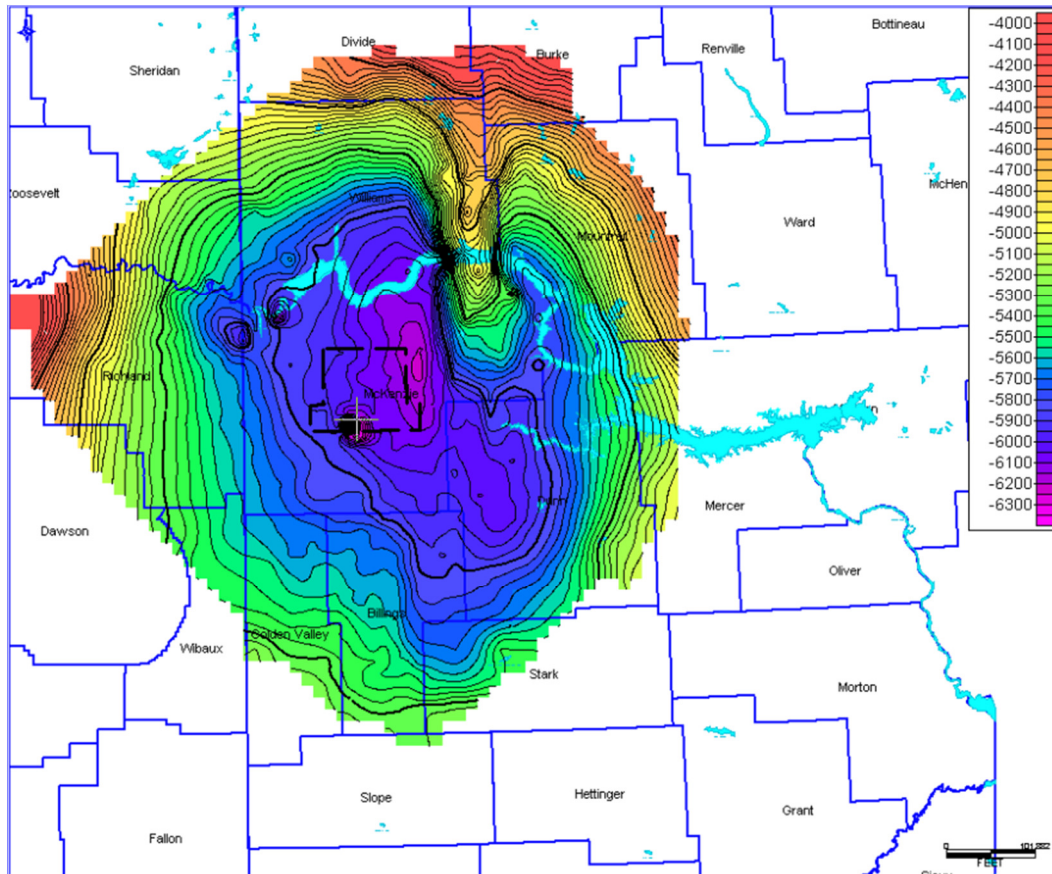
Figure 4.21 Structure map of the top of the Big Snowy Group in the Williston Basin.

This shows a rough estimate of the amount of accommodation space (approximately 2,000 feet)
available at the beginning of Tyler Formation deposition**.**
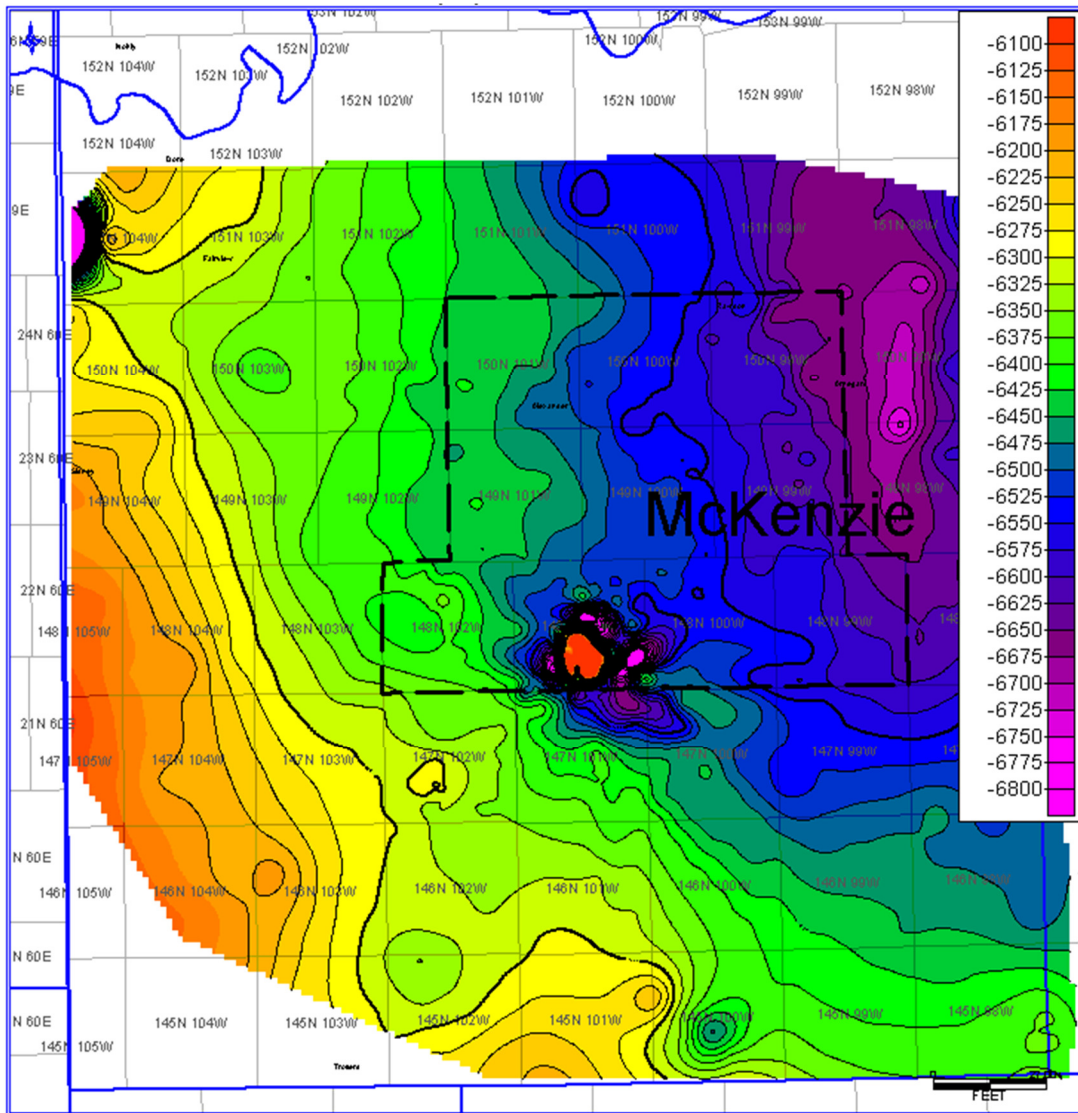
Figure 4.22 Structure map of the top of the Charles Salt.
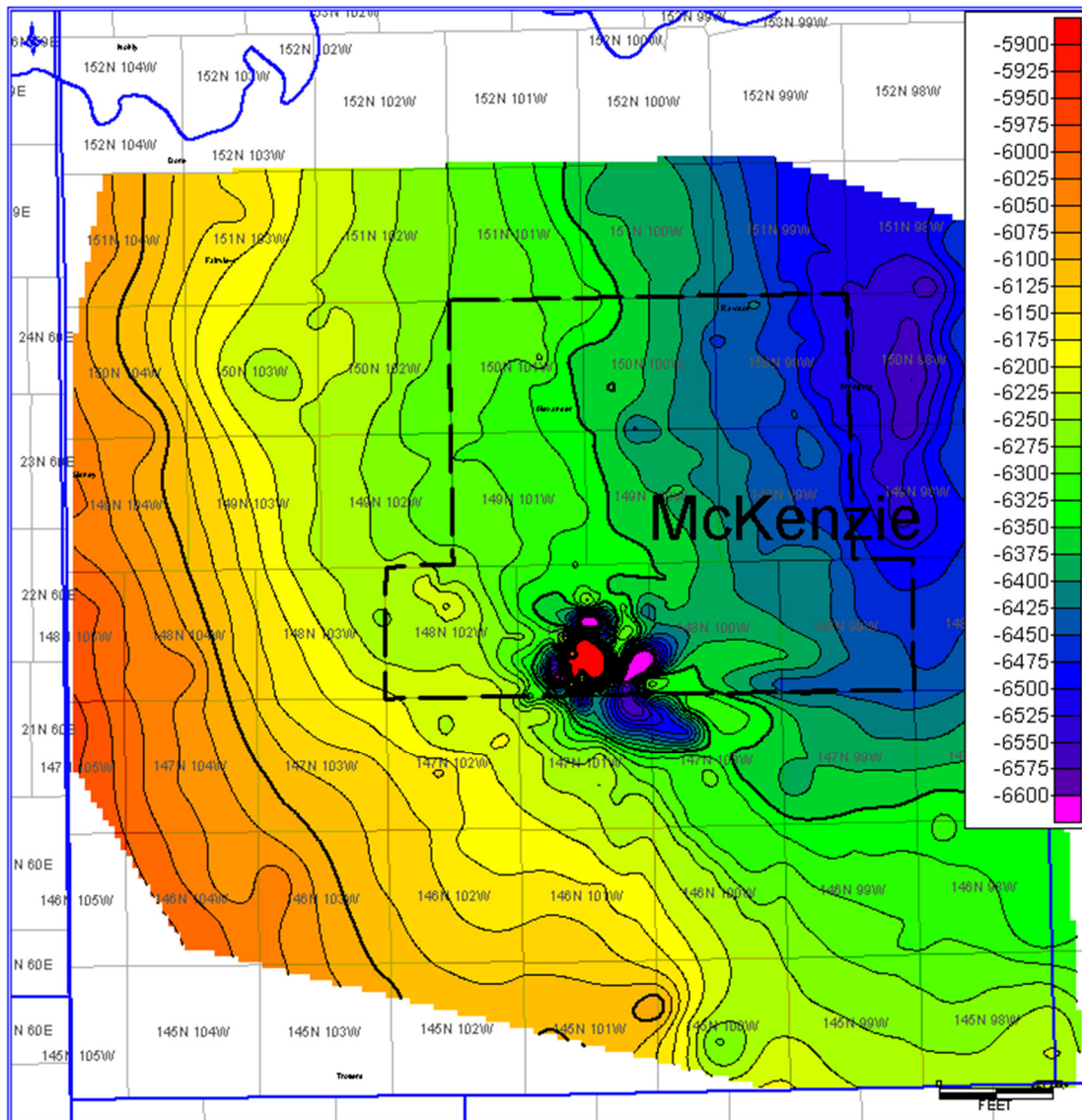
Figure 4.23 Structure map of the top of the Kibbey Lime.
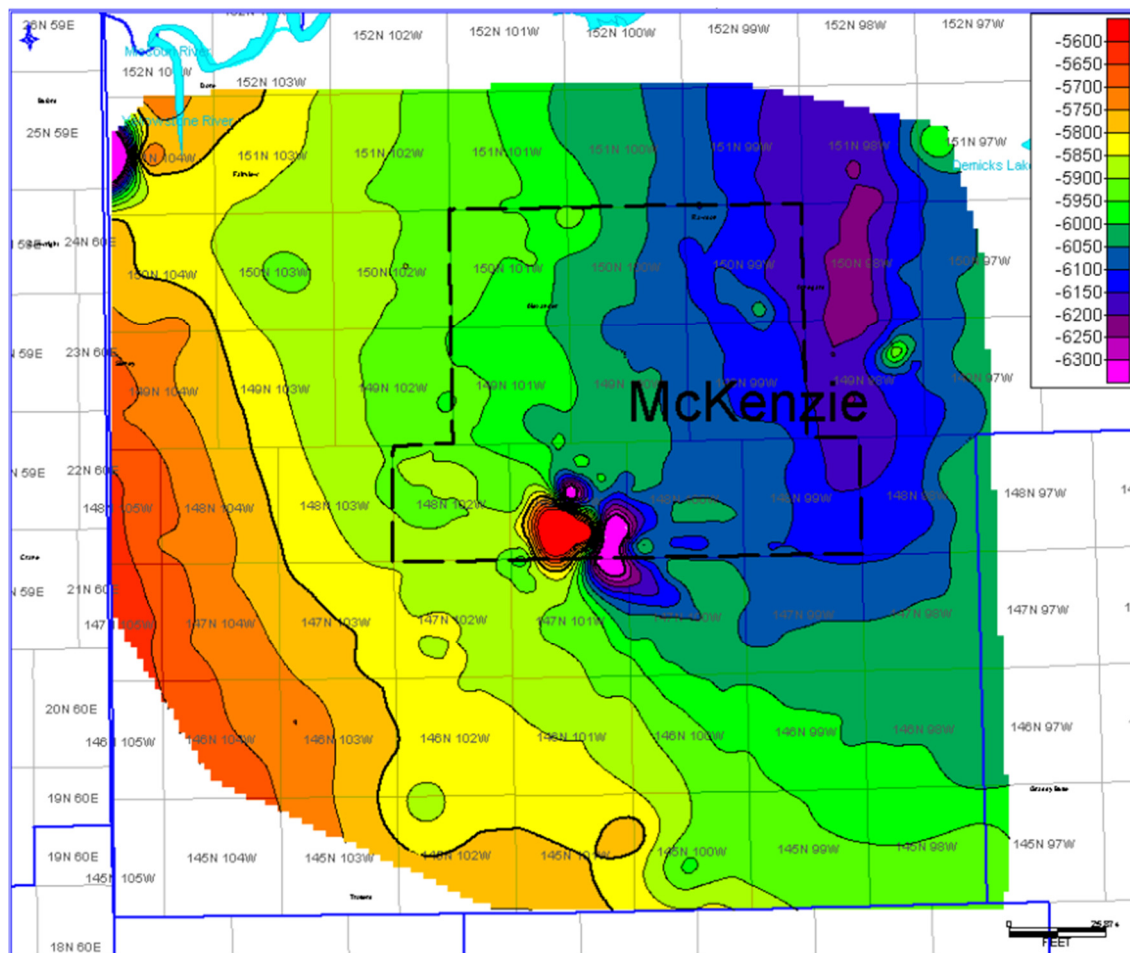
Figure 4.24 Structure map of the top of the Big Snowy Group.
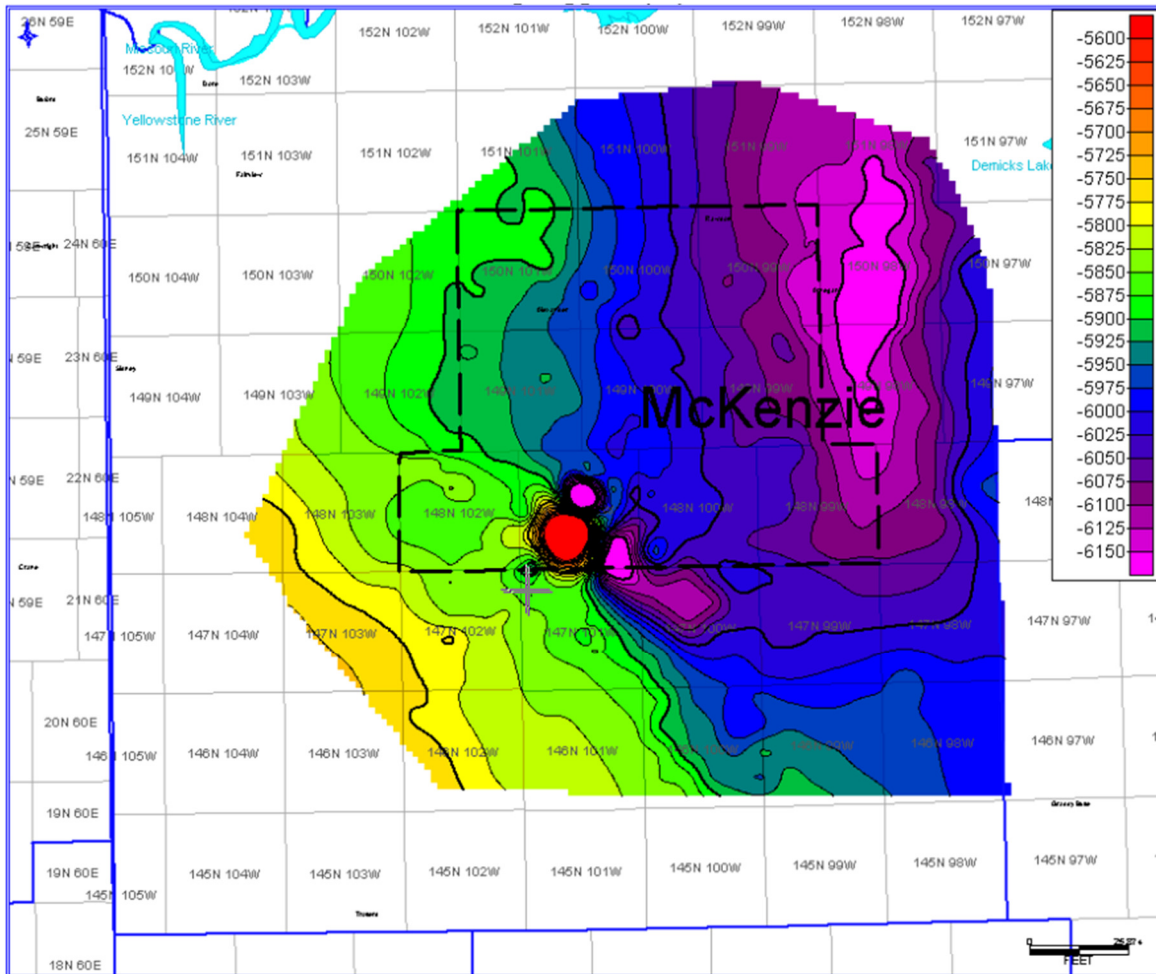
Figure 4.25 Structure map of the top of the first cyclothem.
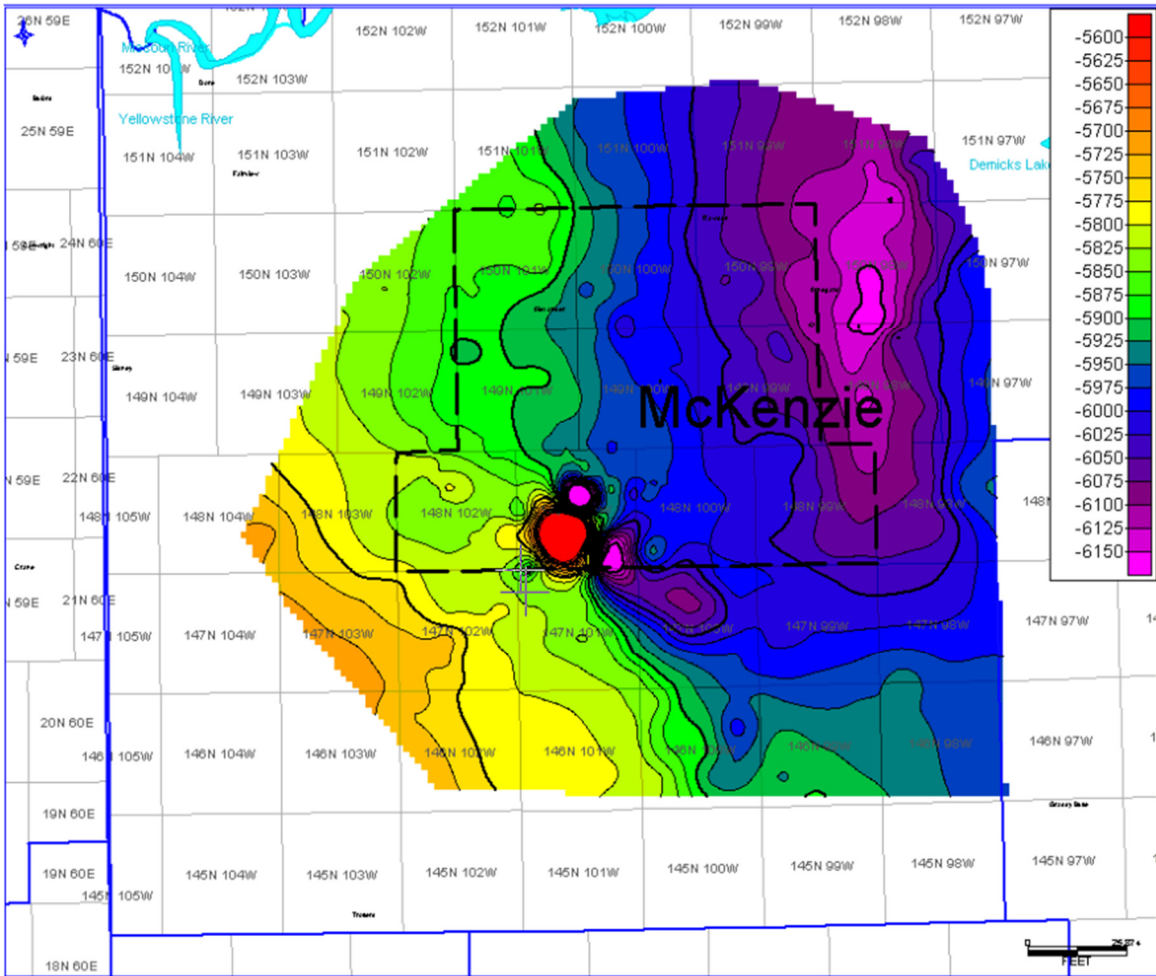
Figure 4.26 Structure map of the top of the second cyclothem.
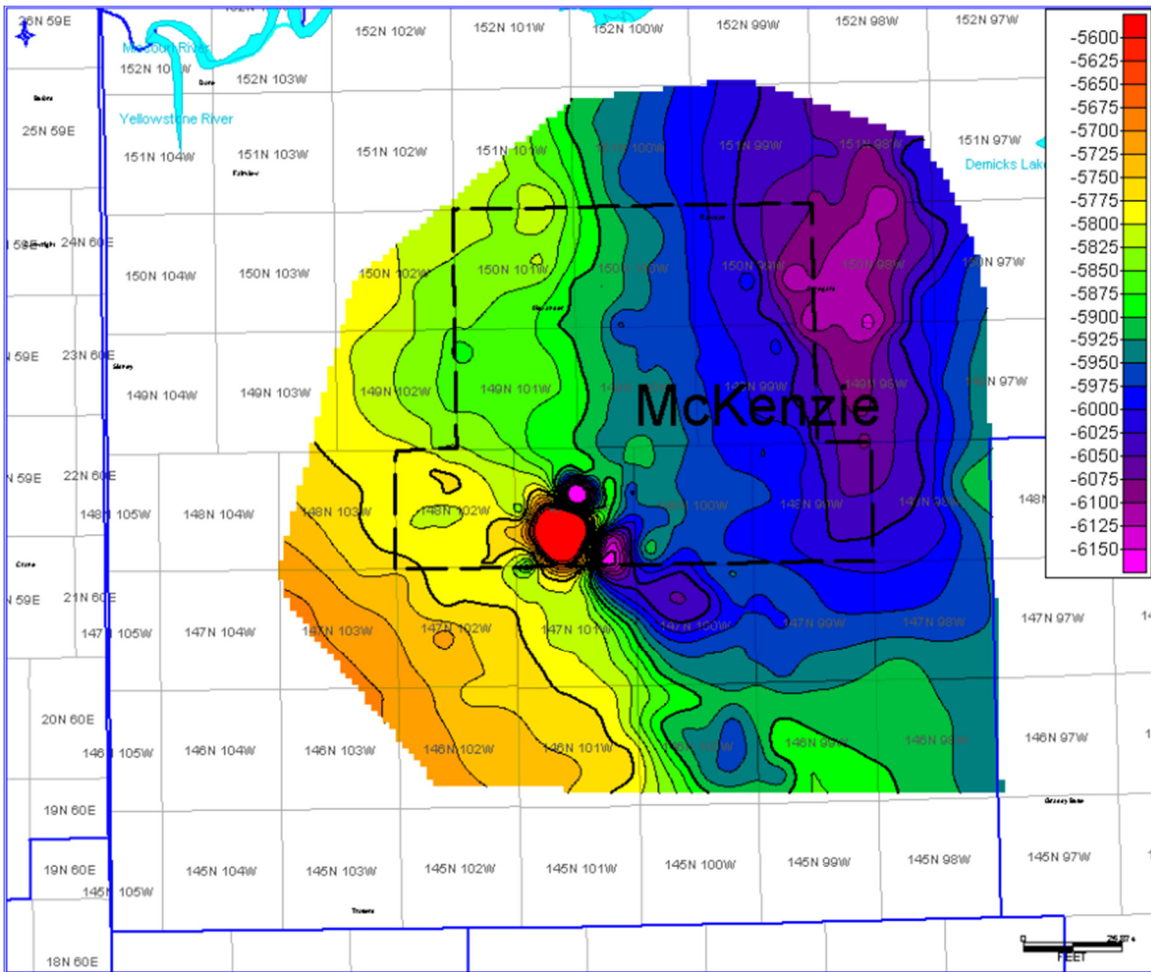
Figure 4.27 Structure map of the top of the third cyclothem.
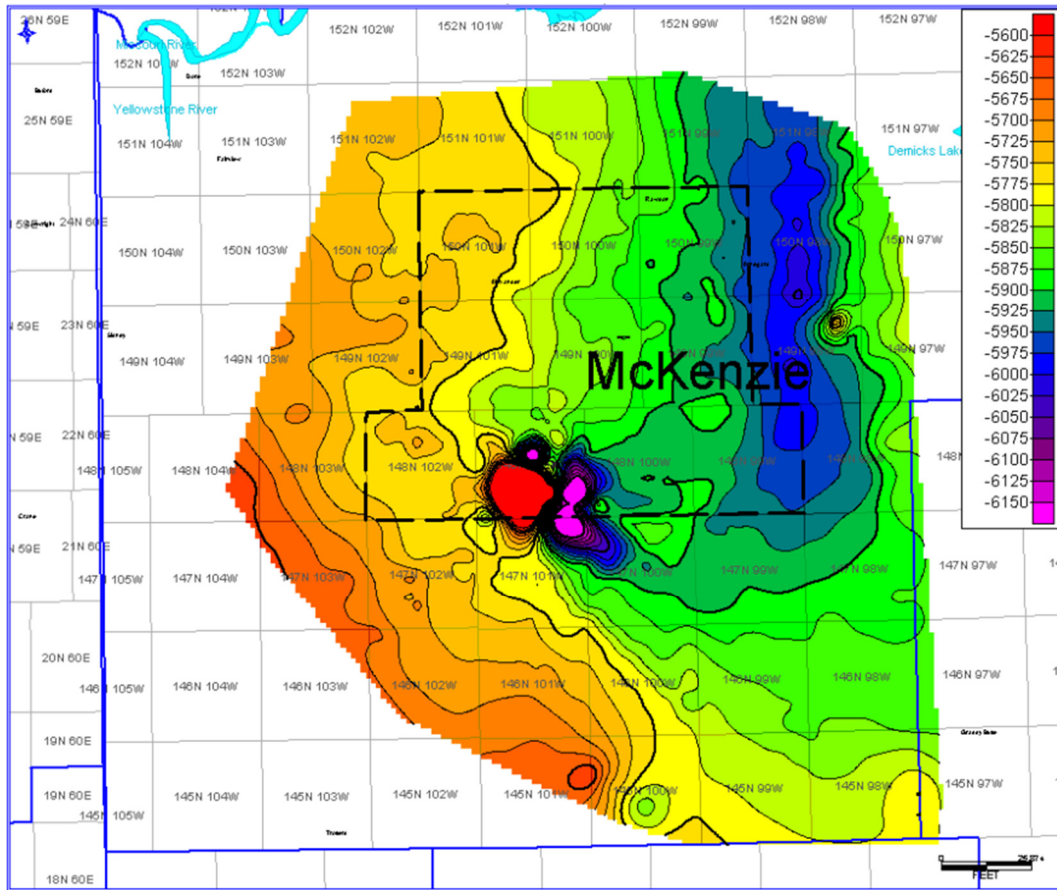
Figure 4.28 Structure map of the top of the Tyler Formation.

4.5 Isopach Maps

The depositional pattern of the Tyler Formation and its cyclothem packages are characterized by five interval thickness maps which can be found in Figures 4.29-4.33. The Tyler Formation is shown to exist within the area of the Red Wing astrobleme uplift found in the structure maps due to the gridding algorithm from IHS PETRA©. The Tyler Formation in the astrobleme, however, is non-existent due to impact of the Red Wing meteor.

The first cyclothem is depicted in Figure 4.29. Linear trends of sediment thicknesses in Figure 4.29 suggest deposition in erosional channels from the Big Snowy Group erosional surface. The average thickness of this cyclothem is approximately 35 feet (10.7 meters) which supports the stratigraphic cross sections. The first cyclothem sustains a steady thickness throughout the study area, 30-50 feet (9-15 meters).

The isopach for the second cyclothem is shown in Figure 4.30. This cyclothem has an average thickness of approximately 20 feet (6.09 meters) according to the thickness maps. The variation in thickness is less than the first cyclothem, averaging 25-35 feet (7.6- 10.6 meters), indicating the depositional surface was smoothed out by the end of the first cyclothems deposition. The extreme low thicknesses seen in the isopach is related to erosion caused by the overlying cycles, which is shown clearly in the isopach for the third cyclothem (Figure 4.31).

The third cyclothem has been widely affected by erosion caused by the overlying upper Tyler Formation. This is shown in the isopach for the cyclothem in Figure 4.31. Lineations that trend east-west and then north-west cut the third cyclothem. Variation in thickness to the south of the study area could have been caused by Facies B development in that region.

The upper Tyler Formation thickness map is shown in Figure 4.32. This interval has the most variation of the four in the Tyler Formation. A large increase in thickness towards the depocenter and in the central-northern portions of the study area occurs. The contours near the center of the study area are very tight, signaling that subsidence was occurring in the center of the basin near the depositional center during the time of deposition. Large variations in

63

thicknesses are seen in the northern-most sections of the study area. These "bull's-eyes" overlap the areas where the third cyclothem was eroded and additional accommodation space was available locally.

The last isopach shows the thickness of the sands found in upper Tyler Formation identified with the cross-sections (Figure 4.33). These sand thicknesses have a primary east-west orientation and north-south secondary orientation. The thickest sand package can be found in township 150N-100W. This sand package is in the stratigraphic cross-section D-D' (Figure 4.18).
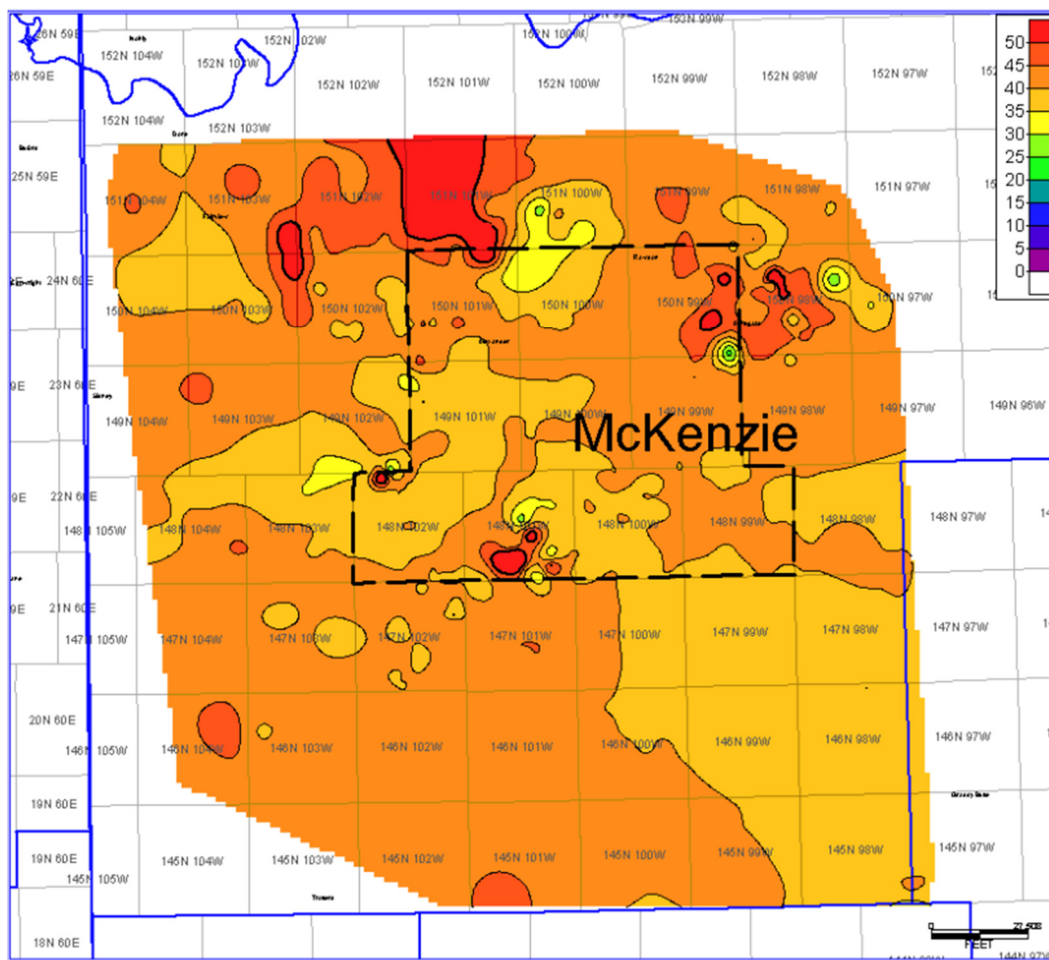
Figure 4.29 Isopach of the first cyclothem in the Tyler Formation.
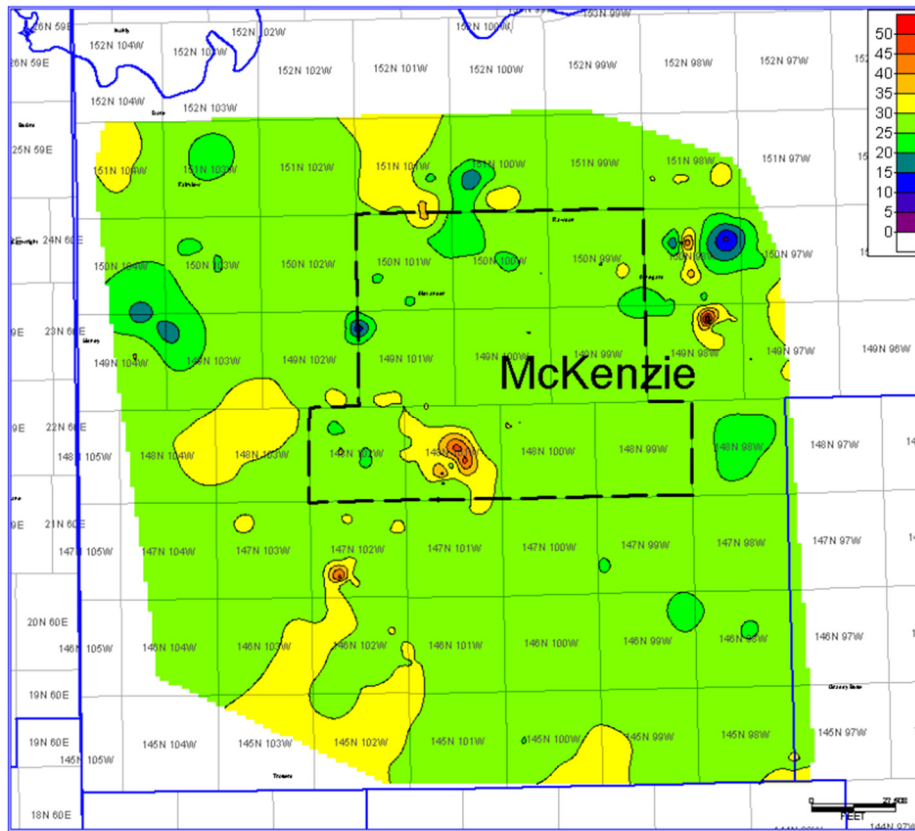
Figure 4.30 Isopach of the second cyclothem in the Tyler Formation.
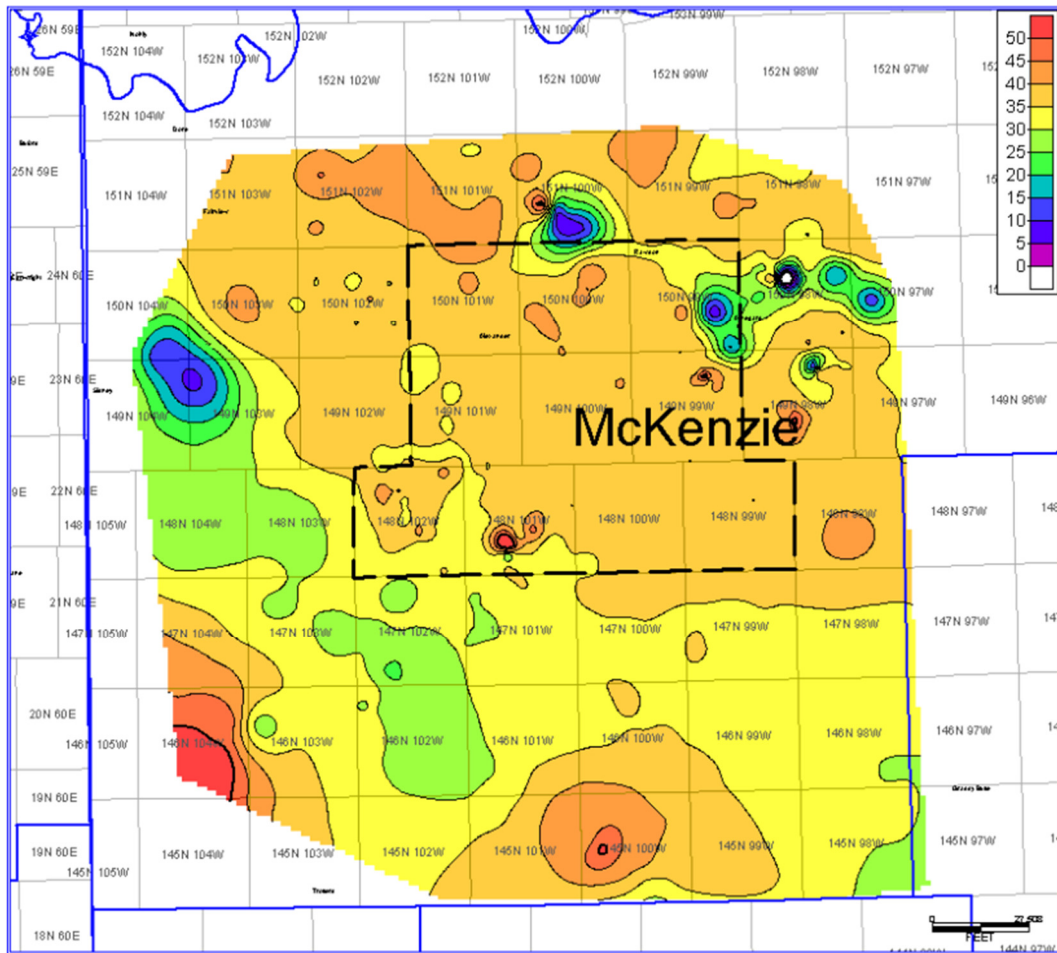
Figure 4.31 Isopach of the third cyclothem in the Tyler Formation.
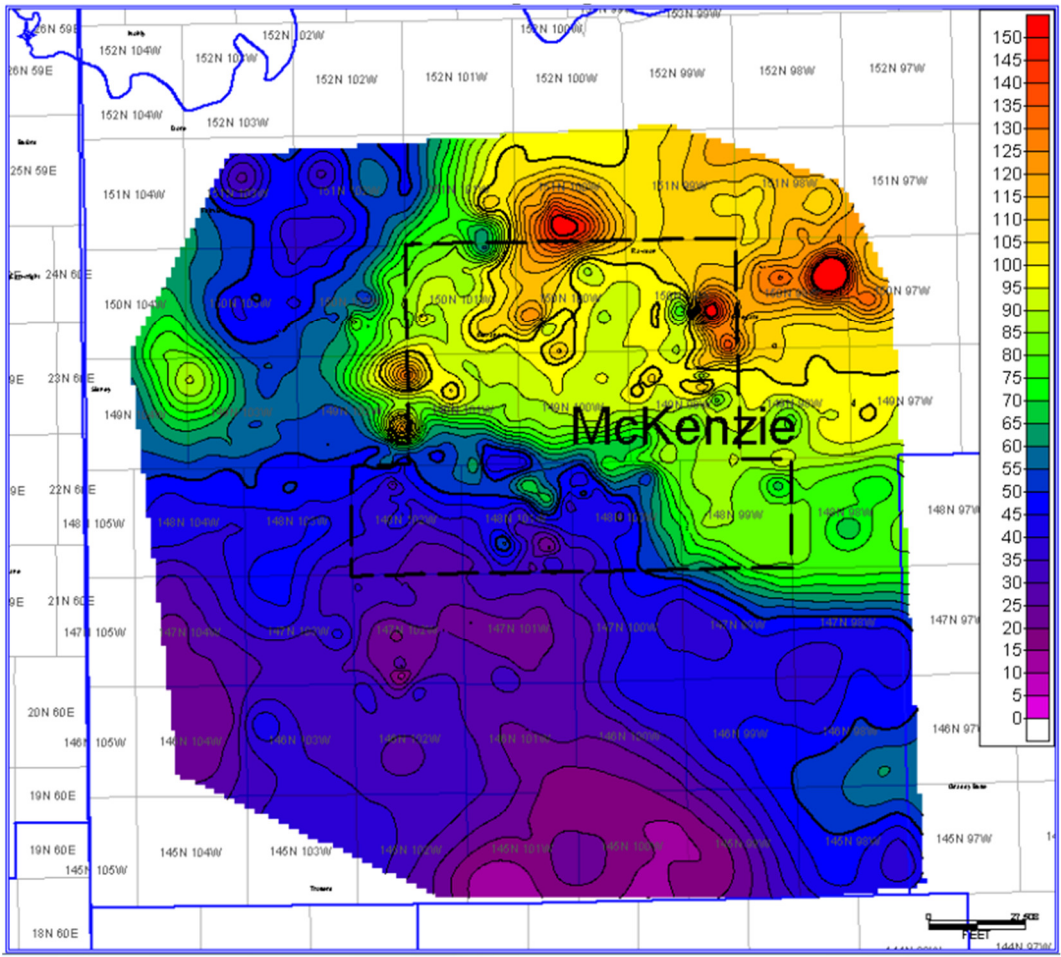
Figure 4.32 Isopach of the upper Tyler Formation.
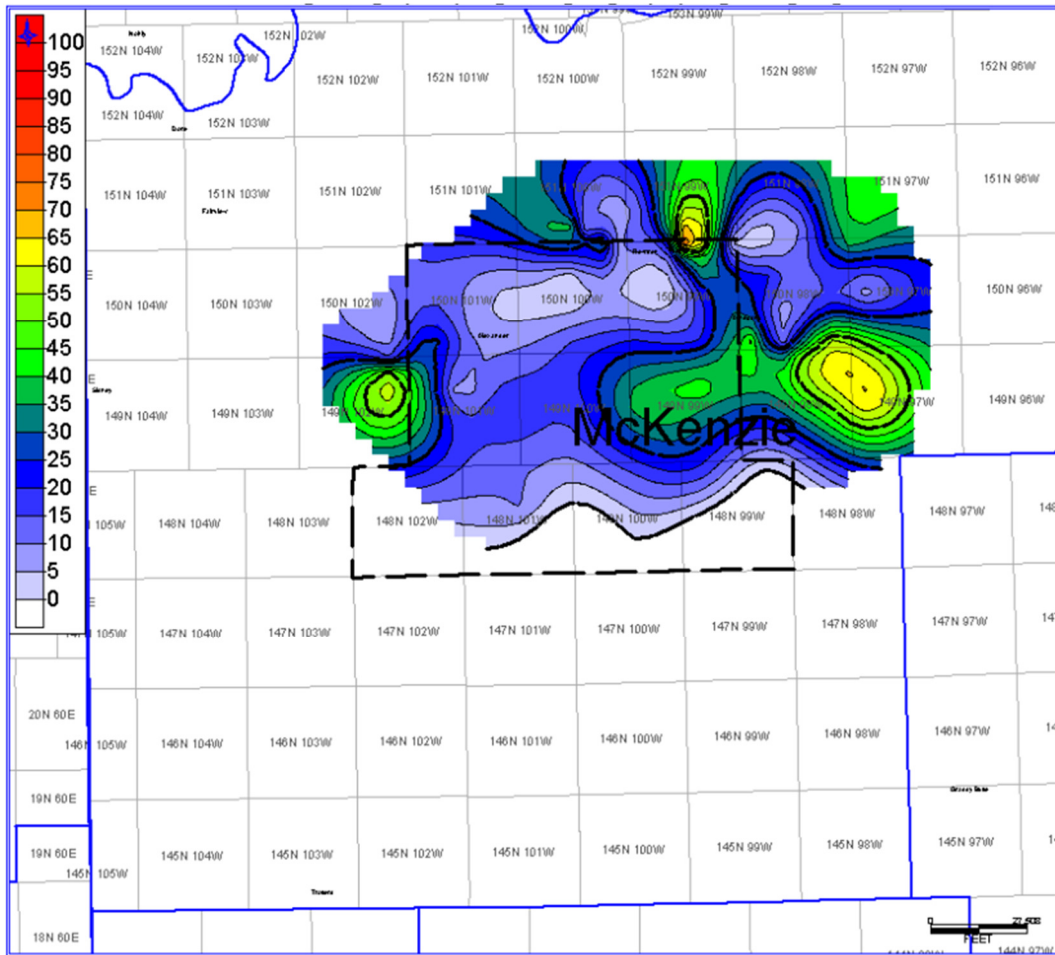
Figure 4.33 Isopach of sands located in upper Tyler Formation

4.6 Depositional Model

During Early Pennsylvanian time, glacial-interglacial fluctuations at high latitudes caused eustatic sea level fluctuations that, in turn, impacted depositional conditions. The Tyler Formation occurs above a major unconformity marking the boundary between the Big Snowy Group and the Tyler Formation. This unconformity represents a falling sea level exposing the Big Snowy Group.

4.6.1 Lower Tyler Formation

Sedimentation above the Big Snowy Group disconformity commenced with the low-stand systems tract which is not present in the core. This tract would have been characterized by red beds and/or estuary deposits of sandstone which were not observed with logs. The lower half of the Tyler Formation is interpreted to have been deposited in a marginal-marine deltaic environment. Within the lower Tyler Formation there are three identified cyclothems which contain higher order cycles, as identified by Nesheim & Nordeng (2012). Each cyclothem contains offshore marine mudstone from Facies A which is indicative of a transgressive systems tract. The dark-gray skeletal limestone from Facies B overlying the marine mudstone is interpreted as the base of the regressive unit. This limestone indicates the commencement of the high-stand systems tract. Mudstone deposited in a lagoonal or bay environment such as from Facies C occasionally overlies the regressive limestone. These mudstones grade from the Facies A mudstone into a brown to tan color and contain sparse carbonate material within its matrix.

The caliche and paleosol of Facies D1 and D2 represent subaerial exposure and low-stand conditions. Well-developed soil horizons (21.36 – 143.25 cm) occur over a large area suggesting apex regression and a long period of subaerial exposure (Reinhardt & Sigleo, 1988).The paleosol facies may account for the thickest depositional time period within the cyclothems. Coal from Facies E may represent subsequent transgression, in which rapid subsidence approximated the accumulation rate of peat. Figure 4.34 depicts the depositional environment during the onset of a high-order transgressive systems tract. As sea level began to rise, the terrestrial areas began to slowly flood with marine water. These regions became the

renowned Pennsylvanian swamplands, wherein accumulations of significant amounts of coal developed (Boggs, 2005).

As transgression continued, the swamplands retrograded towards the basin margins. The third cyclothem illustrates this in Figure 4.35. The third cyclothem consists entirely of marine to marginal marine sediment, unlike the first and second cyclothems. Slowly increasing thickness of offshore facies and decreasing thickness in the terrestrial facies in the lower Tyler Formation indicates retrogradation of the terrestrial to offshore facies. This retrogradation of the shoreline indicates a lower-order transgressive systems tract is found within the cyclothems. This introduces the onset of dominantly marine sedimentation onto the study area. During the third cyclothems' deposition sea level high stand had been reached and sea level then progressively fell, until the red beds found at the topmost section of the core. These red beds are a possible sequence boundary which indicate there was possible subaerial exposure in the basin during this time period, implying a period of low stand overlying the third cyclothem. This lowstand leads into the upper Tyler Formation.

4.6.2 Upper Tyler Formation

A low- order transgression commenced after a sea level lowstand overlying the high-order high stand systems tract of the lower Tyler Formation, represented by the topmost cyclothem. Higher-order systems tracts within this interval may have been present, but were not identifiable through the well logs. Mudstones, interpreted as mid-to-outer shelf deposits due to their macro- and micro-fossil assemblages, dominate the upper Tyler Formation and, considering a lack of clearly regressive strata, are interpreted to indicate pervasive shelfal-marine deposition. Interbedded carbonate within the interval indicate a preferential deposition of carbonate within the basin. Carbonate deposition in the upper Tyler Formation indicates a possible subtle decrease in sea level to allow carbonate mud to precipitate within the study area. Sandstone bodies within this interval could indicate submarine channel and lobe systems. These sand bodies might

possibly be delta-front siliciclastic run-off from the upper unit of the Tyler Formation (Sturm, 1982).
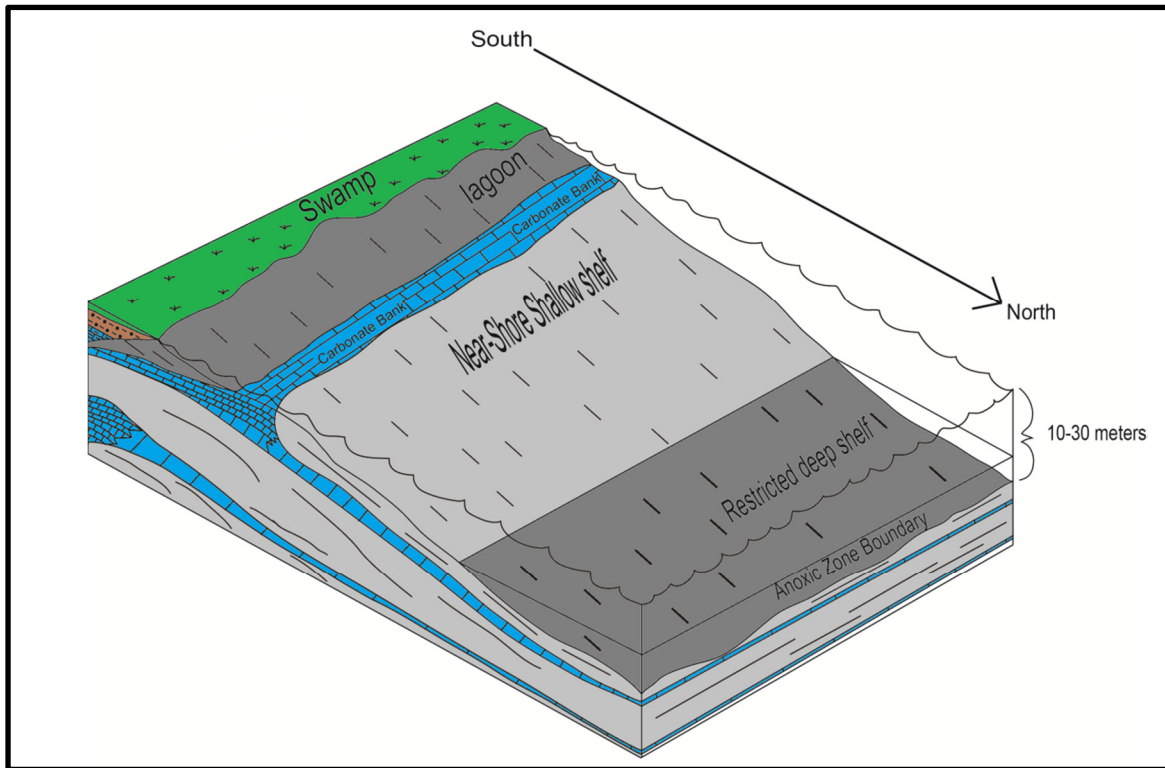
Figure 4.34 Paleographic reconstruction of facies relationships in the Tyler Formation, central western North Dakota.

This block diagram represents the facies at the commencement of a transgressive systems tract.
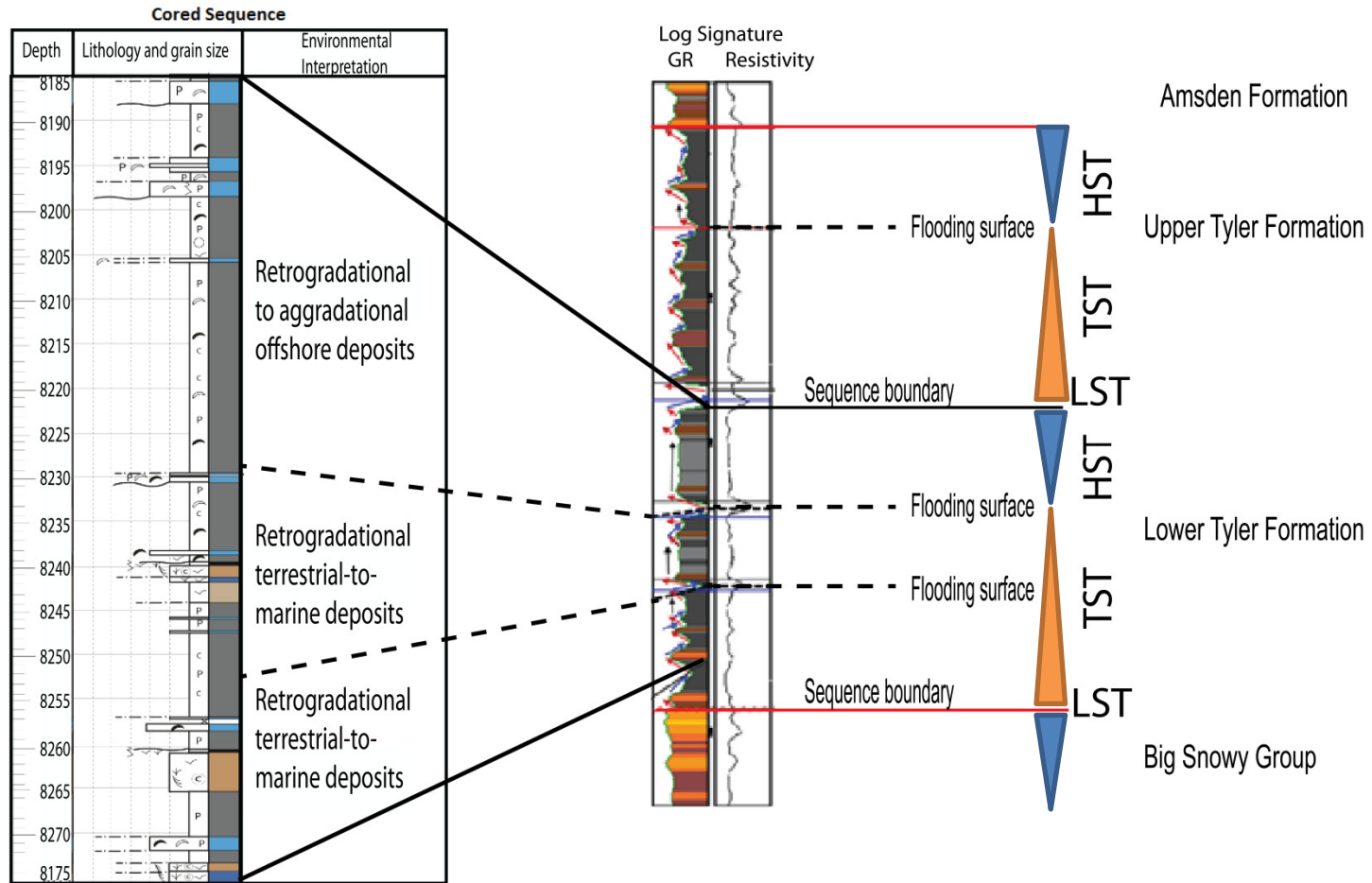
Figure 4.35 Cored sequence and log signature from the Curl 23-14 well showing the Tyler Formation in a sequence stratigraphic context.

Lithology and grain size legend is found in Figure 4.8.

4.7 Core Properties Analysis

Routine core analysis provided information on porosity, permeability, and grain density. The values were collected from the North Dakota Industrial Commission (https://www.dmr.nd.gov-oilgas/) and from the MIP experiments done for this study. These values can be found in Table 4.1. Facies C and E had no data points in their intervals due to thinness of the interval or inconsistent depositional behavior of facies in the core. The cross plot of the core porosity and permeability values found in Figure 4.35 show some general trends for each of the facies. All facies with data with exception of D1 have a permeability of less than 0.0001 microdarcies. Porosity values do exhibit general correlations with facies.

Facies A had core porosity values ranging from 1.6- 9.4% with an average value of 5.76%. The porosity for Facies A is highly heterogeneous and dependent on organic-matter pores and interparticle pores formed during compaction and pyrolysis.

Facies B had core porosity values ranging from 0.8-2.7% with an average of 1.8%. This facies is the least porous and equally as low in permeability as the other facies found in the Curl 23-14 Tyler Formation core. Its low porosity is a characteristic of mudstone-wackestone. Possible diagenesis could have also caused pores to have been sealed during deposition.

Facies D1 had a core porosity value of 2.3%. Low porosity in this facies is highly likely due to the porosity and permeability analysis done by Whiting Oil and Gas occurring in a limestone nodule. Calcite cement and clay particles in the matrix between the grains can reduce the void space within this facies (Boggs, 2005). The permeability in this facies, however, seems to have occurred by preserving an open framework in-between the clay particles which exist in between the limestone nodules. The permeability may also have been enhanced by dissolution of the original limestone during Tyler deposition, which increased the connectivity of the pores.

Facies D2 had core porosity values ranging from 7.4-10.9% with an average of 8.78%. The porosity in this facies is the highest in the Curl 23-14 core and is caused by the unconsolidated characteristic of the paleosol and lack of calcite cement within the interval.

Table 4.1 Core analysis table.

Sample numbers labeled with (*) were gathered by Whiting Oil and Gas Corporation.

Sample Number	Sample Depth	Permeability, millidarcys	Porosity, percent	grain density, gm/cc
A	8185.00	<0.0001	1.4	2.67
B	8286.00	<0.0001	0.7	2.78
1-10(f)*	8194.40	-	1.2	2.84
1-11*	8195.50	<0.0001	0.8	2.85
1-14*	8198.00	<0.0001	2.1	2.87
1-22(F)*	8206.65	-	7	2.79
1-46*	8230.40	<0.0001	1.6	2.83
1-56(F)*	8240.50	-	10.9	2.72
1-58*	8242.00	0.015	2.3	2.78
1-59(F)*	8243.40	-	8.9	2.71
1-60(F)*	8244.65	-	9.4	2.72
1-63(F)*	8247.70	-	3	2.85
1-64(F)*	8248.75	-	7.8	2.73
1-73*	8257.40	<0.0001	1.6	2.77
1-73A*	8257.60	<0.0001	2.7	2.85
1-78(f)*	8262.50	-	8.2	2.84
1-79(F)*	8263.50	-	7.4	2.77
1-80(f)*	8264.50	-	9.2	2.78
1-89(F)*	8273.40	-	8.2	2.77
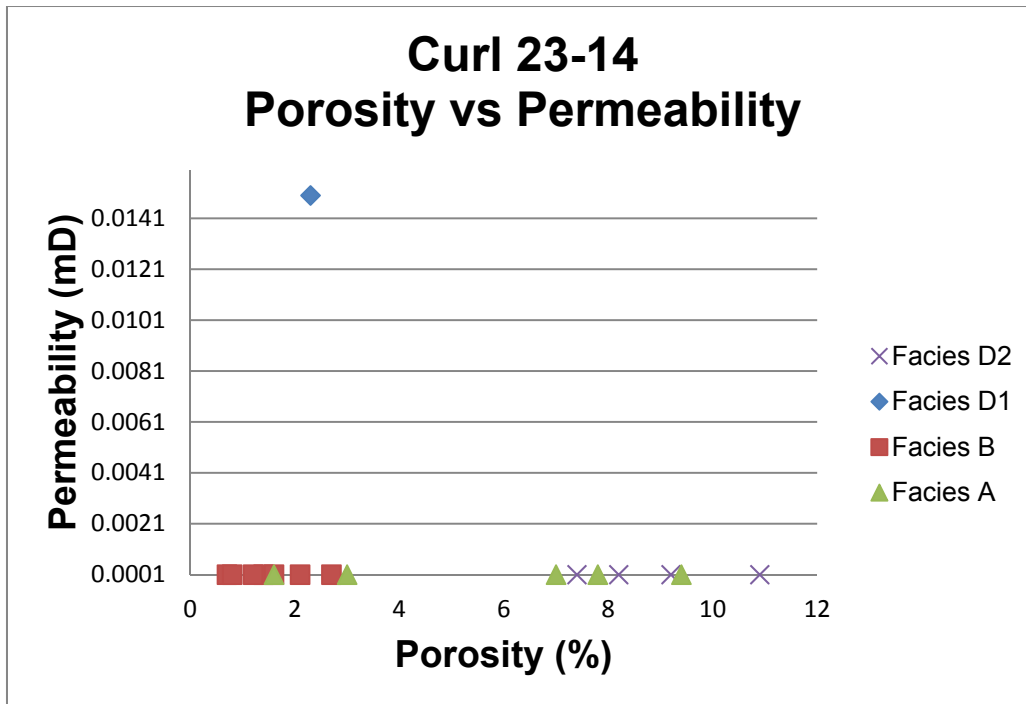
Figure 4.36 Porosity and permeability cross plot of the Curl 23-14 Tyler Formation core.

4.8 Conventional Well Log Analysis

The well log characteristics for the three cyclothems are similar. The GR log for each cyclothem does not vary much and remains in the 90-110 API range. Several lower API readings indicate the presence of calcite, such as in Facies B, or silica. The resistivity logs in these cyclothems remain fairly consistent in the 1-10 ohm range. The variations in the neutron log readings are due to the presence of hydrogen in the clays. Differentiation of the facies within the cyclothems was not possible because several of the facies are too thin for the resolution of the logging tool.

In between the cyclothems lies the highly organic mudstone source rock which is part of Facies A. In these intervals, the GR log shoots off the scale indicative of a high concentration of radioactive material. The accumulation of radioactive material, specifically uranium, is commonly associated with organic material. The organic mudstone also are characterized by an increase in

the resistivity logs, reading up to 100 ohms-meter. Due to the limestone matrix correction for the density log, the porosities for the mudstone will be a lot higher than their actual value.

The upper Tyler Formation consists of marine mudstone with submarine channel sands. The mudstone in this interval is similar to log characteristics of mudstone in the cyclothems. The channel sands within this system typically have an API value of 20-40 in the GR log. The resistivity in these sands is generally very low which conversely means high conductivity, indicating a water-rich zone. At the north-eastern boundary of the study in township and range 148-150N 99W, the sands are water saturated and all show similar log readings as that is shown in Figure 4.37. The cross-over in the porosity logs is a possible indicator of sandstone or accumulation of hydrocarbons, specifically gas, and is shaded red in Figure 4.37 (Asquith, et al., 2004). The porosity logs indicate that the sands have approximately 15% porosity and the spread in the different resistivity logs indicate good permeability. The photoelectric log (PDPE) has a cut off of 3.14 for dolomite (shaded blue), and shows a value of approximately 2.2- 2.5 for the sandstone. Clean sandstone has a value in the vicinity of 2 thus affirming that these are sandstones (Asquith, et al., 2004).

Figure 4.37 Well log example of sandstone bodies within the Tyler Formation in the study area.
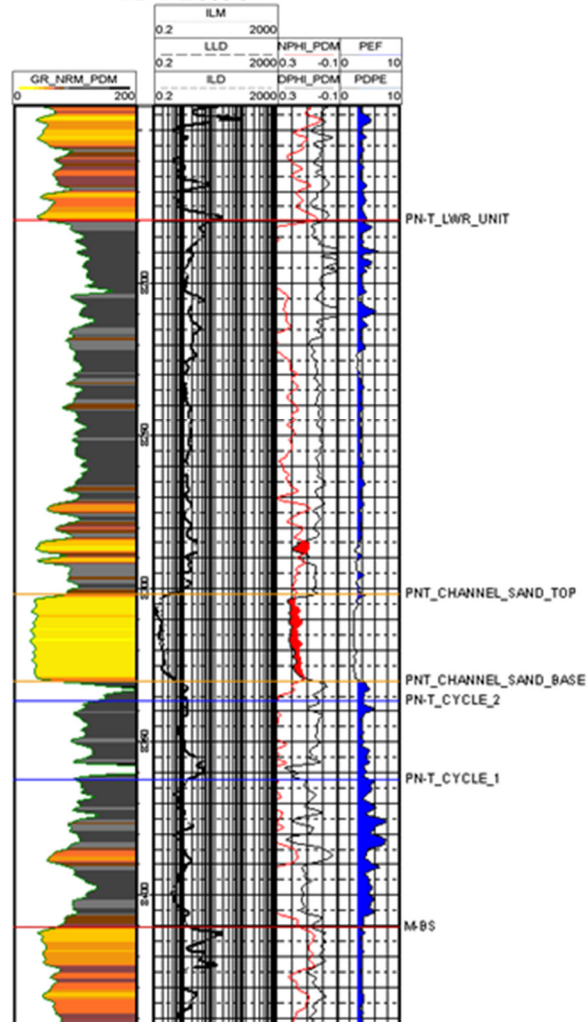
The GR log is shaded in from yellow (0 to 20 API) to black (greater than 150 API), having intermediate colors in between. The PE curve has a geocolumn shading (blue) cut-off of anything greater than 3.14. Porosity cross-over shaded red

Chapter 5

Conclusions and Recommendations

5.1 Conclusions

There are six facies present in the Tyler Formation core from the Curl 23-14 well, which represent offshore to deltaic environments. Facies A and B were deposited in offshore to near-shore marine environments characterized by marine fauna such as: ostracods, shell fragments, algae, and crinoids. Facies A is a black mudstone with laminar bedding. Facies B also contained similar fauna as Facies A with the exception of crinoids and algae. Facies B was a calcareous mudstone and contained occasional fractures filled by calcite. Facies C through E were deposited in near-shore marine to deltaic terrestrial environments. Facies C consists of terrestrial to near-marine mudstone deposited shortly after regression. Facies D1 and D2 are terrestrial sediments deposited at the end of the sea level low-stand. These facies can be used to determine low-stand conditions during Tyler Formation deposition. Facies E, bituminous coal, marks the commencement of the transgressive systems tract within the cyclothems. These thin intervals of coal are overlain by lagoonal to bay deposits of black mudstone from Facies A.

Water depth, sediment supply, and depositional energy control the facies variation within the Tyler Formation near the depocenter of the Williston Basin during the early Pennsylvanian. The cyclothemic deposition occurred during low-order transgressive and high stand systems tracts and was observed in the lower half of the Tyler Formation in the form of three cyclothems. The three cyclothems that occur exhibit high frequency, higher-order sequence deposition. Within the lower two cyclothems, Facies E, A, and B occur following the rise of sea-level caused by the high order transgressive systems tract. Facies B marks the commencement of the high-stand systems tract in the form of a regressive limestone unit. Facies A continues to be deposited in a lagoonal or bay setting after the regressive limestone unit, which can potentially become Facies C through weathering and leaching of calcite, originating from Facies D1 and D2. The low-stand systems tract is characterized by the appearance of Facies D1 and D2, terrestrial sediment. This

78

cycle repeats for the lower two cyclothems. A high-order transgressive systems tract forms the boundary between each cyclothem. The third and upper-most cyclothem consists solely of Facies A and B marine sediment deposited during a sea level high stand. Offshore marine deposition dominated the upper half of the Tyler Formation during a lower-order transgressive and possible high stand event. These two different depositional regimes depict a time of eustatic change during the Early Pennsylvanian.

 Although the areal extent of each individual facies could not be mapped and analyzed, the areal of extent of the three cyclothems were mapped. The three cyclothems are part of Sturm's (1982) Lower unit for the Tyler Formation south of the study area in the Dickinson, Fryburg, Medora, Rocky Ridge, and Tracy Mountain fields. The upper Tyler Formation identified in this study is the basinal equivalent of Strum's (1982) Upper unit and consists of mudstone, thin lenses of carbonate material, and sandstone intervals that are highly variable in thicknesses.

<div align="center">5.2 Recommendations</div>

A more detailed look at the mineralogical composition of the Tyler Formation near the depocenter of the Williston Basin would be beneficial to further understand this potential oil and gas play. This work could quantify the brittleness of the Tyler Formation to see if it has potential as an unconventional reservoir.

Geochemical analysis on the facies of the Tyler Formation can be done to prove the heterogeneous nature of the formation. This would highlight the highly variable trends which characterize the Tyler Formation.

The rich organic mudstones and coals have gone through the oil window and have generated hydrocarbons, but the cyclothems seem to lack any lithological unit that resembles a conventional reservoir. For production purposes within the cyclothems in this region of the basin, a horizontal hydraulic fracturing campaign would be advisable.

References

Anna, L., Pollastro, R. & Gaswirth, S., 2011. Williston Basin Province- Stratigraphic and structural framework to a geologic assessment of undiscovered oil and gas resources, chap 2 of. *f U.S. Geological Survey Williston Basin Province Assessment team, Assessment of undiscovered oil and gas resources of the Williston Basin Province of North Dakota, Montana, and South Dakota, 2010,* Volume U.S. Geological Survey Digital Data Series 69-W, p. 17.

Anon., 2000. *Depositional History of the Pennsylvanian Rocks in Illinois.* [Online] Available at: http://www.isgs.uiuc.edu/maps-data-pub/publications/geonotes/geonote2.shtml

Anon., 2011. *North Dakota Oil & Gas Division.* [Online] Available at: https://www.dmr.nd.gov/oilgas/stats/2011CumulativeFormation.pdf

Asquith, G. B., Krygowski, D. & Gibson, C. R., 2004. *Basic well log analysis.* 2nd ed. s.l.:Association of Petroleum Geologists.

Bebout, D. G. & Loucks, R. G., n.d. *Handbook for logging carbonate rocks: Bureau of Economic Geology, University of Texas at Austin, Handbook 5, 43 p.* s.l.:s.n.

Berner, R. A., 1984. Sedimentary pyrite formation: An update. *Geochimica et Cosmochimica Acta, vol. 48,* pp. p. 605-615.

Bisnett, A. J. & Heckel, P. H., 1996. Sequence stratigraphy helps to distinguish offshore from nearshore black shales in the Midcontinent Pennsylvanian succession. *Geological Survey of America, Special paper 306,* pp. 341-350.

Blakey, R., 2013. *Paleogeography and Geologic Evolution of North America.* [Online] Available at: http://www2.nau.edu/rcb7/nam.html

Boggs, S., 2005. *Principles of Sedimentology and Stratigraphy.* 4th ed. Columbus: Prentice Hall.

Carlson, C. G., 1960. Stratigraphy of the Winnipeg and Deadwood Formations in North Dakota. *North Dakota Geological Survey Bulletin V.35,* p. 149 p.

Crowley, K. D., Ahern, J. L. & Naeser, C. W., 1985. Origin and epeirogeneic history of the Williston Basin: Evidence from fission-track analysis of apatite. *Geology,* pp. 620-623.

Dorobek, S. L. et al., 1991. Subsidence across the Antler foredeep of Montana and Idaho: Tectonic versus eustatic effects. *Kansas Geological Survey bulletin 233,* pp. 232-251.

Dow, W. G., 1974. Application of oil-correlation and source-rock data to exploration in Williston Basin. *AAPG Bulletin V 58,* pp. 1253-1262.

Fairbridge, M. & Rampino, 2003. Diagenetic structures. In: *Encyclopedia of Sediments and Sedimentary Rocks.* s.l.:Kluwer Academic Publishers, pp. 219-225.

Gao, Z. & Hu, Q., 2013. Estimating permeability using median pore-throat radius obtained from mercury intrusion porosimetry. *Journal of Geophysics and Engineering,* pp. 1-7.

Geology, M. B. o. M. a., 2013. *Stratigraphic charts index.* [Online]
Available at: http://www.mbmg.mtech.edu/sp28/strat.htm

Gerhard, L. C., Anderson, S. B., Lefever , J. A. & Carlson, C. G., 1982. Geological development, origin, and energy mineral resources of Williston Basin, North Dakota. *AAPG Bulletin, V.66,* pp. 989-1020.

Gerhard, L. C., Fischer, D. W. & Anderson, S. B., 1990. Petroleum Geology of the Williston Basin. In: *M 51: Interior Cratonic Basins.* s.l.:AAPG, pp. 507-559.

Giesche, H., 2006. Mercury porosimetry: a general (practical) overview. *Part. Part. Syst. Charact.,* pp. 1-11.

Gile, L. H., Peterson, F. F. & Grossman, R. B., 1966. Morpological and genetic sequences of carbonate accumulation in desert soils. *Soil Science v. 101,* pp. p. 347-360.

Green, A., Hajnal, Z. & Weber, W., 1985a. An evolutionary model of the western Churchill Province and wester margin of the Superior Province in Canada and the north-central United States. *Tectonophysics, v.116,* pp. 281-332.

Grenda, J. C., 1978. Paleozoology of Oil Well Cores from the Tyler Formation (Pennsylvanian) in North Dakota, U.S.A.. *Williston Basin Symposium,* pp. 249-260.

Hallam, A., 1986. Origin of minor limestone-shale cycles: Climatically induced or diagenetic?. *Geology v. 14,* pp. 609-612.

Harrison, R. S. & Steinen, R. P., 1978. Subaerial crusts, caliche profiles, and breccia horizons: Comparison of some Holocene and Mississipian exposure surfaces, Barbados and Kentucky. *Geological Society of America Bulletin, v.89,* pp. p. 385-396.

Heckel, P., 2008. Pennsylvanian cyclothems in Midcontinent North America as far-field effects of waxing and waning of Gondwana ice sheets. *GSA Special paper 441,* pp. 275-289.

Heckel, P. H., 1996. Evaluation of evidence for glacio-eustatic control over marine Pennsylvanian cyclothems in North America and consideration of possible tectonic effects. *Tectonic and Eustatic controls on Sedimentary Cycles,* Volume SEPM Concepts in Sedimentology and Paleontology #4, pp. 65-87.

Hoyt, J. H., 1967. Barrier Island Formation. *GSA Bulletin Vol. 78,* pp. 1125-1136.

Jones, B., 1986. The Influence of Plants and Micro-Organisms on Diagenesis in Caliche: Example From The Pleostocene Ironshore Formation on Cayman Brac, British West Indies. *Bulletin of Canadian Petroleum Geology, VOL. 36, NO.2,* pp. P. 191-201.

Katz, A. J. & Thompson, A. H., 1986. A quantitative prediction of permeability in porous rock. *Phys. Rev. B 34,* pp. 8179-8181.

Katz, A. J. & Thompson, A. H., 1987. Prediction of rock electrical conductivity from mercury injection measurements. *J. Geophys. Res.92,* pp. 599-607.

King, P. B., 1976. Precambrian geology of the United States; an explanatory text to accompany the geologic map of the United States. *U.S. Geological Survey Professional Paper 902,* p. 85 p.

Koeberl, C., Reimold, W. U. & Brandt, D., 1996. Red Wing Creek structure, North Dakota: Petrographical and geochemical studies, and confirmation of impact origin. *Meteoritics and Planetary Science,* Volume 31, pp. 331-342.

Kraus, M., 1999. Paleosols in clastic sedimentary rocks: their geologic applications. *Earth Science Reviews 47,* pp. P. 41-70.

Land, C. B., 1976. Stratigraphy and petroleum accumulation, Tyler sandstones (Pennsylvanian), Dickinson area, North dakota. *AAPG Bull. 60 (Abstract),* pp. 1401-1402 .

LeFever, R. D., 1996. Sedimentology and stratigraphy of the Deadwood-Winnipeg interval (Cambro-Ordovician), Williston basin, in Longman, M.W., and Sonnenfeld, M.D., eds., Paleozoic systems of the Rocky Mountain region. *Rocky Mountain Section SEPM ,* pp. 11-28.

Lochman-Balk, C., 1972. Cambrian System in Geologic Atlas of the Rocky Mountain region, U.S.A.. *Denver, Rocky Mountain Association of Geologists,* pp. 60-76.

Mack, G. H., James, W. C. & Monger, H. C., 1993. Classification of paleosols. *Geological Society of America Bulletin, v. 105,* pp. p. 129-136.

Maughan, E. K., 1984. Paleographic Setting of Pennsylvanian Tyler Formation and Relation to Underlying Mississipian Rocks in Montana and North Dakota. *AAPG V. 68, No.2 ,* pp. 178-159.

McCabe, W. S., 1957. Wiliston Basin Paleozoic Unconformities. *Bulletin of AAPG Vol. 38, No. 9,* pp. 1997-2010.

Mücke, A., 1994. Postdiagenetic ferruginization of sedimentary rocks (sandstones, oolitic ironstones, kaolins and bauxites) - including a comparative study of the reddening of red beds.. *Developments in Sedimentology,* 5(1), pp. 361-395.

Nelson, K. et al., 1993. Trans-Hudson orogen and Williston Basin in Montana and North Dakota-New COCORP deep-profiling results. *Geology v.21,* pp. 447-450.

Nesheim, T. O. & Nordeng, S. H., 2013. *North Dakota Petroleum Council.* [Online] Available at: www.ndoil.org/image/cache/Nesheim-Tyler__WBPC2012_.pdf

Nordeng, S. H. & Nesheim, T. O., 2012. *An Evaluation of the Resource Potential of the Tyler Formation (Pennsylvanian) using a Basin Centered Petroleum Accumulation Model,* Grand Forks, ND: North Dakota Geological Survey.

Olariu, C. & Bhattacharya, J. P., 2006. Terminal Distributary Channels and Delta Front Architecture of River-Dominated Delta Systems. *Journal of Sedimentary Research v. 76,* pp. 212-233.

Pederson, T. F., 1990. Anoxia vs. Productivity: what controls the formation of organic-carbon-rich sediments and sedimentary rocks?. *American Association of Petroleum Geologists Bulletin, v. 74,,* pp. p. 454-466.

Peterson, J. A., 1981. General stratigraphy and regional paleostructure of the western Montana overthrust belt. *Field Conference and Symposium Guidebook, Southwest Montana; Montana Geological Society,* pp. 5-35.

Peterson, J., 1995. Williston Basin Province, in U.S. Geological Survey 1995 National Assessment of United States Oil and Gas Resources, Digital Data Series DDS-30, Release 2, CD-ROM

Rankey, E. C., 1997. Relations between relative changes in sea level and climate shifts: Pennsylvanian- Permian mixed carbonate-siliciclastic strata, western United States. *GSA Bulletin 109, no. 9,* pp. 1089-1100.

Reinhardt, J. & Sigleo, W. R., 1988. *Paleosols and weathering through geologic time: principles and applications,* Boulder: Geological Society of America.

Sloss, L., 1984. Comparative anatomy of cratonic uncomformities, in Schlee, J.S., ed., Interregional unconformities and hydrocarbon accumulation. *AAPG Memoir 36,* pp. 7-36.

Spray, J. G., Kelley, S. P. & Rowley, D. B., 1998. Evidence for a late Triassic multiple impact event on Earth. *Nature,* pp. 171-173.

Sturm, S. D., 1982. Depositional Environment and Sandstone Diagenesis in the Pennsylvanian Tyler Formation of Southwestern North Dakota. *4th International Williston Basin Symposium,* pp. 251-262.

Sturm, S. D., 1987. Depositional History and Cyclity in the Tyler Formation (Pennsylvanian), Southwestern North Dakota. *Williston Basin: Anatomy of a Cratonic Oil Province Symposium,* pp. 209-221.

Tourtelot, H. A., 1979. Black Shale- Its deposition and Diagenesis. *Clays and Clay Minerals, No. 5,* pp. 313-321.

Tourtelot, H. A., 1979. Black Shale- Its Deposition and Diagenesis. *Clay and Clay Minerals, vol. 27, no. 5,* pp. p. 313-321.

Vail, P., Mitchum, R. & Thompson, S., 1977. Seismic stratigraphy and global changes of sea level, Part 3: Relative changes of sea level from coastal in, C.E. Payton, ed., Seismic Stratigraphy- Application to hydrocarbon exploration. *AAPG Memoir 26,* pp. 63-81.

Walker, R. G., 2006. Facies Models Revisited in Posamentier, H.W., and R.G., Walker, Facies Models Revisited. *Society for Sedimentary Geology (SEPM),* p. p. 375.

Watney, W. L., 1980. Cyclic sedimentation of the Lansing- Kansas City Groups in northwestern Kansas and southwestern Nebraska. *Kansas Geological Survey Bulletin 220,* p. 72 p..

Ziebarth, H. C., 1972. The Stratigraphy and economical potential of Permo-Pennsylvanian strata in southweestern North Dakota.. *University of North Dakota Ph.D thesis,* p. 414 pp.

Biographical Information

Paul David Monahan is the oldest of two children of Paul Conrad Monahan and Lourdes Monahan. He graduated with his Bachelors of Science in Geology from Florida Atlantic University in Boca Raton, FL in 2011, and Masters of Science in Geology from University of Texas at Arlington in 2014. His research interest while at University of Texas at Arlington was petroleum geology, with a specific interest in unconventional resources and exploration. This led to a focus towards stratigraphy and sedimentation along with basic sequence stratigraphy. After graduation Paul intends to work in the oil and gas industry, preferably in exploration.